ALMA MATER STUDIORUM - UNIVERSITÀ DI BOLOGNA
CAMPUS DI CESENA
SCUOLA DI INGEGNERIA E ARCHITETTURA

Corso di Laurea Magistrale in Ingegneria Elettronica e delle Telecomunicazioni per l'Energia

TITOLO DELLA TESI

RFID TAG LOCALIZATION WITH VIRTUAL MULTI-ANTENNA SYSTEMS

Tesi in
Sistemi di Telecomunicazioni LM

Relatore:
Chiar.mo Prof. Ing.
DAVIDE DARDARI

Presentata da:
FEDERICO BERTI

Correlatori:
Dott. Ing.
NICOLÓ DECARLI
Prof. Ing.
ANDREA GIORGETTI

SESSIONE III
ANNO ACCADEMICO 2014-2015

Keywords

RFID

Localization

Phase

Multi-antenna

Tag

Alla mia famiglia...

List of Acronyms

3D three dimensional

AOA angle-of-arrival

CW continuous wave

DOA direction-of-arrival

GPS Global Positioning System

IoT Internet of Things

LLRP Low Level Reader Protocol

LOS line-of-sight

NLOS non-line-of-sight

PDOA phase-difference-of-arrival

RFID radio frequency identification

RMSE root mean square error

RSS received signal strength

RV random variable

RX receiver

SNR signal-to-noise ratio

TDOA time-difference-of-arrival

TOA time-of-arrival

TX transmitter

UWB ultra-wide band

WSN wireless sensor networks

Contents

Abstract

In questa tesi si sono valutate le prestazioni di un sistema di localizzazione multi-antenna di tag radio frequency identification (RFID) passivi in ambiente indoor. Il sistema, composto da un reader in movimento che percorre una traiettoria nota, ha come obiettivo localizzare il tag attraverso misure di fase; piú precisamente la differenza di fase tra il segnale di interrogazione, emesso dal reader, e il segnale ricevuto riflesso dal tag che é correlato alla distanza tra di essi.

Dopo avere eseguito una ricerca sullo stato dell'arte di queste tecniche e aver derivato il criterio maximum likelihood (ML) del sistema si é proceduto a valutarne le prestazioni e come eventuali fattori agissero sul risultato di localizzazione attraverso simulazioni Matlab.

Come ultimo passo si é proceduto a effettuare una campagna di misure, testando il sistema in un ambiente reale. Si sono confrontati i risultati di localizzazione di tutti gli algoritmi proposti quando il reader si muove su una traiettoria rettilinea e su una traiettoria angolare, cercando di capire come migliorare i risultati.

Introduction

In recent years the importance of localizing and tracking objects and people has grown considerably. Also the birth of the Internet of Things (IoT) and its expansion, where every object can communicate to each other, caused the need of interconnect many devices. In this context the information about their locations could be important.

Simultaneously the technological progress of RFID systems has brought an enormous diffusion of this technology. Originally they were created for the purpose of automatically identifying and automatic storage of information relevant to objects, animals or people. This technology thanks to its simplicity, low cost and small dimensions, has found use in many environments like logistic, airport baggage management, inventory process, security and access control. A RFID system is composed at least of two devices: a reader that makes interrogations to the tag and the tag which answers with its ID by modulating the interrogation. The reader can measures only the received signal strength (RSS) level of the signal and the phase difference between the interrogation and the response of the tag.

Thanks to the low cost of RFID tags, this technology can be used to design innovative and low-cost localization systems. Imagine a warehouse where each object is provided with a passive RFID tag. A reader, free to move inside the environment, that performs phase measurements can localize all tags and then through the information acquired realize an automatic inventory process (see Figure 1). Otherwise cars provided with antenna arrays through their motion can localize the relative position and velocity of an object, equipped with a passive RFID tag, and prevent possible collisions.

In literature there are present many RFID locating system that use the RSS level of the received signal, but the disadvantage of these methods is that the RSS is affected by multipath and interference effects.

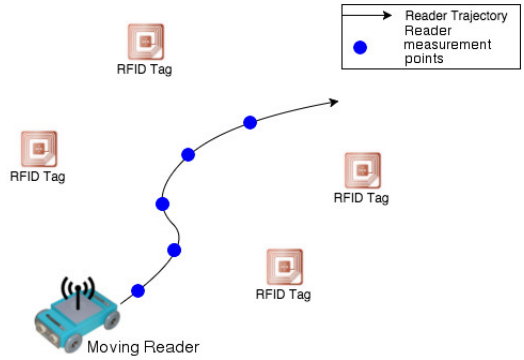

Figure 1: Example of localization in a warehouse environment using a moving reader.

The objective of this thesis is to evaluate the performance and how improve it of a RFID localization system formed by a reader, moving in a known trajectory, that performs phase measurements.

This work is organized as follows:

- *Chapter 1:* describes the principal indoor localization techniques and the architecture of RFID-based technologies. Also the principal RFID phase-based spatial identification methods are introduced.

- *Chapter 2:* contains a mathematical analysis in order to derive the ML criterion of the system and describes the algorithms proposed.

- *Chapter 3:* this chapter collects the simulation results of our system obtained through Matlab simulators in order to discover the performance and the features of the locating system implemented.

- *Chapter 4:* shows the measurement setup adopted and the principal standard protocols that are used in RFID technologies.

- *Chapter 5:* describes the measurement campaign carried out in a real indoor environment and compares the localization result of the different algorithms investigation, trying to minimize the root mean square error (RMSE).

- *Chapter 6:* reports the conclusions of the work.

This thesis has been carried out within the European project XCYCLE. Its objective is to reduce accidents and fatalities of cyclists in urban traffic and improve its comfort. XCYCLE has an objective of developing user-friendly, technology-based systems to make cycling safer in traffic [1].

RFID localization technologies could be used in this contest, for example, to localize cyclists at junctions and prevent possible collisions.

XCYCLE consortium is composed by: Alma Mater Studiorum-University of Bologna, ITS-University of Leeds, Volvo Group, DLR Germany, University of Groningen, VTI, Imtech, Kite Solutions and Jenoptik.

Chapter 1

Localization Methods

1.1 Classic Indoor Localization Methods

The localization methods are processes that perform physical measurements, like distances or angles, in order to find the exact position of a mobile device [2]. A locating system is composed at least by: mobile devices or target that are moving in an area; base stations at known positions and data processing subsystems. Propagation in indoor environment is affected by many problems like multipath, diffraction, reflection, non-line-of-sight (NLOS) path and absorption [4]. There are several localization methods in literature [5]. The methods can be divided into three classes: distance-based estimation, scene analysis based and proximity-based [6].

Distance estimation methods can be divided into:

- Received Signal Strength (RSS);
- Time-of-Arrival (TOA);
- Time-Difference-of-Arrival (TDOA);
- Received Signal Phase (RSP);
- Angle of Arrival (AOA);

Scene analysis methods can be divided into:

- k-Nearest-Neighbor (kNN);
- Probabilistic Approaches.

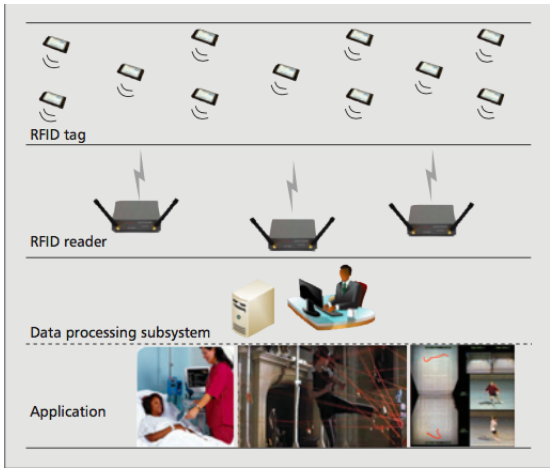

Figure 1.1: RFID-based localization system [3].

1.1.1 Distance Estimation-Based Methods

These algorithms use a triangulation or lateration approach to estimate the mobile device location. They convert physical measurements of the system, like propagation time or received power, in equivalent distance values.

- **RSS-Received Signal Strength Method:** Technique based on the measure of the power of the signal received at the reader/base station. The distance measurement can be obtained knowing the path-loss of the radio channel. The attenuation of the signal is function of the distance between the transmitter and the receiver. Therefore, the device with unknown position is placed on a circumference with radius equal to the distance estimated. Having at least three base stations or readers doing the RSS measure it is possible estimate the position of the device resolving a triangulation problem. This method is very sensitive to shadowing and multipath effects; they can cause a large distance error that determines a wrong localization.

- **TOA-Time of Arrival Method:** Technique based on the measure of the signal propagation time between base stations and the mobile device with unknown position. The distance measurement can be obtained from the time measurement knowing the propagation speed of the signal. Therefore, the device with unknown position should be placed on a circumference with radius equal to the distance estimated. Having

at least three base stations or readers doing the time-of-arrival (TOA) measure it is possible estimate the position of the device resolving a triangulation problem. This method is more robust than RSS with respect to shadowing and multipath effects. The system need to know the time instant of the signal transmission or in alternative use a two way ranging method.

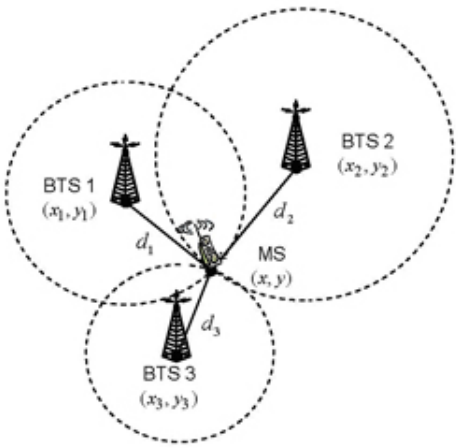

Figure 1.2: Example of localization with RSS or TOA method [7].

- **TDOA-Time Difference of Arrival Method:** Technique based on the measure of the signal propagation time difference between two base stations of the network. The time-difference-of-arrival (TDOA) principle lies on the idea of discovering the position of a transmitting device by using the difference in time at which the signal arrives at multiple base stations. Therefore, the device with unknown position should be placed on a hyperbole where the base stations are in the focus of the curve. Having at least three base stations or two TDOA measurements it is possible estimate the position of the device. The system requires strong base station synchronization.

- **RSP-Received Signal Phase:** This method, also called Phase of Arrival (POA), uses the delay, expressed as phase measurements, to estimate distance. The localization can be done using the same algorithm than TOA or TDOA. This method strongly needs a line-of-sight (LOS) path in order to limit locating error.

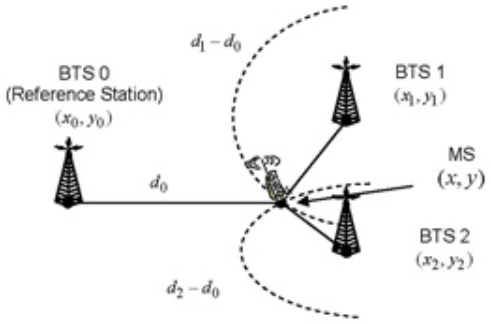

Figure 1.3: TDOA method [7].

- **AOA-Angle of Arrival Method:** Technique based on the measure of the direction of arrival of the signal to the base station. Therefore, the device with unknown position should be placed on a straight line with direction equal to one measured before. Having at least two base station it is possible estimate the position of the device as the intersection of the two straight lines. This method requires directional antennas or smart antennas.

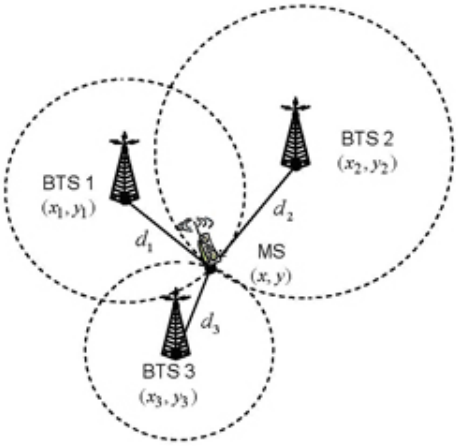

Figure 1.4: AOA method [7].

1.1.2 Scene Analysis-Based Methods

Scene analysis approaches have a first step for collecting the fingerprint of the environment. First of all the ambient is divided into several subareas, then at each zone a value obtained through preliminary measurements is assigned, so a database of the area is built. In the second step of the method the target performs a measure and compares its value with the database values in order to find the subarea of membership. Generally, RSS-based fingerprinting is used. The two main techniques are: k-Nearest-Neighbour (kNN) and probabilistic method.

- **k-Nearest-Neighbour (kNN):** It consists in a first time measuring RSS at known location in order to make a database called radio map. Then a mobile device can perform RSS measurements to find the k closest matches in the signal space previously built. Finally, a root mean square algorithm is applied in order to find the estimated location of the device.

- **Probabilistic Approach:** This method assumes that there are n possible locations and one observed strength vector during the second phase according to Bayes formula. The location with the highest probability is chosen.

1.1.3 Proximity-Based Methods

This approach relies on dense deployment of antenna. When the target enters in the radio range of a single antenna, its position is assumed as the same of this receiver. If more than one antenna detect the target, the mobile device is collocated in the position of the receiver with the strongest signal. The accuracy of this method is equal of the size of the cells.

1.1.4 Performance Metrics

Different applications or technologies may have different requirements on localization system. There are different performance metric to evaluate in order to reach a performance objective.

Performance metrics for indoor wireless location systems are [3, 8]:

- **Accuracy:** In general this parameter evaluates the localization error, that is the distance between the real position of the target and the estimated position. This is the most important parameter in these systems; higher is the accuracy, better is the system but often there is a trade off between this parameter and other performance metrics.

- **Precision:** This parameter is an indicator of how uniformly the system works. Accuracy only evaluates the mean of the distance error. Precision parameter represents the robustness of the localization technique i.e., the variations on its performance over many tentative. Many scientific papers indicate precision as geometric dilution of precision (GDOP) or location error standard deviation.

- **Complexity:** It depends from hardware, software and data processing.

- **Scalability:** The scalability represents how the system can work correctly in a different environment keeping the same performance.

- **Latency:** It is an important performance metric to evaluate a localization system. Latency is defined as the time required by the system to generate the new estimated position when the target moves to a new location. In real time system it is very important to have a low latency.

- **Robustness:** A high robustness ensures that a system could work in complicated environments where there is incomplete information, some signals are not available, a wireless sensor network with disabled nodes or high presence of multipath or interference effects.

- **Cost:** Cost is another performance metric to evaluate when a localization system is designed. Costs include money, time, energy, space and weight.

1.2 RFID Tag

RFID tags, also called transponders or labels, are simple devices formed by an antenna and an integrated circuit. There are three different type of RFID tags:

- *Passive tags*: tags are not powered. They use the electromagnetic field coming from the reader to power up.
- *Semi-passive tags*: they are powered only for data process or maintenance. The electromagnetic field from the reader is used to send the answer after the interrogation.
- *Semi-active tags*: chip and transmitter are both powered by a battery but the tag is normally disabled. The tags are enable by a receiver that works with the technology of passive tag. The main advantage is the long life of battery.
- *Active tags*: tags are totally powered and contain their own transmitter. They have an high working distance reachable.

In this thesis we consider only passive tags. They use a part of the electromagnetic field from the reader to power them-self and generate, through a backscatter modulation, the response. The advantages of passive tags are: very long useful life, they are very cheap and have small dimensions. The major disadvantage is that they can be read only at very short distances. Passive tags cannot start a communication but only respond after an interrogation. They are made up by an integrated antenna, typically printed on a insulating substrate, and a miniaturized integrated circuit. The total thickness of the tag is very low so they can be integrated in credit cards, adhesive labels, small plastic objects and tickets. Their data memory can be read-only or read-writable. The last type permits also, in additions to reading operations, the possibility to modify data memorized. Generally tags can made by different material in order to use it in different environments and situations.

RFID tags can operate in different frequency bands. In this thesis we decided to use only passive tags that operate in the UHF band (860MHz-960MHz).

1.3 RFID Localization Schemes

Nowadays there are a lot of RFID localization techniques. Due to the limited energy of the tags the localization and the data processing are centralized. With passive tags it is suggested the proximity approach; differently in an

(a) Example of HF passive tag.

(b) Example of active tag-Identec.

(c) Example of semi passive tag integrated in an adhesive label.

Figure 1.5: Different type of RFID tags [9].

environment full or readers technique more elaborated can be applied. We can classify RFID localization scheme into three classes: distance estimation, scene analysis and constraint-based.

1.3.1 Distance Estimation

These algorithms use a triangulation or laterations approach to estimate the mobile device location. They convert physical measurements of the system, like propagation time or received power, in equivalent distance values. Laterations are used to localize the tag.

- **SpotON [10]:** This scheme is very simple: readers collect signal strength measurements to approximate the distance through a function built with empirical data.

- **SAW ID-tags [11]:** Surface Acoustic Wave Identification interrogates passive tags with the time inverse of its pulse response. Then tags retransmit the correlated signal. This signal shows a peak in the autocorrelation function and the response with the highest amplitude recognizes the searched tag. The distance between the reader and the tag is measured using a TOA approach.

- **LPM [12]:** Local Position Measurement (LPM) readers are synchronized thanks to a reference tag (RT) positioned in fixed location. This method is based on the TDOA approach. Selective active tags after an interrogation responds at the time t_{MT}. The time difference t_{diff} of the signals between reader R_i and tag can be calculate as:

$$ct_{diff}(R_i) = c(t_{MT} - t_{RT}) + \|MT - R_i\| - \|RT - R_i\| \tag{1.1}$$

  where c is the speed of light and MT indicates the measurement transponder.

- **RSP [13]:** Two readers at fixed locations calculate the phase difference of a moving tag. When they collect a lot of measures the estimation can be done through a least square fitting technique. With two pairs of readers it is possible a triangulation to find the tag position and its direction. It is an example of direction-of-arrival (DOA) method.

1.3.2 Scene Analysis

The principal RFID localization scheme belonging to scene analysis category found on scientific papers are the following.

- **Landmarc [14]:** This method is based on the kNN concept. Fixed tags with know positions (reference tags) cover the area to be monitored. Tracking tags are on the target object. When an object is inside the area, readers perform RSS measures of both reference and tracking tags. The reference tag with the closest RSS value to the tracking tag is used to compute the localization. Multipath and interference may influence the performance of that system.

- **VIRE [15]:** This method uses the principle of the previous case. It is used the concept of proximity map. The monitoring area in divided into regions, where reference tags are placed in the center of them. Each reader has its own proximity map. Readers perform RSS measures of the unknown tags and reference tags and if the difference is smaller than a threshold the corresponding region is marked as '1'. The fusion of all n reader proximity maps creates a global map localizing the tag.

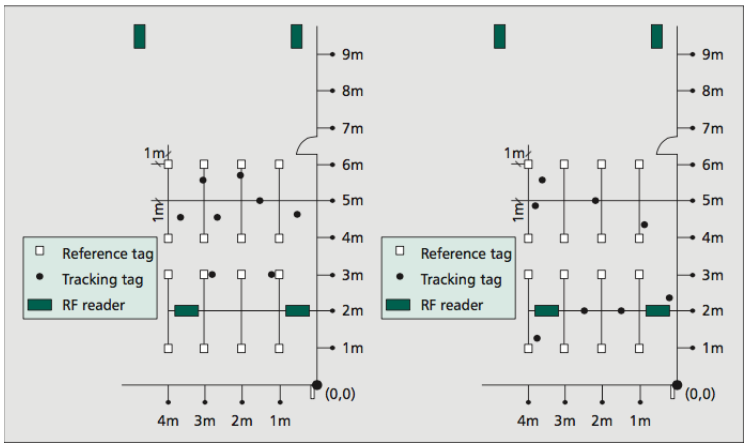

Figure 1.6: Landmarc method example [3].

- **Simplex [16]:** This method is based on reference tags placed in the monitoring area. It requires that the n readers have different trasmissione power level. Each reader starts with the lowest power level and increases it until it receives a response from the tag. The distance between the reader and the tag is estimated by averaging the distance between the reader and all reference tags detected with the same power level. This method is called *simplex* because it use the simplex algorithm in order to minimize the localization error function.

- **Kalman filtering [17]:** This method is divided into two steps. The first step consists in calculating the distance D_j between each reference tag and tag with unknown position using RSS measurements from two readers. Solving the following system of equation through a minimum square error algorithm it is possible to find the coordinates of the target tag.

$$(x_j - x_e)^2 + (y_j - y_e)^2 = D_j^2 \qquad \forall j = 1, \cdots n \tag{1.2}$$

where (x_i, y_i) are the coordinates of the ith reference tag and (x_e, y_e) are the coordinates of the target. The second step builds a probabilistic map of the localization error for the reader's detection area. A Kalman filter is used on this online map in order to increase the accuracy of the localization and reduce the error due to RSS measures.

1.3.3 Constrain-Based Approach

The main method that belongs to this category is *3-D Constraints* [18]. It is based on connectivity information and it defines that if a reader can detect a tag then the distance between them is inferior of the reader's read range. The area is discretized into points in order to delimit the detection area of the readers.

1.4 RFID-Based Technology

Another way to classify RFID systems is depending on their technologies. It can be classified into four categories: tag based, reader based, transceiver free and hybrid technologies [3].

- **Tag-based technologies**

  Tag-based technologies require that the target object carry a tag, for example an active tag that periodically transmits beacon messages. An example of this technology is LANDMARC system [14]. It use reference tag in known positions and RSS measurements in order to find or track a target carrying an active tag. It is very simple to implement but it suffers of multipath and interference effect.

- **Reader-based technologies**

  In this technologies classical roles of readers and tags are reversed: tags are placed at known and fixed position and a reader is attached to a object or is carried by an user [19]. The position of the user is determined using tag IDs or RSS value read by the reader. This method is also called as reverse RFID. It permits to remove the dependence on the infrastructure of networked readers, very useful in many applications concerning tracking people in dangerous situations like natural disaster where the preexisting infrastructure can be damaged.

  Active or passive tags can be used with this technology.

- **Transceiver-free technologies (RADAR)**

  The basic idea of this technology is to locate object or people without they carry any tag or reader. Wireless signal in a static environment

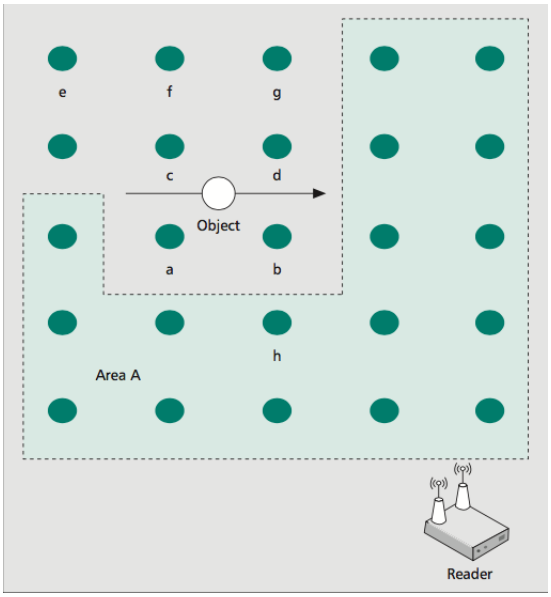

Figure 1.7: Transceiver-free technologies example [3].

are quite stable. When an object are moving in a monitored area it cause changes on the signal.

A simple implementation of this technology is the following [20]: an area is covered with an array of tags and few readers are placed on the ground. Readers periodically read the RSS value of tags. These values are stable in a static environment. When an object is moving in the area it causes changes in the RSS values of nearby tags. This information it used to track and localize the object. See Figure 1.7.

This algorithm requires a training step where for an amount of time the system collects RSS values of tags. The main advantage of transceiver-free technologies is that the target does not carry a device but the localization and tracking of multiple object are very hard.

- **Hybrid technologies**

  Hybrid technologies try to join advantages of different technologies. The first example is Cocktail [21]. It is an implementation that joins RFID technologies to wireless sensor networks (WSN) theory with objective to improve localization accuracy in a large area. In large area accuracy of traditional RFID system decrease due to multipath and

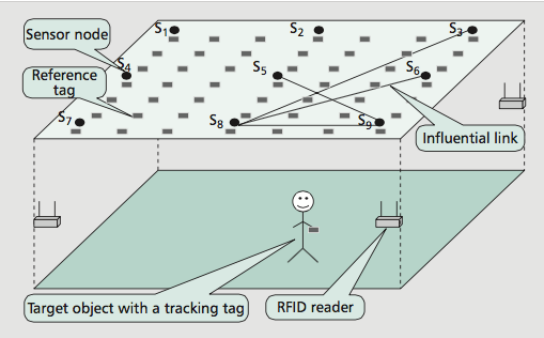

Figure 1.8: Cocktail architecture example [3].

interference effects. Cocktail employs a sparse WSN network to cover the area using reference tags and sensor nodes. Sensor nodes have a sparse grid deployment respect to tags grid because they are expensive. When a target is moving in the area it causes changes in RSS values of some sensor link, called influential links. Influential links tend to be clustered around the object [22].

The a LANDMARC [14] approach or Support Vector Regression (SVR) [23] is applied.

Cocktail improve the localization accuracy respect to previous technologies. However tracking multiple objects is very hard if they are very close to each other.

The second example is a technology that joins RFID to inertial navigation system (INS) using inertial and non-inertial sensors.

In a hybrid Reverse-RFID/INS system the target carry a reader and a portable inertial navigation sensor. When the object is out of range of a tag, the INS is used to track the trajectory. As soon as the object enter in the read range of a tag, it know coordinates are used to correct the trajectory estimated. This technology have good results only if the time spend using the inertial sensor are small.

1.5 RFID Phase-Based Spatial Identification

The previously seen locating system mainly use the RSS indicator or TDOA measurements. Using UHF RFID tags, RSS measurements could be very

unreliable due to multipath and interference effects or reliable only in a short distance. Moreover RFID tags and readers cannot operate in short impulse mode as required by a TOA approach because they are a very short range narrowband technology.

Thanks to modern RFID readers that perform fully coherent detection and recover the phase of the tag signal, tag phase information could be used to determine the position and the velocity of the moving tag. This application is also called as *spatial identification* [24].

Tag phase information depends from the propagation channel. Using a phase-difference-of-arrival (PDOA) approach it is possible erase some additive factors, like the phase introduced by cables or by the hardware, that affect the phase read by the reader.

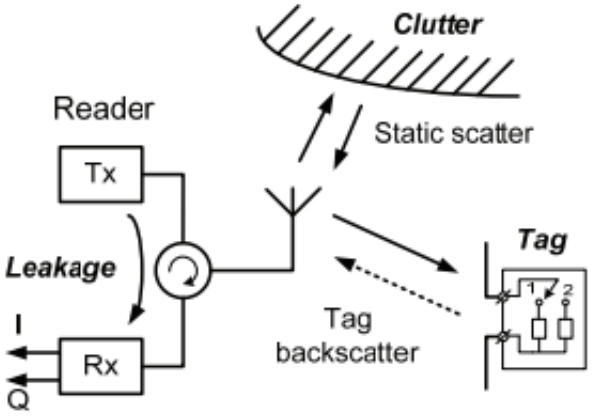

Figure 1.9: Phase identification schematic [24] .

The phase of the signal received by the reader is:

$$\varphi_d = \varphi + \varphi_0 + \varphi_{BS} \tag{1.3}$$

where φ is the phase due to the electromagnetic propagation, φ_0 is the phase deriving from cables and other system components and φ_{BS} is the backscatter phase from the tag.

$$\varphi = -2\frac{2\pi f}{c}d \tag{1.4}$$

where c is the propagation velocity, f is the frequency of the signal and d is the distance between reader antenna and the tag.

1.5.1 Time Domain Phase-Difference-of-Arrival (TD-PDOA)

This method estimates the velocity of the tag by measuring phases at different time instants. Using a fixed signal frequency and measuring the tag phase in two different time instants, assuming that φ_0 and φ_{BS} do not change in time we can derive:

$$V_r = -\frac{c}{4\pi f}\frac{\delta\varphi}{\delta t} \tag{1.5}$$

where V_r is the instantaneous tag velocity and φ is the phase measured.

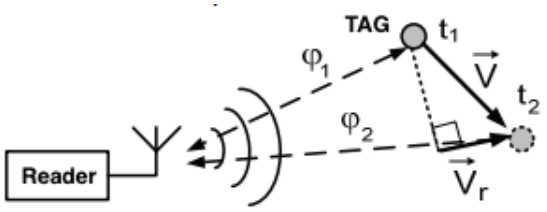

Figure 1.10: TD-PDOA technique [24].

1.5.2 Frequency Domain Phase-Difference-of-Arrival (FD-PDOA)

This method estimates the distance between tag and reader through phase measurements at difference frequencies. Measuring the phase of the tag at different frequencies, assuming that φ_0 and φ_{BS} do not change in frequency or can be considered calibrated and the tag is fixed during measurement process, it is possible find the distance d between reader antenna and tag as:

$$d = -\frac{c}{4\pi f}\frac{\delta\varphi}{\delta f} \tag{1.6}$$

This technique is very similar to frequency modulated continuous wave (FM CW) [25].

1.5.3 Spatial Domain Phase-Difference-of-Arrival (SD-PDOA)

This technique estimates the direction of arrival of a backscattered signal by measuring the phases at several receiving antennas. Supposing to have the

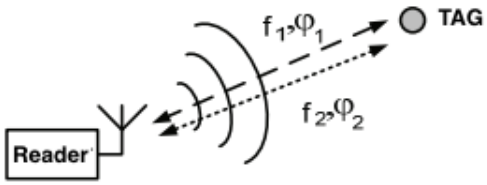

Figure 1.11: FD-PDOA technique [24].

antennas spaced of a factor a and supposing to have the tag to be located out a distance longer than a, it is possible calculate the DOA as:

$$\theta \approx arcsin\left[-\frac{c}{2\pi f}\frac{(\varphi_1 - \varphi_2)}{a}\right] \tag{1.7}$$

A simple scheme is reported in Figure 1.12. In these years many signal

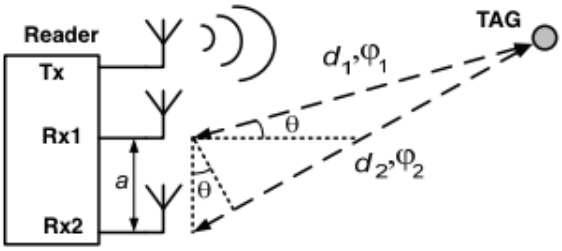

Figure 1.12: SD-PDOA technique [24].

processing techniques have been developed to improve accuracy [26].

1.5.4 Synthetic Aperture Radar and Holographic Localization

This method is very similar to phase difference of arrival technique. A Synthetic Aperture Radar (SAR) is realized by moving the reader antenna on a known trajectory collecting several phase measurements. Target's position can be obtained through a holographic algorithm [27, 28] or multi angulation approach (see Figure 1.13).

In the holographic approach a special correlation function is derived thanks to the phase measurements. The maximum of this function represents the estimated target position. This particular method will be studied and explained in this thesis.

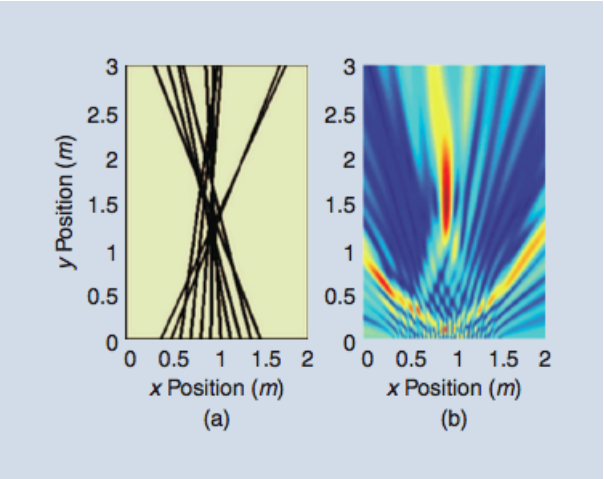

Figure 1.13: Comparison between multi angulation (a) and holographic approach (b) [29].

1.6 RFID-UWB technology

A recent technology studied for accurate indoor mapping is the ultra-wide band (UWB) technology. In fact, the adoption of UWB signals permit to obtain a sub-meter localization accuracy. This technology can be a solution for next generation RFID systems to overcome most of the limitations of the narrow bandwidth RFID technology like: insufficient ranging accuracy, sensitivity to interference and multipath and reduced area coverage [30]. For future RFID systems, important requirements will be very accurate localization at the submeter level, management of large number of tags, small size, low cost and low power consumption.

A promising wireless technique that can be used in next generation RFID systems is the UWB technology characterized by the transmission of sub-nanosecond duration pulses. The employment of wideband signals enables the resolution of multipath and high localization precision based on TOA estimation. Also, it includes low power consumption, low detection probability and efficient multiple channel access [31].

Also, UWB technology can be used in a novel network able to combine passive RFID and radar sensor networks (RSN) in order to identify and localize tags and moving objects in a monitored area through the analysis of their backscattered response to a common interrogation signal [32].

Chapter 2

Localization Algorithms using Virtual Arrays

2.1 Virtual Array

Our system is composed by a moving reader equipped with a single UHF antenna. It moves on a known trajectory performing phase measurements of the signal received from the tag with unknown position. Supposing that the tag is in a fixed location during the motion of the reader and supposing to know the exact positions of the reader when the measures was taken, it is possible to combine and process measurements taken at different time instants corresponding to different antenna positions as if they were obtained from an antenna with multiple spatially distributed elements.

This technique is called *virtual antenna array* and it creates an equivalent virtual antenna with large aperture, able to discriminates directions of arrivals of different signals.

The objective of this thesis is evaluating the effectiveness of a virtual array solution where the motion of the reader is used to create an antenna with large aperture.

Figure 2.1 shows an example of localization setup using virtual antenna array.

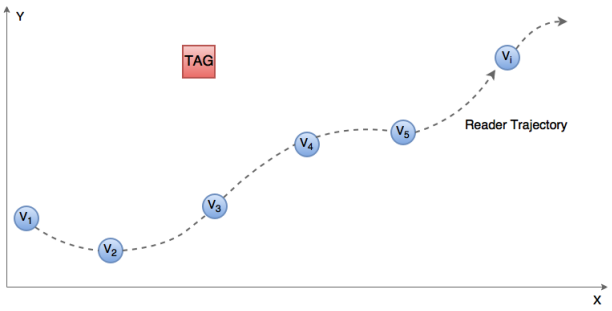

Figure 2.1: Example of localization using a virtual antenna array. $\mathbf{v}_i$ indicates the ith position of the reader performing the ith phase measurement.

2.2 Problem Definition

The advantage of using a backscatter transponder, as a passive tag, is that it reflects the incident signal modulating it in amplitude after an interrogation, performed by the reader. The phase shift between the interrogation signal and the response is related to the distance that separates the reader and tag.

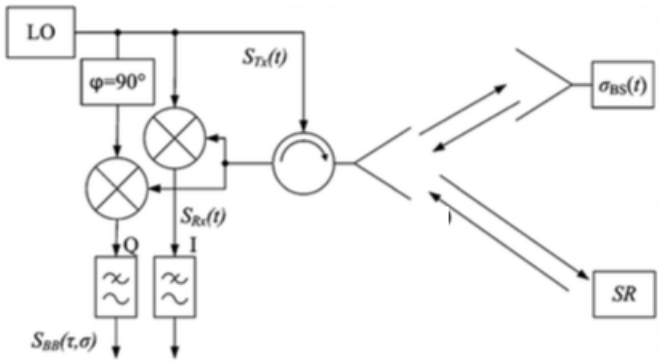

Figure 2.2: Block diagram of interrogator and backscatter transponder [33].

In order to recover the phase information is necessary to execute a fully coherent demodulation, shown in Figure 2.2.

To simplify the model we suppose that the RFID reader transmits a continuous wave (CW) signal

$$s_{\mathrm{Tx}}(t) = a_{\mathrm{Tx}} \cos(2\pi f_0 t) \tag{2.1}$$

where a_{Tx} and f_0 are, respectively, the amplitude and the frequency of the signal. After traveling to the tag situated in a fixed position at distance d_i from the reader and coming back, the reader receives the following signal:

$$r(t) = \tilde{a}_i \, s(t - \tau_i) + n(t) \tag{2.2}$$

$$\tau_i = 2d_i/c \tag{2.3}$$

where $\tilde{a}_i$ is the amplitude of the received signal, c is the speed of the signal, τ_i is the traveling delay due to the distance d_i between reader and tag and n is the phase noise. Then

$$r(t) = \tilde{a}_i \cos(2\pi f_0(t-\tau_i)) = \tilde{a}_i \cos(2\pi f_0 t - 2\pi f_0 \tau_i) = \tilde{a}_i \cos(2\pi f_0 t + \varphi_i) \tag{2.4}$$

$$\varphi_i = -2\pi f_0 \tau_i = -\frac{4\pi d_i}{\lambda} \tag{2.5}$$

where $\lambda = c/f_0$ is the wavelength of the signal. The phase value that the reader provides is obtained as:

$$\varphi_i \bmod 2\pi = -\frac{4\pi d_i}{\lambda} \bmod 2\pi \tag{2.6}$$

2.3 Maximum Likelihood Estimator

In this paragraph the maximum likelihood estimator will be derived with two different assumptions. The first considers constant the amplitude of the received signals; the second case uses the information about the received power to derive the estimator.

Our system is composed of a moving reader along a know trajectory interrogating a tag supposed in a fixed unknown position $\mathbf{p} = (\mathbf{x}, \mathbf{y})$. In each interrogation the reader performs a phase measurement which is related to the distance between the reader and the tag. While moving the reader collects N tag reads in positions $\mathbf{v}_1, \mathbf{v}_2, \ldots, \mathbf{v}_N$, where $\mathbf{v}_i = (x_i, y_i)$, according to Figure 2.3. The ith reader-tag distance is defined as:

$$d_i(\mathbf{v}) = \sqrt{(x - x_i)^2 + (y - y_i)^2} \tag{2.7}$$

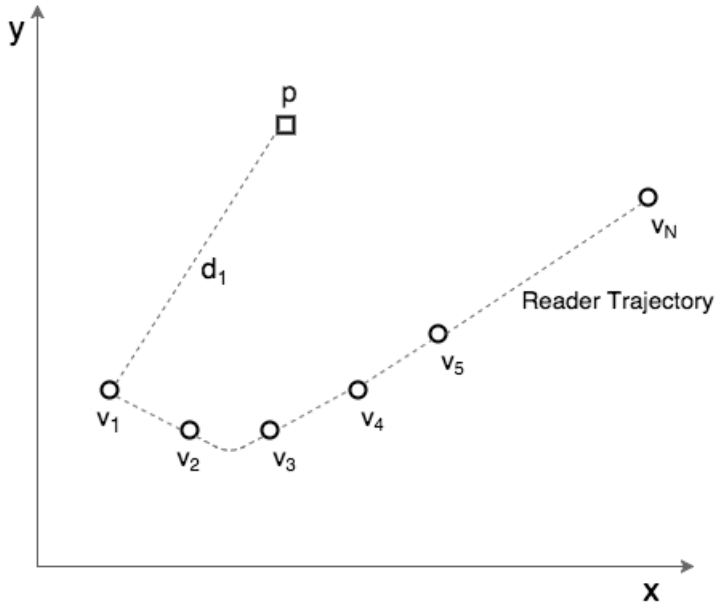

Figure 2.3: Simple scheme of the system where the tag is located in $\mathbf{p}$ and the reader evaluates the phase from the N positions $\mathbf{v}_i$.

2.3.1 ML Estimator with Constant Amplitudes

In this simplified model we assume that the amplitude of the received signals is constant for all reader positions. The observation vector $\mathbf{r}$ that collects all phase differences due to the reader-tag-reader propagation is (in equivalent low-pass)

$$\mathbf{r} = [r_1\, r_2\, \ldots\, r_N]^{\mathrm{T}} = \left[e^{j\varphi_1}\, e^{j\varphi_2}\, \ldots\, e^{j\varphi_N}\right]^{\mathrm{T}} = \mathbf{s} + \mathbf{n} \tag{2.8}$$

where

$$\mathbf{s} = [s_1(\mathbf{p})\, s_2(\mathbf{p})\, \ldots\, s_N(\mathbf{p})]^{\mathrm{T}} = \left[e^{j\phi_1(\mathbf{p})}\, e^{j\phi_2(\mathbf{p})}\, \ldots\, e^{j\phi_N(\mathbf{p})}\right]^{\mathrm{T}} \tag{2.9}$$

$$\phi_i(\mathbf{p}) = -\frac{4\pi f_0}{c} d_i(\mathbf{p}) = -\frac{4\pi f_0}{c}\sqrt{(x-x_i)^2 + (y-y_i)^2} \tag{2.10}$$

The noise vector $\mathbf{n} = [n_1\, n_2\, \ldots\, n_N]^{\mathrm{T}}$ has independent elements $n_i = n_{\mathrm{I}i} + jn_{\mathrm{Q}i}$. Considering $n_{\mathrm{I}i}$ and $n_{\mathrm{Q}i}$ independent random variables, it is

$$n_{\mathrm{I}i},\ n_{\mathrm{Q}i} \sim \mathcal{N}(0, \sigma^2) \tag{2.11}$$

$$n_i \sim \mathcal{CN}(0, 2\sigma^2) \tag{2.12}$$

which is a circular Gaussian random variable.

The likelihood function of the ith observation given $\mathbf{p}$ is

$$f(r_i|\mathbf{p}) = \frac{1}{\sqrt{2\pi\sigma^2}} \exp\left\{-\frac{|r_i - s_i(\mathbf{p})|^2}{2\sigma^2}\right\} \tag{2.13}$$

so then

$$\begin{aligned} f(\mathbf{r}|\mathbf{p}) = \prod_{i=1}^{N} f(r_i|\mathbf{p}) &= \frac{1}{\left(\sqrt{2\pi\sigma^2}\right)^N} \prod_{i=1}^{N} \exp\left\{-\frac{|r_i - s_i(\mathbf{p})|^2}{2\sigma^2}\right\} \\ &= \frac{1}{\left(\sqrt{2\pi\sigma^2}\right)^N} \exp\left\{-\frac{1}{2\sigma^2}\sum_{i=1}^{N}|r_i - s_i(\mathbf{p})|^2\right\}. \end{aligned} \tag{2.14}$$

Then, the maximum likelihood estimate $\hat{\mathbf{p}}$ of the tag position $\mathbf{p}$ is

$$\begin{aligned} \hat{\mathbf{p}} &= \underset{\mathbf{p}}{\operatorname{argmax}} \ln f(\mathbf{r}|\mathbf{p}) = \\ &= \underset{\mathbf{p}}{\operatorname{argmax}} \left\{-\sum_{i=1}^{N}|r_i - s_i(\mathbf{p})|^2\right\} = \\ &= \underset{\mathbf{p}}{\operatorname{argmax}} \left\{-\underbrace{\sum_{i=1}^{N}|r_i|^2}_{N} - \underbrace{\sum_{i=1}^{N}|s_i(\mathbf{p})|^2}_{N} + 2\sum_{i=1}^{N}\Re\{r_i s_i^*(\mathbf{p})\}\right\} \\ &= \underset{\mathbf{p}}{\operatorname{argmax}} \sum_{i=1}^{N}\Re\left\{e^{j(\varphi_i - \phi_i(\mathbf{p}))}\right\} = \underset{\mathbf{p}}{\operatorname{argmax}} \sum_{i=1}^{N}\cos(\varphi_i - \phi_i(\mathbf{p}))\,. \end{aligned} \tag{2.15}$$

Note that, according to (2.15), all the N phase measurements have the same weight in the formula. This derives from the assumption that we considered received signals with constant amplitude, so it is equivalent to consider the same signal-to-noise ratio (SNR) for all the N phase measurements.

2.3.2 ML Estimator with Variable Amplitudes

In this second case we consider a model more similar to the reality. Here each phase value measured is related to the received power at the position from witch it was taken. So the model of the system shown in 2.8 changes into:

$$\mathbf{r} = [r_1\, r_2\, \ldots\, r_N]^{\mathrm{T}} = \left[\tilde{a}_1 e^{j\varphi_1}\, \tilde{a}_2 e^{j\varphi_2}\, \ldots\, \tilde{a}_N e^{j\varphi_N}\right]^{\mathrm{T}} = \mathbf{s} + \mathbf{n} \tag{2.16}$$

where

$$\mathbf{s} = [s_1(\mathbf{p}, a_1)\, s_2(\mathbf{p}, a_2)\, \ldots\, s_N(\mathbf{p}, a_N)]^{\mathrm{T}} = \left[a_1 e^{j\phi_1(\mathbf{p})}\, a_2 e^{j\phi_2(\mathbf{p})}\, \ldots\, a_N e^{j\phi_N(\mathbf{p})}\right]^{\mathrm{T}} \tag{2.17}$$

The amplitude value a_i related to the i-th reader positions is considered as deterministic unknown parameter, not correlated to the tag position $\mathbf{p}$ because the RSS is not a good position-related parameter. The amplitude $\tilde{a}_i$ represents the square root of the received power reported by the reader in the ith measurement.

The likelihood function of the ith observation given $\mathbf{p}$ and a_i in this model can be written as:

$$\begin{aligned} f(r_i|\mathbf{p}, a_i) &= \frac{1}{\sqrt{2\pi\sigma^2}} \exp\left\{-\frac{|r_i - s_i(\mathbf{p}, a_i)|^2}{2\sigma^2}\right\} \\ &= \frac{1}{\sqrt{2\pi\sigma^2}} \exp\left\{-\frac{|r_i|^2 + |s_i(\mathbf{p}, a_i)|^2 - 2\Re\{r_i s_i^*(\mathbf{p}, a_i)\}}{2\sigma^2}\right\} \\ &= \frac{1}{\sqrt{2\pi\sigma^2}} \exp\left\{-\frac{\tilde{a}_i^2 + a_i^2 - 2\tilde{a}_i a_i \cos(\varphi_i - \phi_i(\mathbf{p}))}{2\sigma^2}\right\}. \end{aligned} \tag{2.18}$$

It is possible to determine the likelihood function independent of a_i using an estimate $\hat{a}_i$ of a_i into (2.18), which becomes

$$f(r_i|\mathbf{p}) = f(r_i|\mathbf{p}, a_i = \hat{a}_i)\,. \tag{2.19}$$

Using the maximum likelihood (ML) criterion the estimated $\hat{a}_i$ is

$$\hat{a}_i = \underset{a_i}{\operatorname{argmax}} \ln f(\mathbf{r}|\mathbf{p}, a_i) = \underset{a_i}{\operatorname{argmax}} \{-a_i^2 + 2\tilde{a}_i a_i \cos(\varphi_i - \phi_i(\mathbf{p}))\}\,. \tag{2.20}$$

According to

$$\hat{a}_i = a_i : \frac{\partial}{\partial a_i} f(r_i|\mathbf{p}, a_i) = 0 \tag{2.21}$$

we obtaine

$$\hat{a}_i = \tilde{a}_i \cos\left(\varphi_i - \phi_i(\mathbf{p})\right) \tag{2.22}$$

and the likelihood function of the ith observation becomes

$$f(r_i|\mathbf{p}) = \frac{1}{\sqrt{2\pi\sigma^2}} \exp\left\{-\frac{\tilde{a}_i^2 - \tilde{a}_i^2 \cos^2(\varphi_i - \phi_i(\mathbf{p}))}{2\sigma^2}\right\}. \tag{2.23}$$

Finally, the maximum likelihood estimate $\hat{\mathbf{p}}$ of the tag position $\mathbf{p}$ is

$$\hat{\mathbf{p}} = \underset{\mathbf{p}}{\operatorname{argmax}} \ln f(\mathbf{r}|\mathbf{p}) = \underset{\mathbf{p}}{\operatorname{argmax}} \sum_{i=1}^{N} \tilde{a}_i^2 \cos^2(\varphi_i - \phi_i(\mathbf{p}))\,. \tag{2.24}$$

where $\tilde{a}_i^2$ is the received power of the signal given by the reader. In this maximum likelihood estimator the phase values received with a higher power have a greater impact on the function and on the position estimation. Comparing (2.24) to (2.15) we note that in (2.24) more reliable phase measurements (higher $\tilde{a}_i^2$) have a higher weight in the localization process with respect to (2.15).

2.4 Holographic Localization Method

In literature another algorithm is present, called holographic localization method [33]. The principle is the same as previous approach i.e., the relationship between phase values, antenna position and target position is unique if a sufficient number of measurements was taken. This means that a set of N phase measurements and a known reader trajectory identify only one possible tag position.

According to this method the algorithm makes K hypothesis, where $K \gg N$, representing K different possible tag's position. For each hypothesis with coordinates (x_i,y_i) it calculates the distance between it and the position where the reader takes the phase measures (x_m, y_m). Through the value of the distance it derives the phase vector containing the phase values that can be read in the N measurement positions of the reader if it will be the correct coordinates of the tag. For each hypothesis phase vector the algorithm

computes a sort of correlation with the phase measurements vector by:

$$P(\mathbf{p}) = \left| \sum_{m=1}^{N} \tilde{a}_m e^{j\left(\frac{4\pi d_{m,i}}{\lambda_c} - \varphi_m\right)} \right| = \left| \sum_{m=1}^{N} \tilde{a}_m e^{j(-\phi_m - \varphi_m)} \right| \tag{2.25}$$

where $P(\mathbf{p})$ is the correlation function, $d_{m,i}$ is the distance between the current hypothesis and the antenna position m, a_m is the amplitude measured at the antenna position m, λ_c is the carrier wavelength and φ_m is the phase measured at the antenna position m. The hypothesis that maximizes the function (2.25) is the detected position of the tag.

This method is very similar to approaches that calculate the AOA from phase difference of arrival from different positions and calculate the triangulation to find the tag position [34]. This formula is not the rigorous maximum likelihood estimator, but at high SNR where the phase estimation errors are small, holographic localization performance should be very similar to ML derived in (2.24). In fact,

$$\begin{aligned}
\hat{\mathbf{p}} &= \underset{\mathbf{p}}{\operatorname{argmax}} \left| \sum_{m=1}^{N} \tilde{a}_m e^{j(-\phi_m(\mathbf{p}) - \varphi_m)} \right| = \\
&= \underset{\mathbf{p}}{\operatorname{argmax}} \sqrt{\left(\sum_{m=1}^{N} \tilde{a}_m \cos(-\phi_m(\mathbf{p}) - \varphi_m) \right)^2 + \left(\sum_{m=1}^{N} \tilde{a}_m \sin(-\phi_m(\mathbf{p}) - \varphi_m) \right)^2} \\
&= \underset{\mathbf{p}}{\operatorname{argmax}}\ \tilde{a}_m \sqrt{\left(\sum_{m=1}^{N} \cos(-\phi_m(\mathbf{p}) - \varphi_m) \right)^2 + \left(\sum_{m=1}^{N} \sin(-\phi_m(\mathbf{p}) - \varphi_m) \right)^2}
\end{aligned} \tag{2.26}$$

At high SNR, $\sin(-\phi_m(\mathbf{p}) - \varphi_m) \approx 0$ so

$$\hat{\mathbf{p}} \approx \underset{\mathbf{p}}{\operatorname{argmax}} \left(\tilde{a}_m (\cos(-\phi_m(\mathbf{p}) - \varphi_m))^2 \right) \tag{2.27}$$

where $\tilde{a}_m$ is the power received at the m-th antenna positions, φ_m is the phase measured at the m-th antenna positions and $\phi_m(\mathbf{p})$ is the theoretical phase.

Chapter 3

Simulation Results

In this chapter the performance of the localization system are reported through Matlab simulations.

The algorithm used in the simulations is explained in Sec. 2.4.

3.1 Monodimensional Algorithm

For simulating this system in Matlab we made a series of assumptions in order to decrease the computational complexity and understand how several features of the environment and the technology can impact the performance. The assumptions are:

- the tag is fix in a position with coordinates $\mathbf{p} = (x, y)$;
- the reader is moving along a linear trajectory with constant speed;
- the distance between the tag and the reader's trajectory (y) is known, so it transforms the problem in monodimensional localization where the only unknown variable is the longitudinal coordinate (x).

These hypotheses permit to have a faster simulation and a lower complexity than the 2D case [33]. The complexity becomes:

$$N_{\text{calculation}} \sim K N_{\text{antennas}} \tag{3.1}$$

where K is the number of hypothesis along the x-coordinate and N_{antennas} are the number of phase measures that the reader took. In the following

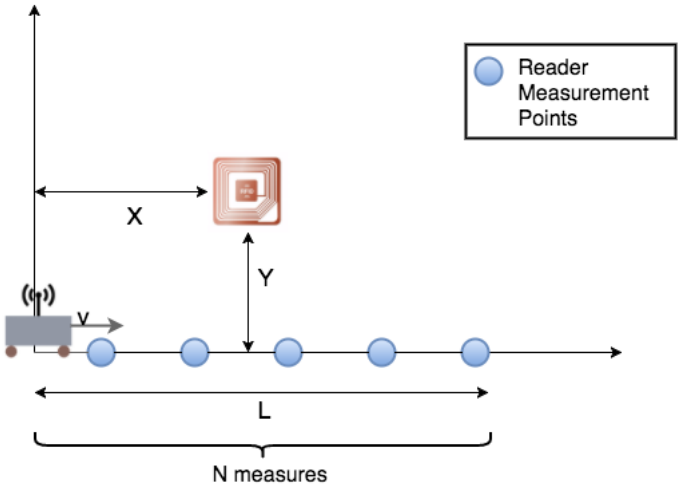

Figure 3.1: Monodimensional localization scheme.

simulations we implemented the holographic localization method explained in Sec. 2.4. The equation (2.25) in a monodimensional localization problem becomes:

$$P(x) = \left| \sum_{m=1}^{N} e^{j\left(\frac{4\pi d_{m,i}}{\lambda_c} - \varphi_m\right)} \right| \tag{3.2}$$

3.1.1 Uniformly Spaced Measure Positions

The first topology that we investigated is a simple system formed by a reader moving along a linear trajectory L with constant speed. It interrogates the tag N times uniformly spaced along the track. The tag position is fixed in $x = \frac{L}{2}$, $y = 1m$ for all different cases that we simulated. In these cases we plot how the RMSE of the detected position and the ratio between the first and the second peak of $P(x)$ change using different values of N or L. Also we consider a Gaussian noise with several variances added to the phase measures. Each simulation is implemented in Matlab through a Monte Carlo approach. Then,

$$\varphi_m = \phi_m + n \tag{3.3}$$

where φ_m is the phase measured, ϕ_m is the theoretical phase without any noise, n is the additive Gaussian noise $\mathcal{N}(0, \sigma^2)$. First of all we derive the RMSE of the detected position when the number of phase measures N

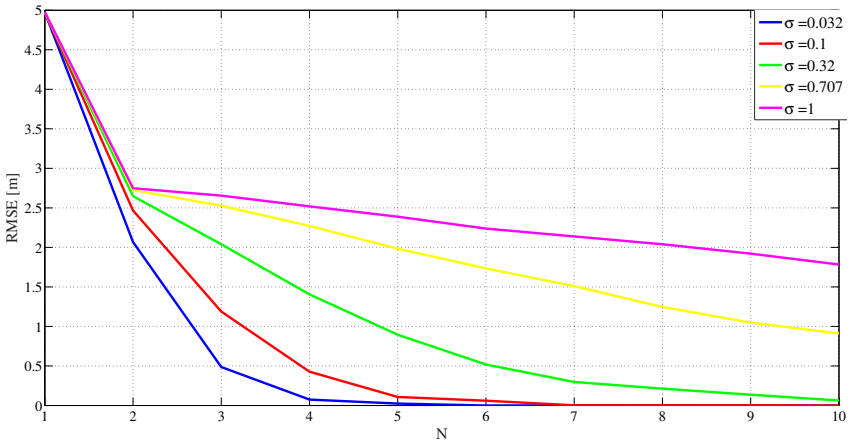

Figure 3.2: RMSE as a function of the number of phase measure N for several noise variances. Monte Carlo simulation with 10000 iterations and $L = 10$.

increase with the length of the trajectory L constant and the opposite case i.e., when N is constant and the length L changes.

From Figure 3.2 is it possible to see that increasing the number of phase measurements for several values of variance of the phase noise, the RMSE decreases. Instead we have an increase of the RMSE when the number N is constant and the length of the trajectory increases (see Figure 3.3).

The same simulation shown in Figure 3.2 is executed monitoring the ratio between the first and the second peak of $P(x)$, showing how the system is strong to the phase noise. It is right to think that increasing the number of phase measures the ratio decreases. In Figure 3.4 this trend is confirmed but growing N the advantage is limited. The curves has a sort of asymptote proving that the amplitude difference between the first and the second peak do not improve beyond a certain value of N. Given the effects on the RMSE or the ratio between the first and the second peak of N or L while the other variable is constant, it is interesting to see how N and L interact each other. To do that, we implemented the same simulations done before looking at the evolution of the functions as the ratio N/L increases. It is rational to suppose that the RMSE tends to 0 for high value of N/L, because it means collect a high number of phase measures for distance unit. Instead, the ratio between the first and the second peak of $P(x)$ has an asymptotic trend like in Figure 3.4. The simulations results are shown in Figure 3.5 and

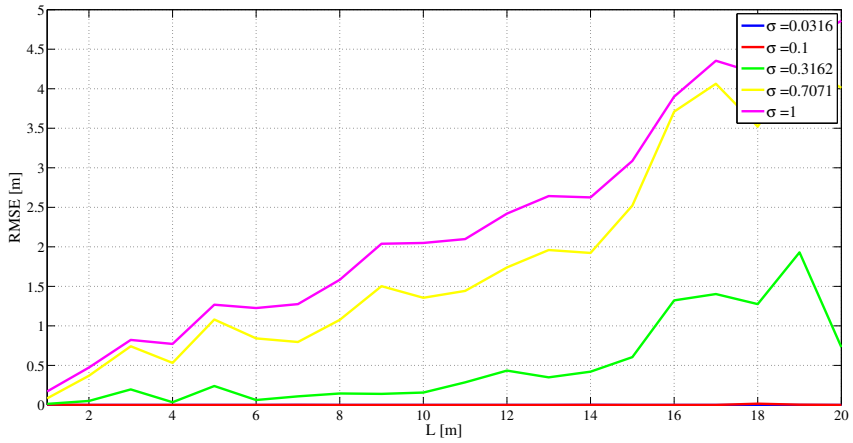

Figure 3.3: RMSE as a function of the length L of the reader's trajectory for several noise variances. Monte Carlo simulation with 10000 iterations and $N = 5$.

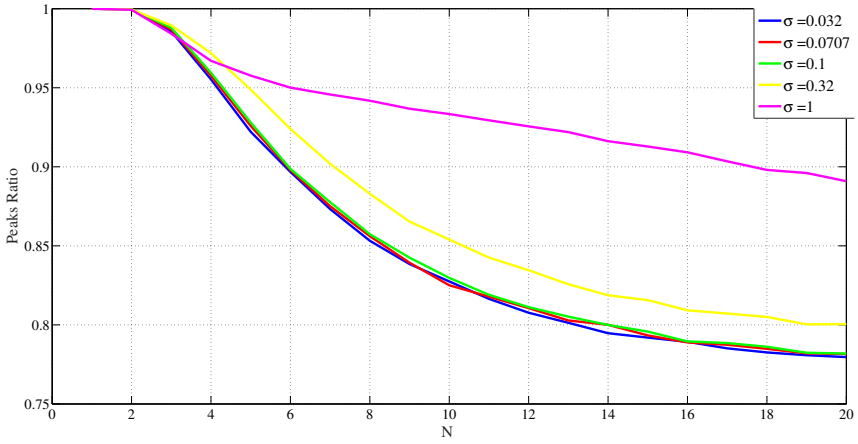

Figure 3.4: Ratio between the first and the second peak of $P(x)$ as a function of the number of phase measure N for several noise variances. Monte Carlo simulation with 5000 iterations and L=10.

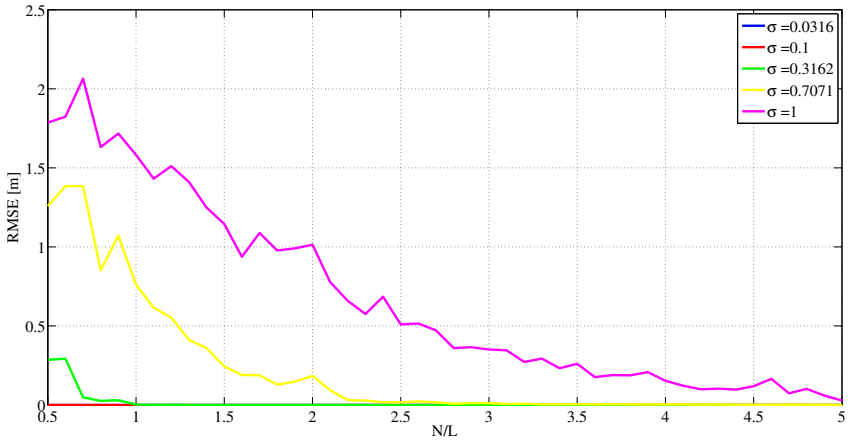

Figure 3.5: RMSE as a function of the ratio N/L of the reader's trajectory for several noise variances. Monte Carlo simulation with 10000 iterations.

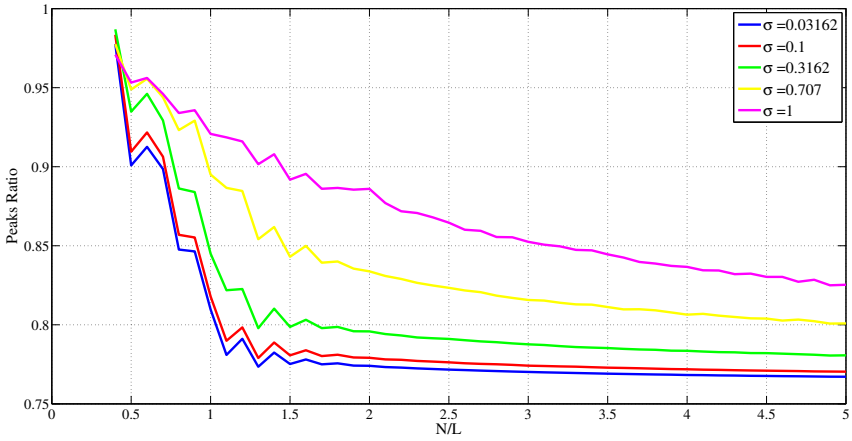

Figure 3.6: Ratio between the first and the second peak of $P(x)$as a function of the ratio N/L for several noise variances. Monte Carlo simulation with 10000 iterations.

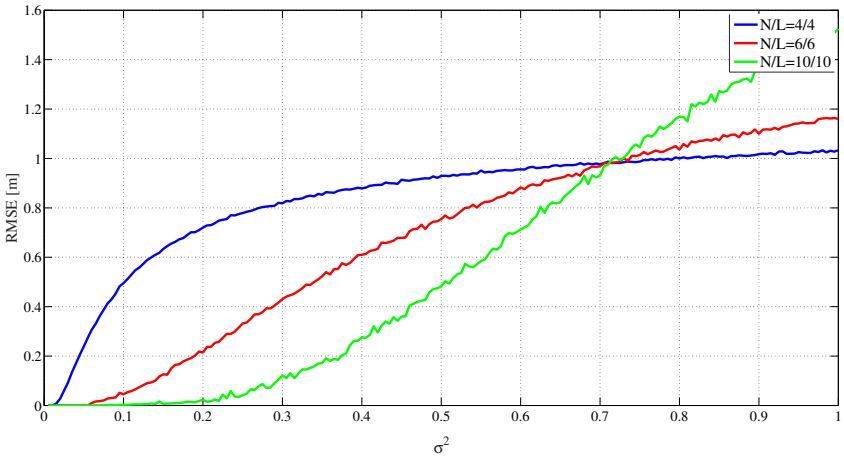

Figure 3.7: RMSE as a function of the noise power for several N/L. Monte Carlo simulation with 20000 iterations.

Figure 3.6. The last simulation compared the same ratio N/L, equals to 1, with different values of N equals to L. The result shown in Figure 3.7 is very interesting. For low noise power is advantageous to use an high number of phase measurements evenly spaced in a long trajectory. Instead, using a short track is better for an higher value of noise power. Also the curves seem to have a common point.

3.1.2 Random Measure Points

The next environment simulated has only one difference from the previous: the measurement points are no more equally distributed along the trajectory but are random placed. For each Monte Carlo iteration a vector containing the coordinates of the phase measure points is random generated. The trend of the following simulations is very similar to the previous case, where the measure points are equally spaced, but the performance is a little bit worse. In Figure 3.13 we can see that the advantage found in the case of uniformly spaced measure points, here is lower; only for very low noise power it is advantageous to use a high number of phase measurements. In general the performance in random measure positions is worse with respect to the previous case. To prove it, we simulated both situations in the same picture for two fix values of phase noise standard deviations: 0.1 and 0.707 (see Fig-

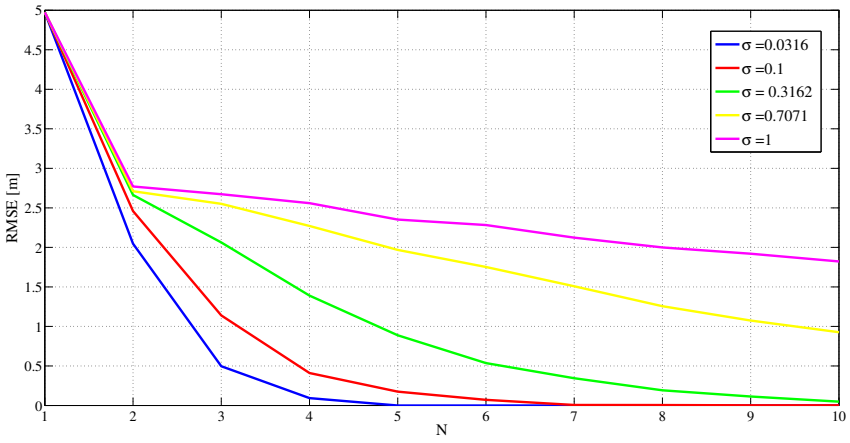

Figure 3.8: RMSE as a function of the number of phase measure N for several noise variances and random measurement positions. Monte Carlo simulation with 10000 iterations and $L = 10$.

ure 3.14 and Figure 3.15).
Simulations of random measure position are from Figure 3.8 to Figure 3.15.

3.1.3 Reader Position with Noise

After having shown the effect of the phase noise on the localisation process we decided to study how the noise on the information about the position of the reader influences the correct localisation of the tag. Supposed to have exact phase measures, so without any uncertainty, we added to each position of the reader an additive Gaussian noise $\mathcal{N}(0, \sigma_s^2)$; where $\sigma_s^2 = [0.00001, 0.00005, 0.0001, 0.0005, 0.001]$.

$$x_i = \tilde{x}_i + n_s \tag{3.4}$$

where $\tilde{x}_i$ is the ith true position of the reader when performs the ith phase measure, x_i is the ith position of the reader with noise and n_s is the noise sample belonging to $\mathcal{N}(0, \sigma_s^2)$. Figure 3.16 and Figure 3.17 shows, respectively, the ratio between the first and the second peak of $P(x)$ and the RMSE. The trends of these figure of merit are very similar to the curves of the previous simulations, where there was noise on the phase measurements. From Figure 3.16 it can be seen that by increasing the number of measure points

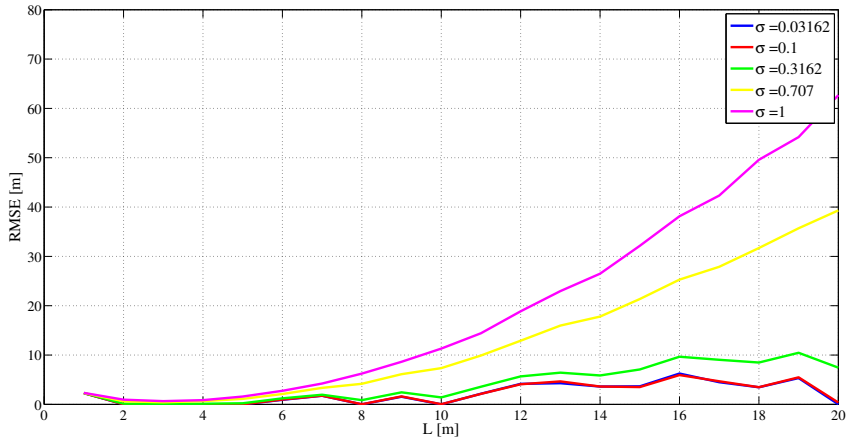

Figure 3.9: RMSE of the detected position as a function of the length L of the reader's trajectory for several noise variances and random measurement positions. Monte Carlo simulation with 5000 iterations and $N = 5$.

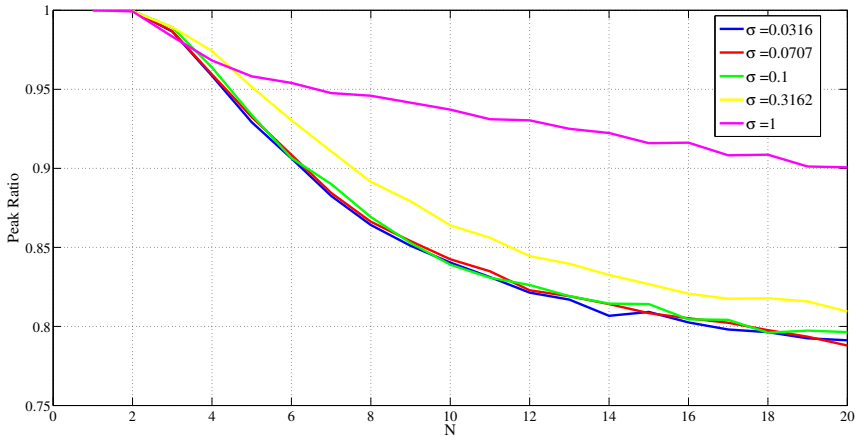

Figure 3.10: Ratio between the first and the second peak of $P(x)$as a function of the number of phase measure N for several noise variances and random measurement positions. Monte Carlo simulation with 5000 iterations and $L = 10$.

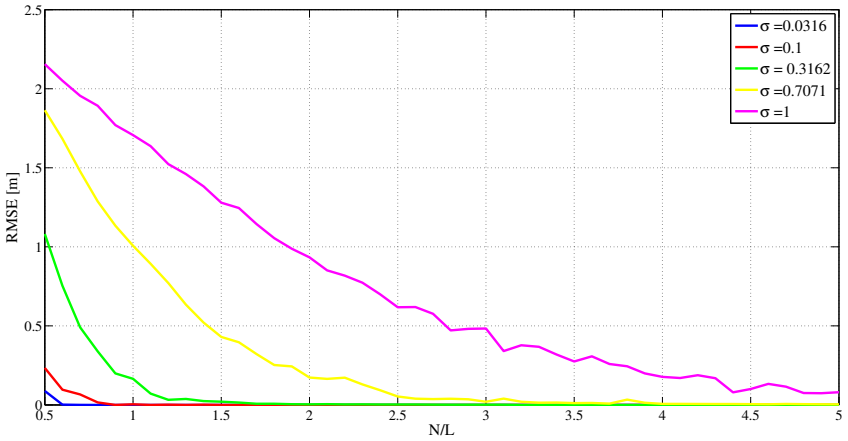

Figure 3.11: RMSE of the detected position as a function of the ratio N/L of the reader's trajectory for several noise variances and random measurement positions. Monte Carlo simulation with 5000 iterations.

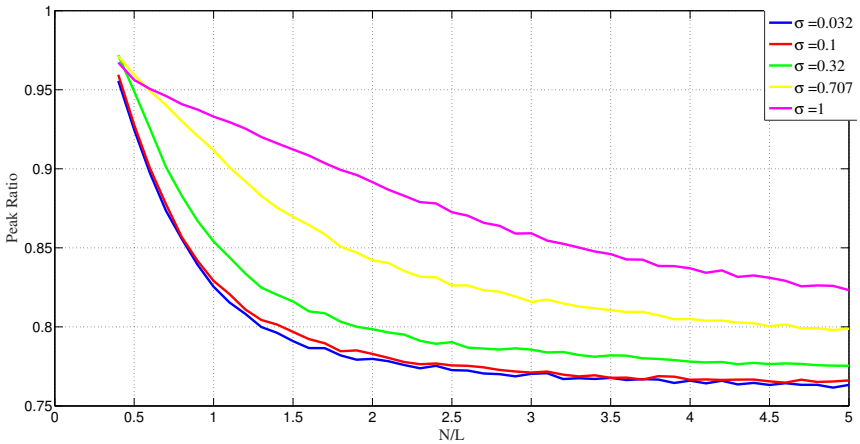

Figure 3.12: Ratio between the first and the second peak of $P(x)$as a function of the ratio N/L for several noise variances and random measurement positions. Monte Carlo simulation with 5000 iterations.

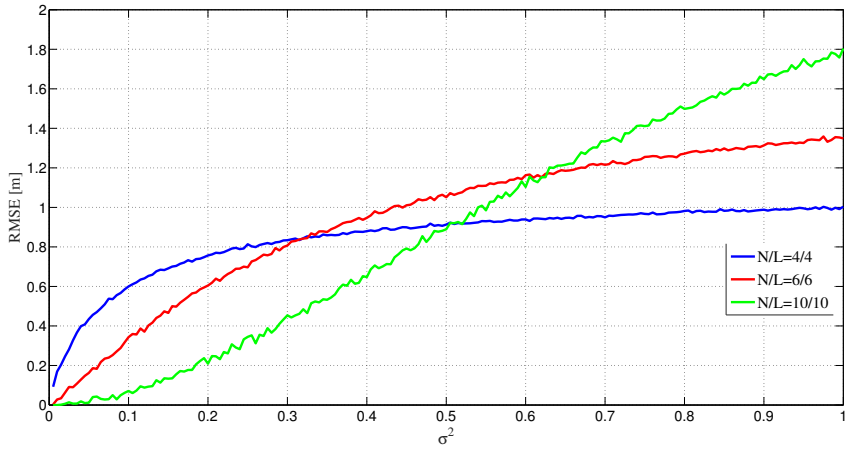

Figure 3.13: RMSE of the detected position as a function of the noise variance for several N/L. Monte Carlo simulation with 20000 iterations.

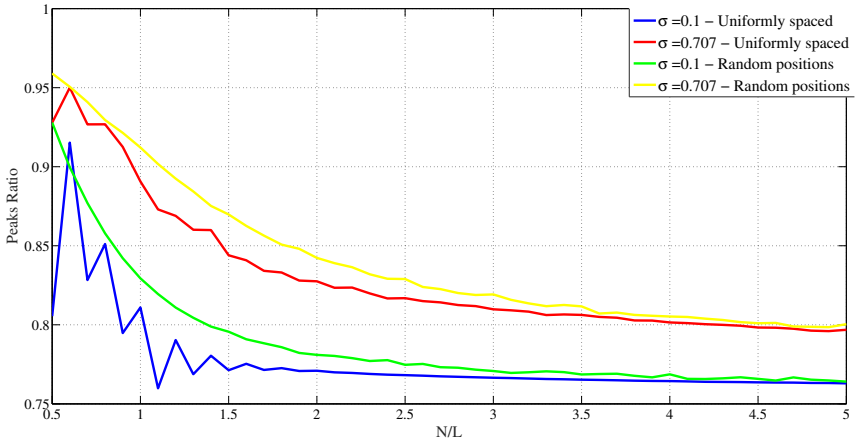

Figure 3.14: Ratio between the first and the second peak of $P(x)$as a function of the ratio N/L for several noise standard deviations. Monte Carlo simulation with 10000 iterations.

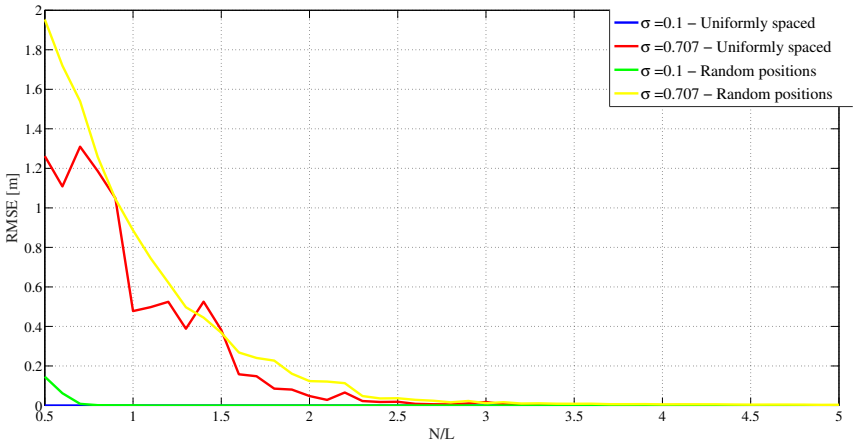

Figure 3.15: RMSE of the detected position as a function of the ratio N/L. Monte Carlo simulation with 10000 iterations.

N the ratio between the first and the second peak decreases and it tend to have an asymptotic behaviour. In Figure 3.17 the RMSE decreases when the ratio N/L raises. The only big difference with the previous cases is the magnitude of the noise variances. In order to have a very good localisation of the tag it is important to know the relative position of the reader with a small error.

Summarizing:

- the largest is the number of phase measurements N, the better is the localization result;
- the longer is the trajectory L, the larger N is necessary for a good results;
- the noise on the position is more degrading with respect to the phase noise.

3.1.4 Relative Position Localization

Imagine an environment, similar to a storage room or a store, where the objective is to know not the absolute position of several products equipped with a RFID tag in the space but the relative positions related to a reference tag

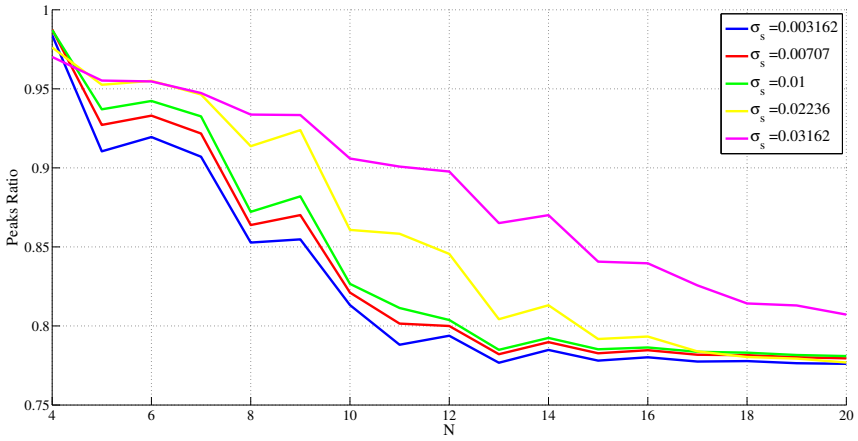

Figure 3.16: Ratio between the first and the second peak of $P(x)$as a function of N for several standard deviations of the position noise with noise in the reader trajectory. Monte Carlo simulation with 5000 iterations.

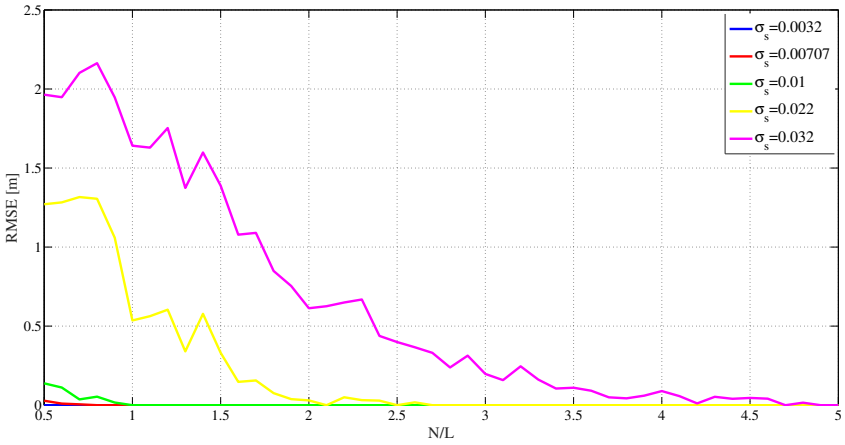

Figure 3.17: RMSE as a function of the ratio N/L with noise in the reader trajectory. Monte Carlo simulation with 5000 iterations.

with known location. This tag can be positioned on a shelving or in other place. It has been found that, if the reader position errors are independent, locating the reference tag and the tag with unknown position separately, using the algorithm explained before, and then derive the unknown tag position through the error on the first device is not useful. Supposing that the moving reader is equipped with high precision odometers or something similar, it is correct to think that the position error between consecutive locations is negligible for a small trajectory. Only on the starting point of the track a significant error is present. In the simulation program we added the same single sample of position noise to all reader locations. The noise trajectory is a shifted version of the original.

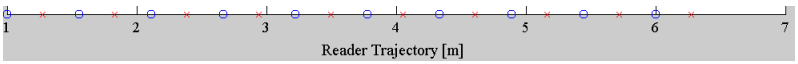

Figure 3.18: Example of reader trajectory: 'o' are the real measurement points of the reader, 'x' are the points with noise.

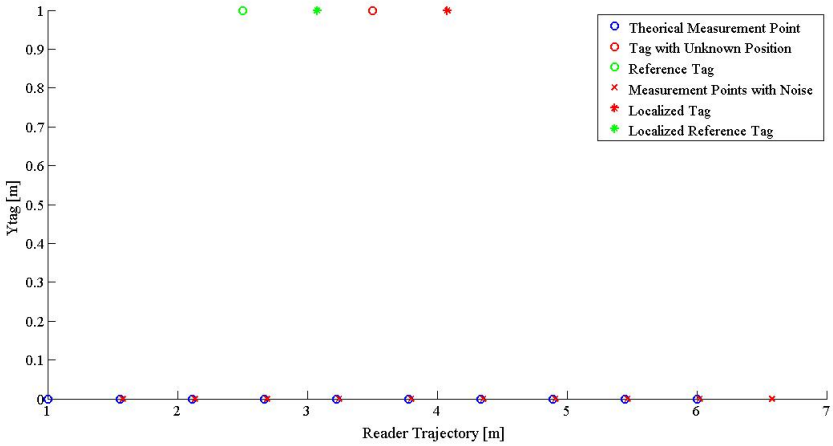

Figure 3.19: Example of localization with tag reference.

Through this assumption the error on the reference tag is equal to the error on tag with unknown position. Knowing the real location of the reference tag it is possible localize the other tag with no uncertainty. To understand the performance of the system and verify that the localization errors of both tags are equal, we simulated this case for several noise variance through a

Monte Carlo simulation where we counted the number of times that localization errors were different each other. The result is an empty histogram for all variance used. This means, under the assumption done before, that always the error on the localized position of the reference tag is equal to the error of the other device with unknown position; so the latter can be localized with precision.

3.1.5 Not Central Tag Position

In previous simulations a strong assumption was that the x-coordinate of the tag was positioned in the middle of the trajectory. The geometry of the system influences the locating process result, so we decided to investigate about the impact of the relative tag position with respect to the reader trajectory. To do that we implemented a simulation where the tag is located in a fixed position and the linear trajectory, with length fixed to L, is moved adding an offset factor, called Δ. When Δ is equal to 0 means that the trajectory is centered with respect to the tag i.e., reader measurement positions are between $-\frac{L}{2}$ and $\frac{L}{2}$. Adding or subtracting a Δ factor to all reader measure positions means move the reader trajectory on the right or on the left with respect to the tag location. For each value of Δ factor we calculated the RMSE using the same position noise samples.

Looking at Figure 3.20, it is possible see that the RMSE modifies its value as the Δ factor changes. In particular the RMSE has zero value when the trajectory is opposite to the tag position and it increases when the trajectory moves from it. Figure 3.21 shows the same simulation but without position noise; in this situation the position of the trajectory with respect to the tag does not influence the localization process result.

3.1.6 Signal-to-Noise Ratio Simulation

The previous simulations considered the phase noise independently to the SNR at the considered reader position. In the following simulation we decided to test the algorithm generating the noise samples with variance according to the effective reader position.

First of all we have extrapolated experimentally the signal to noise ratio at the distance of 1 meter (SNR_0) using the real hardware setup available

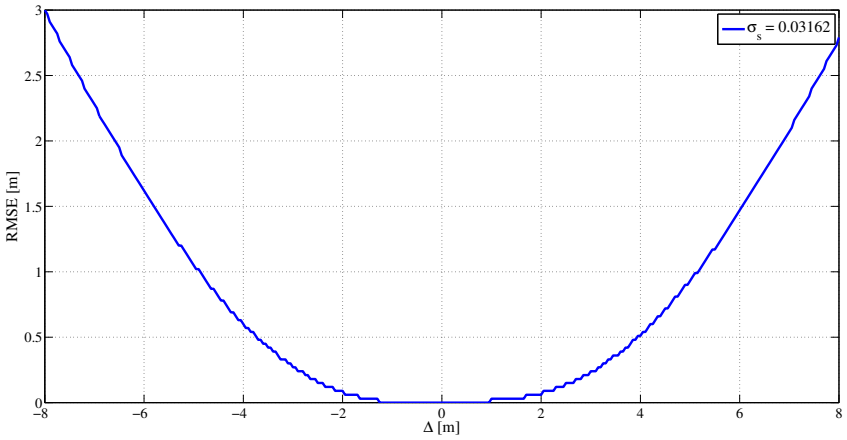

Figure 3.20: RMSE when the relative trajectory position with respect to the tag changes in presence of position noise ($L = 2, N = 21$).

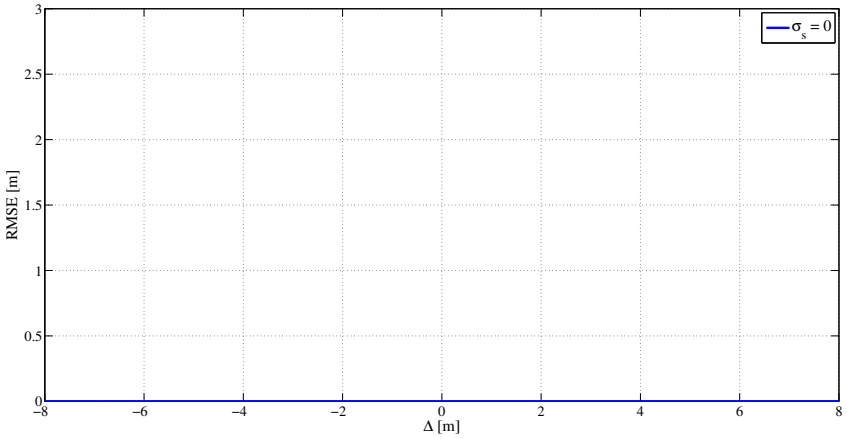

Figure 3.21: RMSE when the relative trajectory position with respect to the tag changes without position noise ($L = 2, N = 21$).

in laboratory (see section 4.2).

$$SNR = SNR_0\, d^{-4} \tag{3.5}$$

Then using the formula (3.5) we calculated the SNR at each reader position distant d from the tag. Now, using the Cramer-Rao Lower Bound

(CRLB) for phase estimation [35] we computed the noise variance as

$$\mathrm{var}(\hat{\varphi}) = \frac{1}{K\,SNR} \tag{3.6}$$

where K is the number of samples of the received signal (we considered $K = 100$ and $K = 1000$).

Thanks to this evaluation, we discovered that the RMSE as function of the number of phase measurements N or the length of the trajectory L is very low. It means that with our hardware the phase noise does not affect significantly the estimation process, so it can be neglected. The factor that most influence the estimation of the tag position is the error on the reader trajectory.

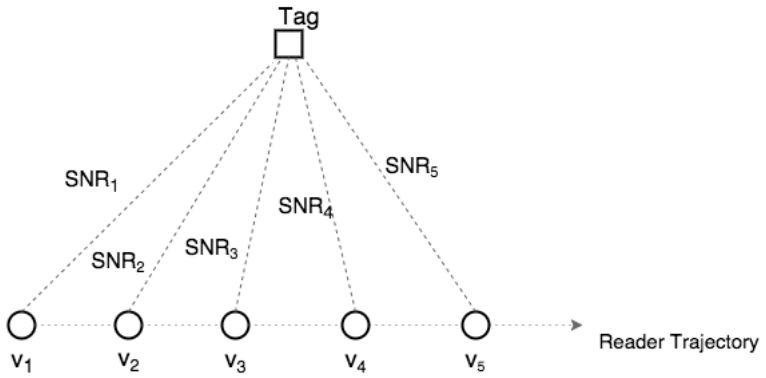

Figure 3.22: Scheme representing the SNR received at different reader positions **v**.

3.1.7 Comparison with ML Criterion

Previous simulations used the monodimensional algorithm deriving from equation (2.25). In this section we compare the performance of this algorithm and the localization using the ML criterion deriving from (2.15). In Figure 3.24 it is shown the ratio between the first and the second peak of $P(x)$ as function of the number of measure points N for several position noise variances. The algorithm that uses the equation (2.25) tends to have the amplitude of secondary lobes very similar to the amplitude of the main peak for high value of noise variance than the localization performed using the

ML criterion. Amplitude of secondary lobes comparable to the main peak can create an ambiguity problem i.e., a secondary lobe can be choosen as estimated position generating a high estimation error. A sharper main peak indicates an estimation with a high accuracy. Using a smaller noise variance both algorithms have a similar peak ratio. Figure 3.23 shows the comparison between the correlation function given by the two algorithms for a specific system configuration.

Figure 3.25 shows the RMSE of the localization result as function of N for several position noise variance. For a small position noise variance and few reader measurements the RMSE results lower using the ML criterion. With a higher noise variance the algorithms seems to have the same performance.

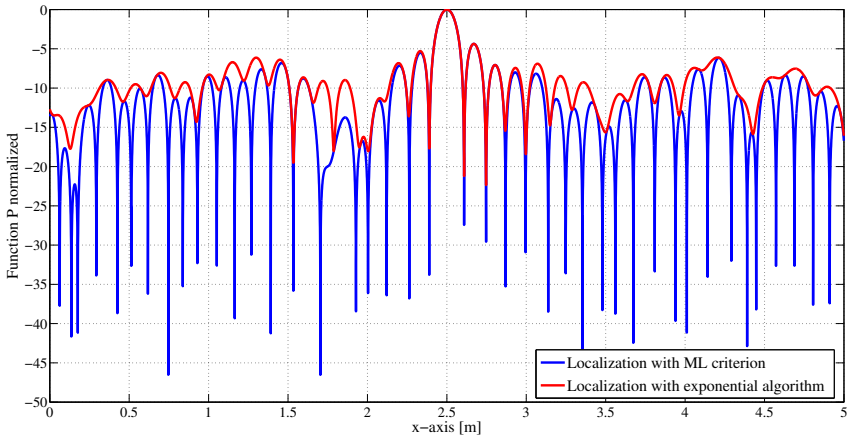

Figure 3.23: Comparison between the correlation functions given by the two algorithms in the same configuration (N=30, L=5 and noise on the reader positions). True tag position x =2.5 m.

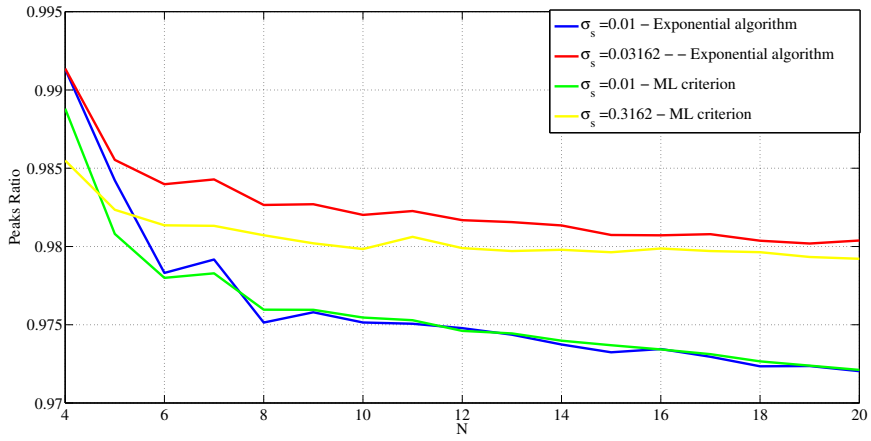

Figure 3.24: Ratio between the first and the second peak of $P(x)$ as a function of the ratio N for several noise standard deviations. Monte Carlo simulation with 10000 iterations.

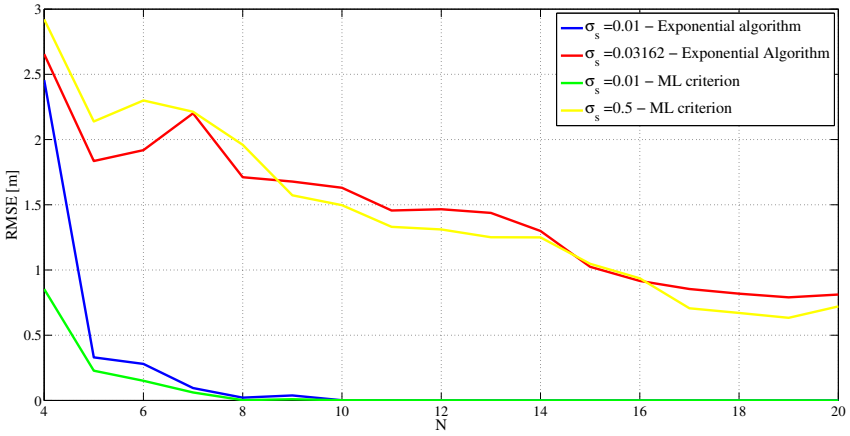

Figure 3.25: RMSE of the detected position as a function of N. Monte Carlo simulation with 10000 iterations.

Chapter 4

Measurement Setup

4.1 Hardware and Software

4.1.1 Reader

The reader used in this research is the Impinj Speedway Revolution R420 shown in Figure 4.1. It is a high performance reader, compatible with EPC-global UHF Gen 2 standard, that provides network connectivity between tag and enterprise software; it is able to maintain high read rates regardless of RF noise or interference as the readers adapt automatically for optimal functionality [36].

The main features of this model are:

- **Low power consumption**: it is capable of using Power over Ethernet (PoE);
- **Compact form factor and robust design**: the compact size permits an easier installation in tight space;
- **High Performance Features**: it has several utilities making possible to read more than 1000 tags per second.

Other characteristics are shown in Table 4.1. Let us note that it has 4 port but, through hubs, it is possible connect 32 antennas. Furthermore, the output power from each port can be set from +10 dBm to +30 dBm with POE power or to +32.5 dBm with an external DC power. The sensitivity of the reader is -82 dBm. In the front panel of the reader, shown in Figure 4.2, it

Figure 4.1: Impinj Speedway Revolution R420 [36].

is possible to see the 4 antenna connectors and the related led, indicating the work status of each port. In the rear panel there are: an ethernet connector and a RS-232 connector used as data interfaces, the power source connector for external power supply and an USB connector for future use.

4.1.2 EPC Radio-Frequency Identity Protocols Class-1 Generation-2 UHF RFID

The EPC protocol [38] defines the physical and logical requirements for an RFID system of interrogators and passive tags, operating in the 860 MHz - 960 MHz UHF range. The system comprises *interrogators*, also known as *readers*, and *tags*, also known as *labels*. The reader transmits information to a label by modulating an RF signal. Tags receive information and power energy from this signal; then they respond at the interrogation by modulating the reflection coefficient of their antennas, thereby backscattering an information signal to the reader. The communications are half-duplex, meaning that readers talk and labels listen, or vice-versa. The protocol specifies: the physical interactions between readers and tags, the operating procedure of interrogators and labels and the collision arbitration scheme used to identify

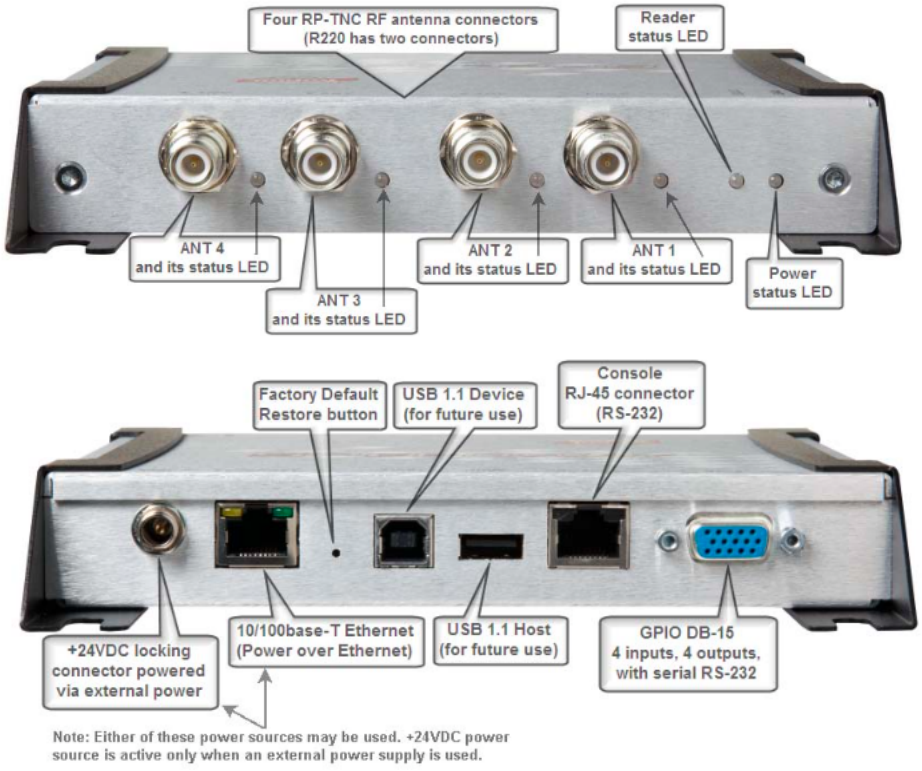

Figure 4.2: Front and rear panel of the reader Impinj Speedway Revolution R420 [36].

Table 4.1: Main features of Impinj Speedway Revolution R420 [37].

Product Details	Speedway R420
Air Interface Protocol	GS1/EPCglobal UHF Gen2 (ISO 18000-6C) or RAIN RFID
Antenna Ports	4 expandable to 32 antennas with Speedway Antenna Hub
Supported Regions or Geographies	FCC (TWYIPJREV), Canada (6324A-IPJREV), Australia, Brazil (Anatel), China (CMIT 2010DJ4065), EU (CE Mark, ETSI EN408 208 v1.4.1), Hong Kong, India, Japan (920MHz band), Korea (UQC-R420), Malaysia, New Zealand (Z233), Singapore, South Africa (ICASA), Taiwan (CCAF10LP1290T5), Thailand, Uruguay, UAE, Vietnam
Transmit Power	+10.0 to +31.5 dBm (PoE) (EU1 limited to +30 dBm), +10.0 to +32.5 dBm(Listed/Certified power supply)
Max Receive Sensitivity	-84 dBm
Min Return Loss	10 dB
Application Interfaces	Low Level Reader Protocol (LLRP): C, C++, Java, and C# libraries, OctaneSDK: Java or C#, On-reader Applications via Octane ETK: C, C++
Network Connectivity	10/100BASE-T auto-negotiate 802.1x with PEAP/TLS and MD5 support, WPA for Wifi and Ethernet, 3rd party Wifi adapters supported via USB interface. Speedway Connect: HID (keyboard) emulation, TCP Socket, Serial/RS-232, HTTP POST
Power Sources	Power over Ethernet (PoE) IEEE 802.3af, Listed/Certified power supply rated minimum 2.5A
Operating Temperature	-20 C to +50 C
Dimensions & Weight	7.5 in H x 6.9 in W x 1.2 in D (19 x 17.5 x 3 cm)

a specific tag in a environment full of different label.

The commands described in the protocol are divided into:

- **Mandatory commands**: Conforming tags and readers shall support all mandatory commands;
- **Optional commands**: Conforming tags or interrogators may or may not support optional commands;
- **Proprietary commands**: Proprietary commands may be enabled in conformance with this specification, but are not specified herein and shall be capable of being permanently disabled. Proprietary commands are intended for manufacturing purposes and shall not be used in field-deployed RFID systems;
- **Custom commands**: Custom commands may be enabled in conformance with this specification, but are not specified herein.

Concerning the tag-identification layer, an interrogator manages tag populations through three basic operations:

- **Select operation**: The operation of choosing a tag population for inventory and access;
- **Inventory operation**: The operation of identifying tags. A reader begins an inventory round by transmitting a query command in one of four sessions. One or more tags may reply. Inventory comprises multiple commands;
- **Access operation**: The operation of reading from and/or writing to a tag. An individual tag must be uniquely identified prior to access.

All commands, RF signal, modulations, and other technique available of this technology are explained in the protocol.

4.1.3 LLRP-Low Level Reader Protocol

The Low Level Reader Protocol (LLRP) [39], written by EPC in 2007, is the standard protocol used to standardize the network interface of the RFID

readers. It specifies an interface between RFID readers and clients and provides control of air protocol operation timing and access to air protocol command parameters. LLRP is situated between clients and readers and his purpose is to maximize the efficiency of operations and facilitates the management of the reader devices to mitigate reader-to-reader and reader-to-tag interference. Also it facilitates device status and error reporting.

The LLRP is specifically concerned with providing the procedures and formats of communications between devices. The data units are called messages. The messages from the client to the reader include configuration, managing and access operation of the reader. Message from the reader to the clients include the reporting of the tag read and the status of the device. It is an application layer protocol and do not permit re-transmission in case of communication errors.

A typical LLRP configurations and execution are:

- Capability discovery;
- Device configuration;
- Inventory and access operations setup;
- Inventory cycles executed;
- RF Survey operations executed;
- Reports to the Client.

Figure 4.4 shows a typical interactions between client, reader and tag.

4.1.4 FOSSTRACK LLRP Commander

In order to send and receive LLRP messages, configure and manage the reader we used the software FOSSTRACK LLRP Commander. It is a plugin with graphical interface working on Eclipse. The program permits to compose easily LLRP messages through a graphical interface or an XML editor or binary code. At the same time it makes possible to receive and view the messages and the reports from the reader.

The basic sequence of operations to read a tag is the following:

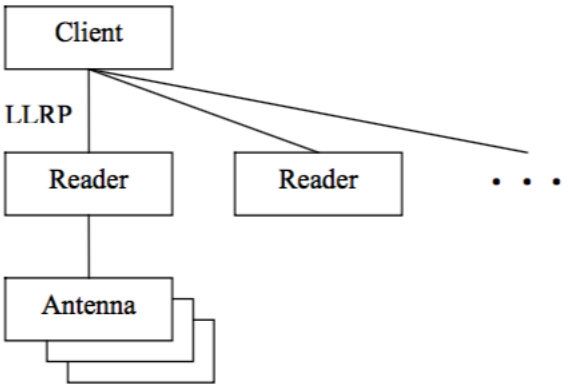

Figure 4.3: LLRP endpoints [39].

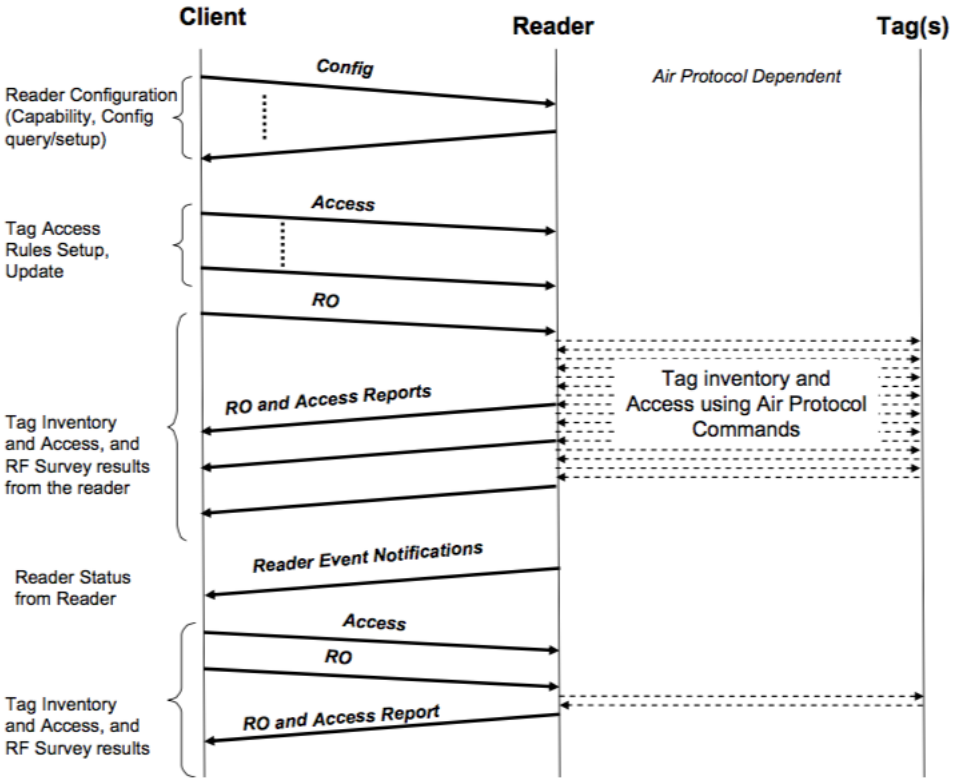

Figure 4.4: Tag-reader-client LLRP interaction [39].

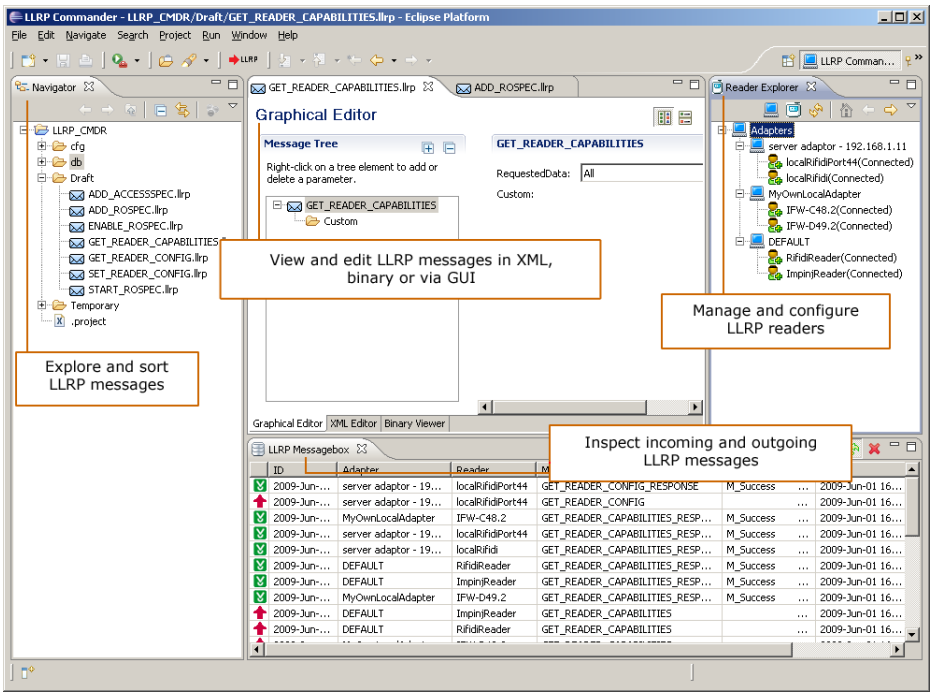

Figure 4.5: Fosstrack LLRP Commander interface [40].

- connect the reader;
- send the set reader configuration (SetReaderConfig) message;
- send the reader operation specification (add_ROSpec) message;
- send enable the reader operation specification (enable_ROSpec) message;
- read the receive operation access report message (RO_access_report) from the reader;
- send disable the reader operation specification (disable_ROSpec) message;
- send the delete reader operation specification (delete_ROSpec) message;
- close the connection.

Set Reader Configuration message (SetReaderConfig) sets the main configurations of the reader, like the antenna and the channel frequency used,

the output RF power and the sensibility of the receiver. Each Set Reader Configuration overwrites the previous set up.

Reader Operation Specification message (addROSpec) defines the behaviour of the reader. Through this message it is possible define most of the parameters used in the inventory process. In one reader can be set more than one Reader Operation Specification, each recognizable with his ROSpec ID, but only one can be active at the same time. Enable the Reader Operation Specification (enable_ROSpec) and Disable the Reader Operation Specification (disable_ROSpec) message enable and disable the relative ROSpec. The principal parameters set in SetReaderConfig message are:

- ROSpecStartTrigger: it describes the condition upon which the ROSpec will start execution;
- ROSpecStopTrigger: it describes the condition upon which the ROSpec will stop;
- AlSpecStopTrigger: it defines when the Inventory process ends;
- InventoryParameterSpec: this parameter defines the inventory operation to be performed at all antennas specified in the corresponding AISpec;
- AntennaConfiguration: this parameter carries a single antenna's configuration;
- ROReportSpec: this parameter describes the contents of the report sent by the reader and defines the events that cause the report to be sent.

Figure 4.6 and Figure 4.7 show respectively, the reader configuration and reader operation specification messages used. The phase of the signal received from the tag is not a standard parameter reported from the reader through LLRP report messages. Impinj provides vendor extensions that permit to obtain these measurements. After have enabled custom messages, it is possible to enable phase measurements adding an extension to our ROSpec message. An extension is described by:

- CustomParameterDefinition: it describes the name of the extension and the vendor identifier;

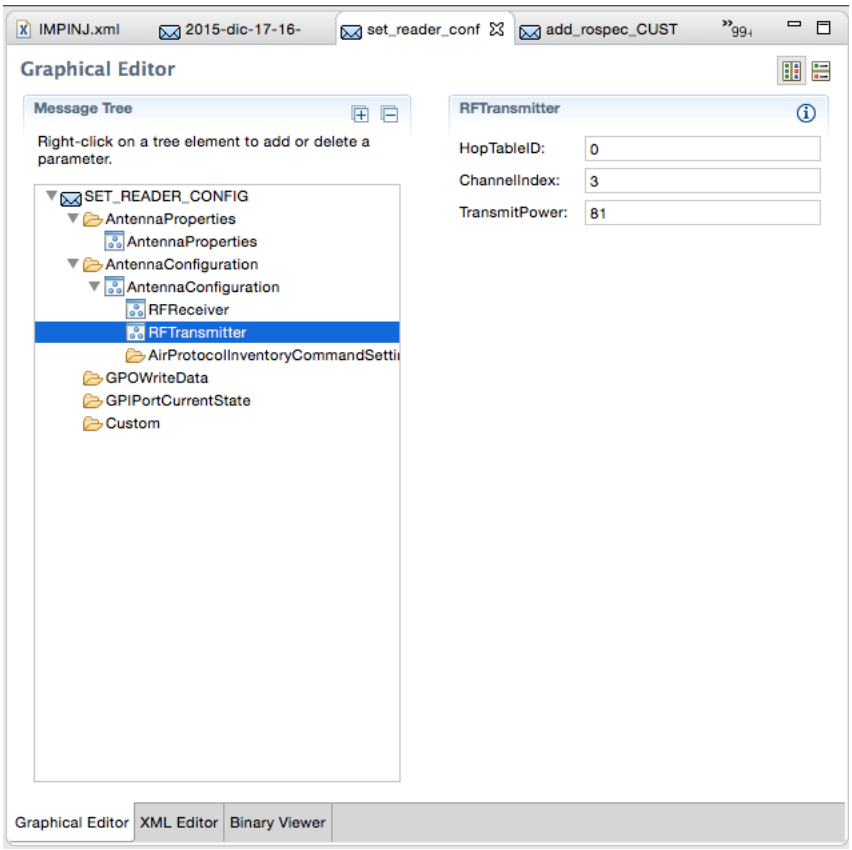

Figure 4.6: Set Reader Configuration message used.

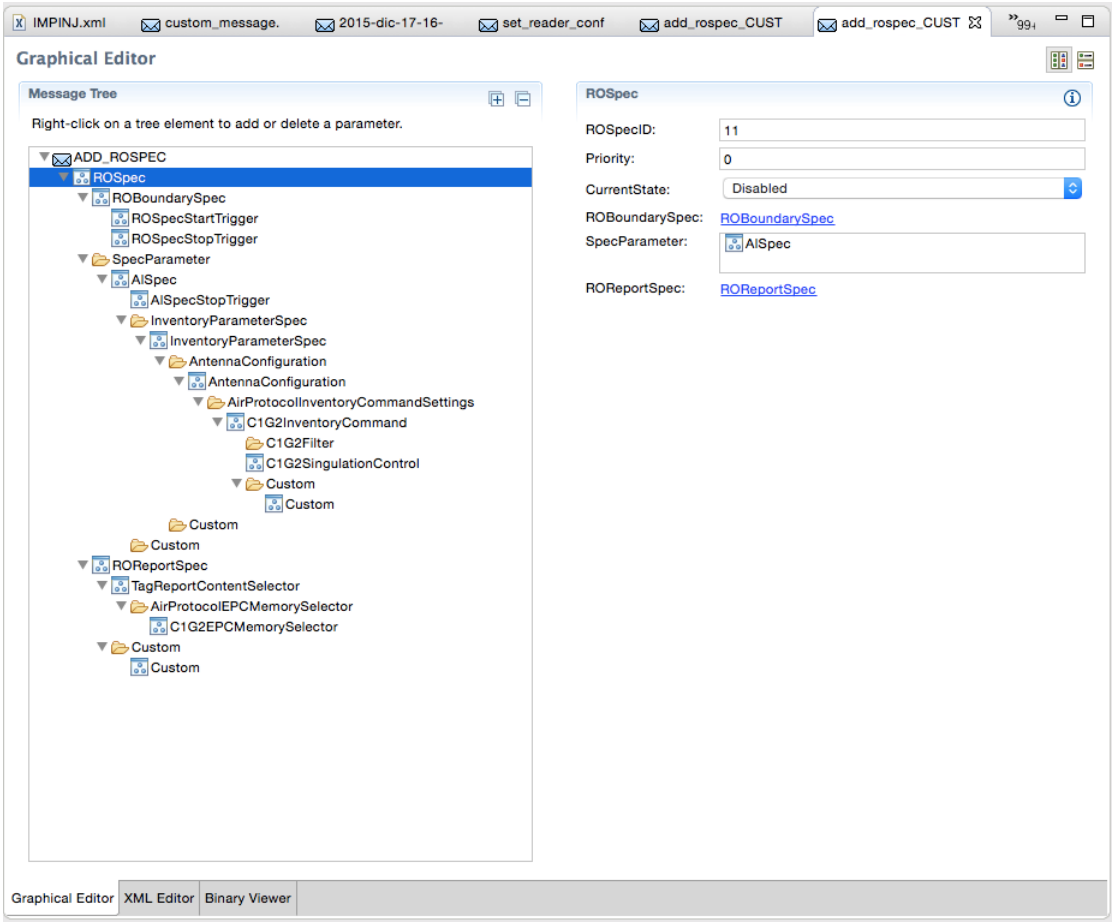

Figure 4.7: Reader Operation Specification message used.

2783 **16.1.42 CUSTOM_MESSAGE**

2784

0										1										2										3	
0	1	2	3	4	5	6	7	8	9	0	1	2	3	4	5	6	7	8	9	0	1	2	3	4	5	6	7	8	9	0	1
Rsvd			Ver			Message Type = 1023										Message Length [31:16]															
Message Length [15:0]																Message ID[31:16]															
Message ID[15:0]																Vendor Identifier [31:16]															
Vendor Identifier [15:0]																Message Subtype															
Vendor Specified Payload																															

2785

2786 See Section 8.1.

2787

Figure 4.8: LLRP custom message parameter.

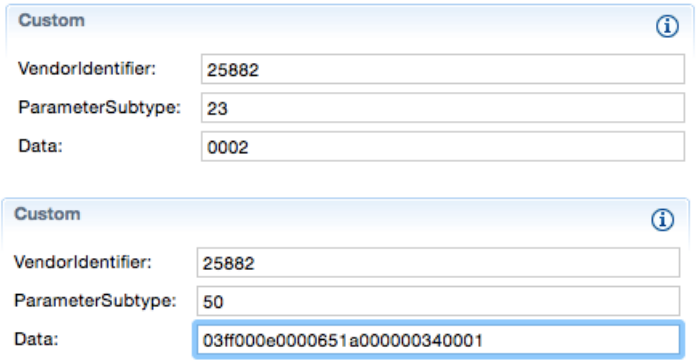

Figure 4.9: Custom parameter configuration to enable phase measurements in Impinj Speedway Revolution reader.

- Field: it describes the data type and the relative name;
- Parameter: another extension nested to the previous;
- AllowedIn: it defines where the extension are insert.

In Figure 4.8 we can see the general custom message parameters while Figure 4.9 shows the configuration of the parameter in order to read the phase value.

The Receive Operation Access Report (RO_access_report), shown in Figure 4.10, include many data generated after an access operation. All parameters shown can be enabled or disabled through tag report specification

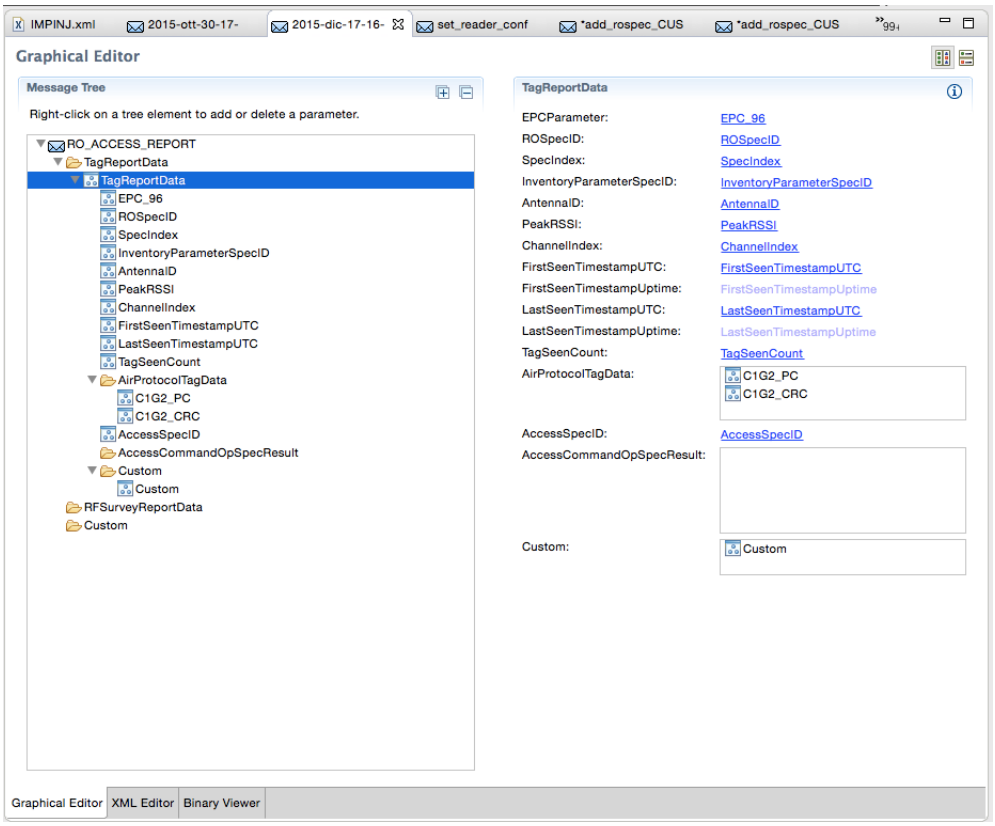

Figure 4.10: Receive Operation Access Report message.

setting inside the ROSpec message.

The principal parameters used are:

- EPC_96: it is the 96-bit tag identifier;
- ROSpecID: it indicates the ROSpecID that performed the report;
- AntennaID: it indicates the number of antenna that performed tag read;
- PeakRSSI: it indicates the received power of the RF signal;
- ChannelIndex: it indicates the channel frequency used;
- Custom: it contains custom parameter measurements sets.

For the phase measure we can obtain the degree value through the following equation:

$$\text{Phase(degree)} = \text{Value} * \frac{360}{4096} \tag{4.1}$$

where Value is the data contained in the custom section inside the Receive Operation Access Report message.

4.1.5 RFID Tag

In this thesis we consider only passive UHF RFID tags.

Tags available in laboratory are shown in Figure 4.11. All of them are made by Impinj and are inlay sticker tags. Comparing their features, we choose two tags, looking at their nominal read range. We have chosen E51 and H47 model; they have a different shape and a different chip but they have an high nominal read range. Table 4.2 reports the nominal read range of available tags.

4.2 Antenna Test

The first type of measurement done was realized to understand the losses due to the channel and the antenna matching in a real environment when reader and tag are in a line of sight. To do that we put the reader antenna on a tripod in a fix position and then we moved the tag on a line in front

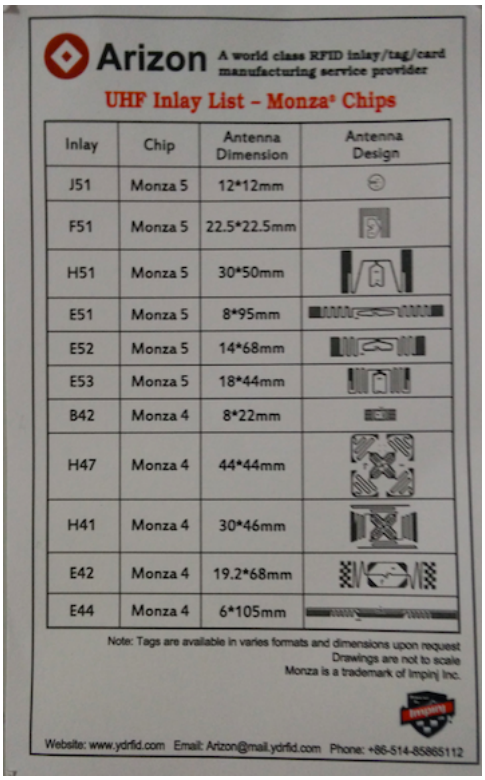

Figure 4.11: Model of tags available in the laboratory.

Tag Model	Nominal Read Range
J51	0.5
F51	0.6
H51	2.9
E51	5
E52	5
E53	3
B42	1
H47	6
H41	2.5
E42	4
E44	4.5

Table 4.2: Nominal read range of tags for transmitted power of 1W.

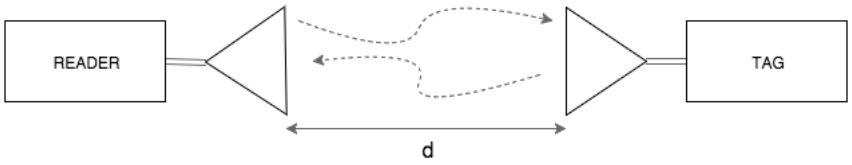

Figure 4.12: Simple schematic of the communication system.

the reader antenna from a distance of 0.5 m until the label could be read, with step of 0.5 m. For each position we collected the RSSI of the signal received. Interpolating these data we could reconstruct the path loss curve and compare it with the theoretical free space path loss curve. The distance between the curves is the values of additional losses in our system. This value help us to calculate the best estimation of received power at the reader antenna and then find the SNR at distance equal to 1 m (SNR_0). The SNR_0 value was used to simulate the system with noise on phase measurements.

We tried to recreate the free space propagation conditions realizing the measurements in an open space. The test was repeated for four different type of antennas and two tag models: E51 and H47.

The antennas used are:

- DLT3-868: Circular antenna with gain G=3 dBi,
- PN6-868: Square antenna with gain G=6 dBi,
- PN8-868: Square antenna with gain G=8 dBi,
- Impinj antenna: Square antenna with gain G=8 dBi.

Using the schematic circuit shown in Figure 4.12 we can define the power received at the reader P_{Rx} as:

$$P_{Rx} = \frac{P_{Tx} G_t^2 G_r^2 \lambda^4}{(4\pi d L_t)^4} \tag{4.2}$$

where P_{Tx} is the transmitted power by the reader, G_{t} is the transmit antenna gain, G_{r} is the receiver antenna gain, λ is the wavelength, d is the distance between tag and reader antenna and L_t are the additional losses due to antenna matching and propagation channel. We can define P_{Rx0} the power received when the distance d is equal to 1 m.

$$P_{Rx0} = \frac{P_{Tx} G_t^2 G_r^2 \lambda^4}{(4\pi L_t)^4} \tag{4.3}$$

(a) Tag E51 model.

(b) Tag H47 model.

Figure 4.13: Tags used for the test.

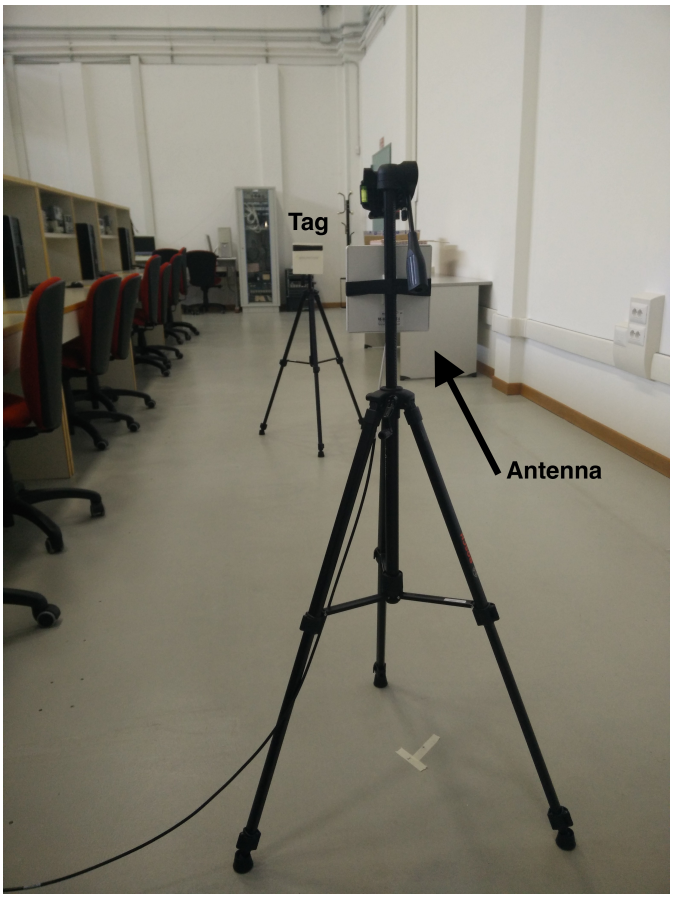

Figure 4.14: Antenna test setup.

We can define the SNR_0 as:

$$SNR_0 = \frac{E}{N_0} \quad \text{where} \quad E = \frac{P_{\text{Rx0}}}{B}, N_0 = kTF \tag{4.4}$$

(a) DLT3-868 antenna with gain G=3 dBi.

(b) PN6-868 antenna with gain G=6 dBi.

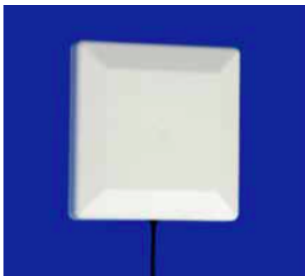

(c) PN8-868 antenna with gain G=8 dBi.

(d) Impinj antenna with gain G=8dBi.

Figure 4.15: Antenna used for the test.

where B is the channel bandwidth equal to 200 KHz, k is the Boltzmann constant, T is the noise temperature equal to 290 K and F is the noise figure equal to 4 dB. So the signal-to-noise ratio SNR at the distance d can be expressed as

$$SNR = SNR_0 \left(\frac{d}{d_0} \right)^{-4} \tag{4.5}$$

where d_0 is equal to 1 meter.

Next figures show the Friis transmission equation (4.2) in a real environment obtained using the RSSI read from the reader for several tag positions in a linear line of sight with it. The red curves represent the equation with $L_t = 1$ i.e., without losses. The green curves are the best Friis transmission equation with losses that get closer to the power points measured. The

transmission equation with losses was estimated finding the L_t factor that minimizes the euclidean distance to the points.

The curves derived from the measurements have the tendency similar to the Friis transmission equation in free-space without losses but they present a very high attenuation for the technologies and the system configuration considered. We used information presented in the datasheets of the hardware.

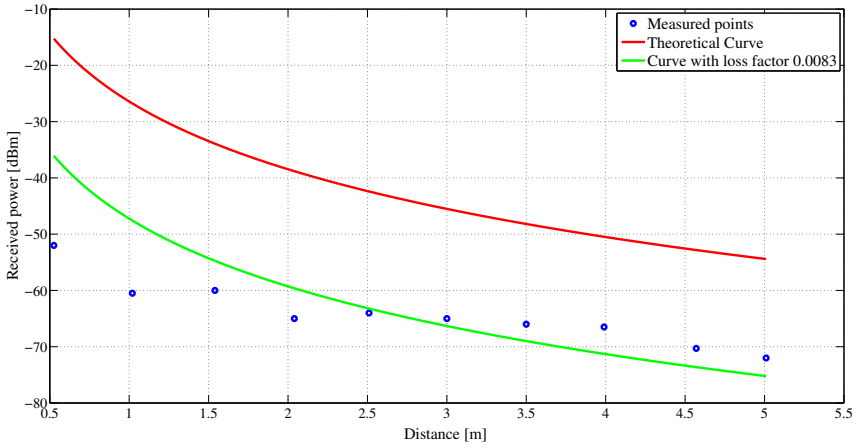

Figure 4.16: DLT3-868 Antenna test with E51 tag.

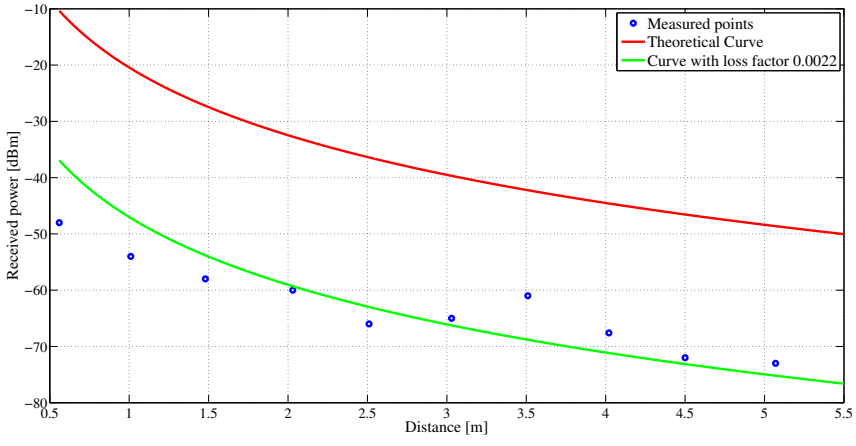

Figure 4.17: PN6-868 Antenna test with E51 tag.

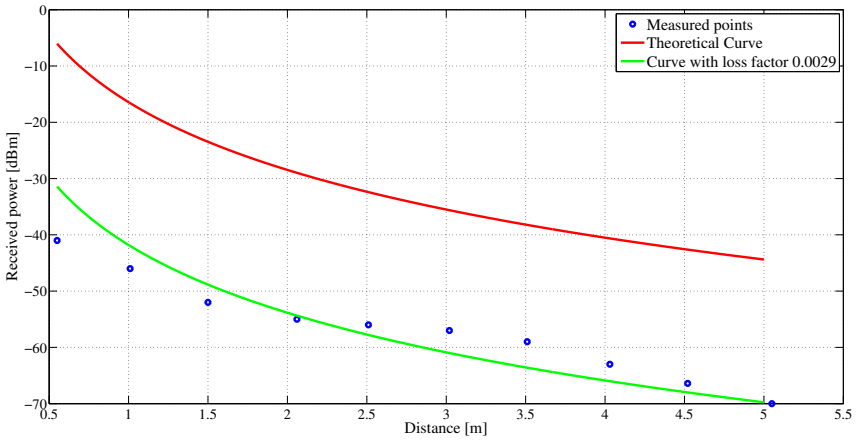

Figure 4.18: PN8-868 Antenna test with E51 tag.

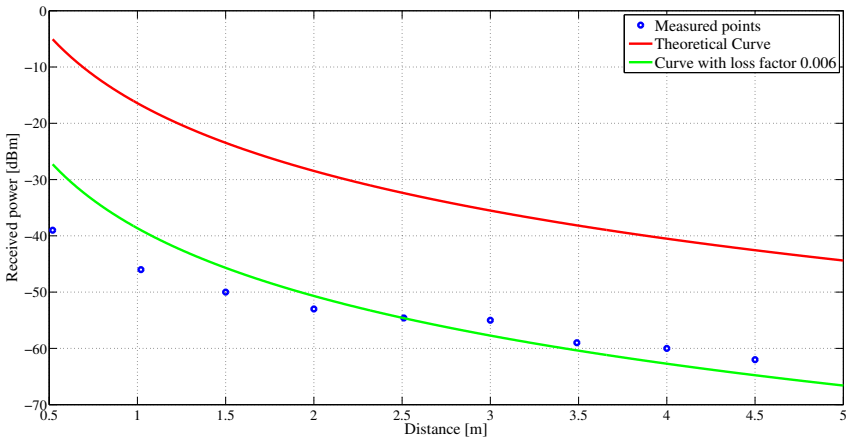

Figure 4.19: Impinj antenna Antenna test with E51 tag.

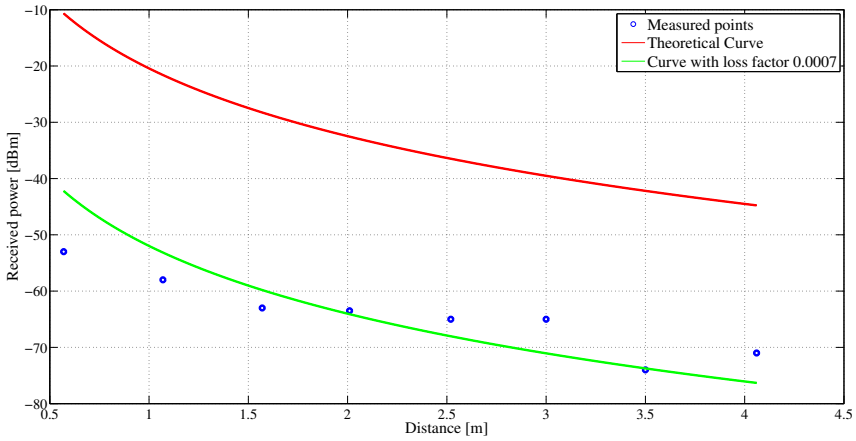

Figure 4.20: PN6-868 Antenna test with H47 tag.

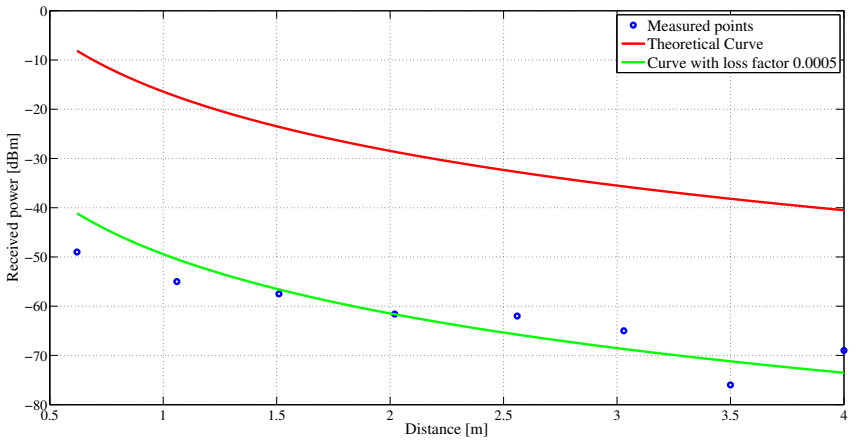

Figure 4.21: PN8-868 Antenna test with H47 tag.

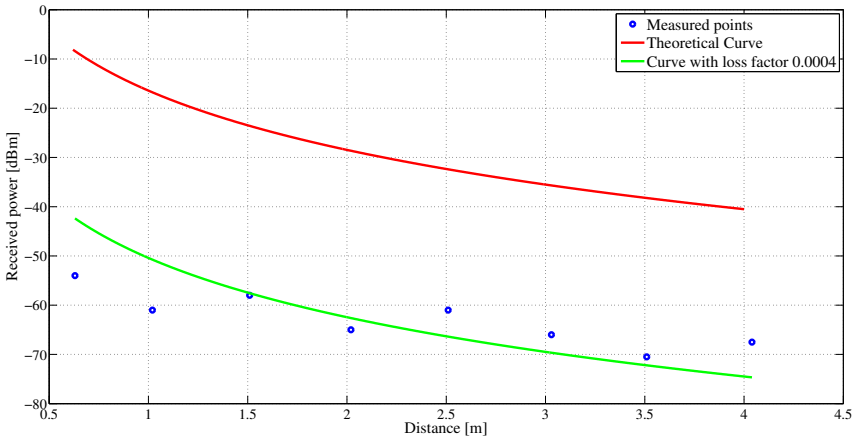

Figure 4.22: Impinj antenna test with H47 tag.

Chapter 5

Measurement Results

5.1 Linear trajectory

After the simulative approach we decided to test the algorithm in a real environment. The first test concerned the lateral relative movements of the reader with respect to the tag. Our questions were: how long the tag can be read while the reader is moving laterally with respect to it? Using the phase measurements, can the tag be located correctly? Which algorithm does have the best performance?

For an easier procedure of measurement we placed the reader antenna fixed in the position of 4.65 m and moved the tag back and forth in a linear trajectory in front of the reader. This situation is equal of the corresponding used in simulations, where the tag was fixed and the reader in movement, because what it is important is the relative motion among them. Tag was moved with step of 0.1 m. For each position the phase and the RSS values was taken as the mean of ten different measures. The test was repeated for three different tag-reader frontal distances, 1 m, 2 m, 3 m and for two antennas: PN6-868 model with 6 dBi gain and PN8-868 model with 8 dBi gain.

The procedure can be summarized as:

1. Put the reader antenna in the fix point with coordinate 4.65 m;

2. Put the tag in front of the reader antenna at the desired distance;

3. Find the maximum reading distance moving the tag on the right with respect to the antenna and put it in this point;
4. Read 10 LLRP packets and calculate the average of the phase and the RSS values read;
5. Move the tag 0.1 m left.
6. Repeat points 4 and 5 until the tag cannot be read.

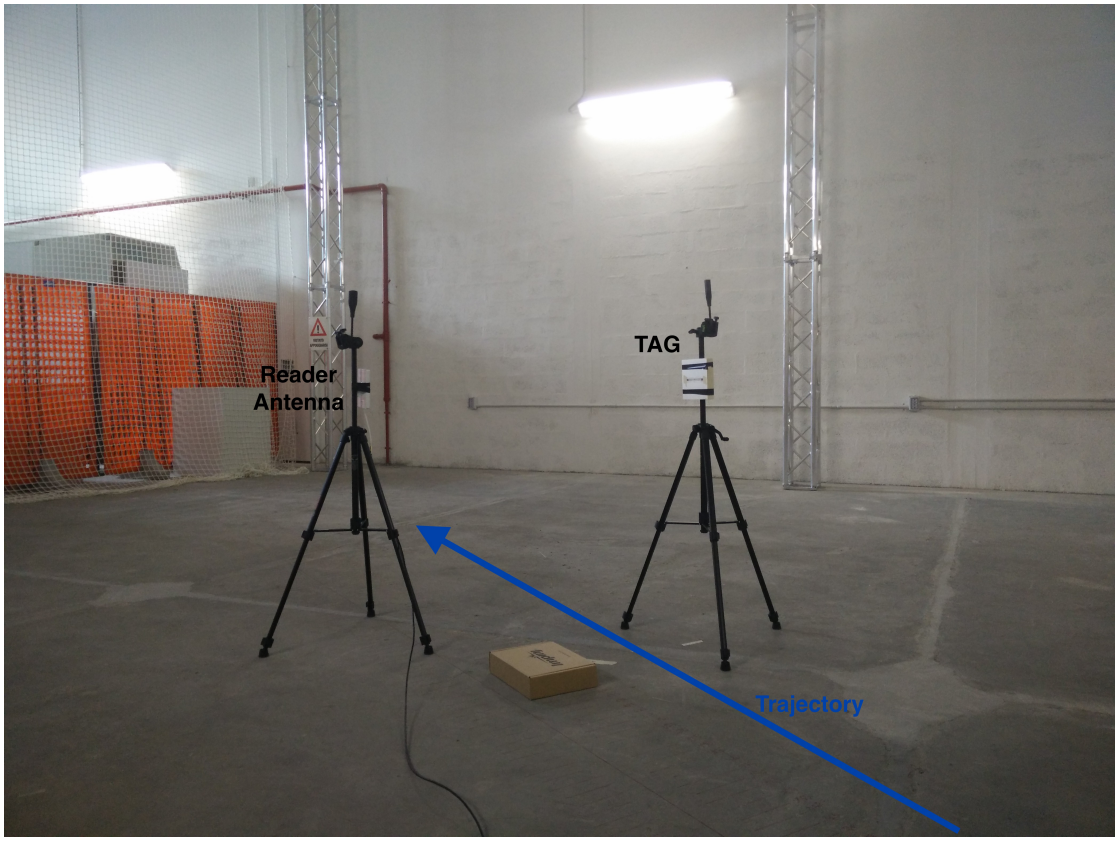

Figure 5.1: Measurement setup.

5.1.1 1D-Localization Results

In this section the performance of the algorithms, explained in Chapter 2. is compared using the phase measurements taken in the laboratory. In particular we tested the one dimensional (1D) localization i.e., we supposed to

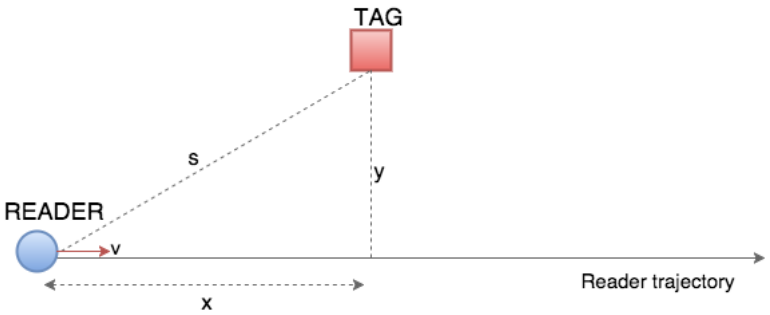

Figure 5.2: Measurement setup.

know *a priori* the distance between the reader and the tag trajectory (y-coordinate) so that the algorithms should localize only the positions of the tag on the linear trajectory (x-coordinate), referring to the lateral offset with respect to the reader position.

Next figures show the function P of the algorithms i.e., the correlation function between the vector containing the phase relative to a hypothetical location and the vector of the phase measurements where its maximum expresses the estimated position of the tag. In particular the figures refer to the situation where the distance between the tag and the reader trajectory was equal to 2 m. In this environment the tag, positioned in $x = 4.65$ m, could be read from the coordinate $x = 2.65$ m to $x = 6.65$ m. We performed phase measurements with step of 0.1 m.

Figure 5.2 shows our environment where a reader moves on a linear trajectory with a constant velocity v and the tag is positioned in a fixed position. Remembering the relation between the distance and the phase of the backscatter signal, it is possible write:

$$\varphi = \left(-4\pi f_0 \frac{s}{c}\right) \bmod 2\pi = \left(-4\pi f_0 \frac{\sqrt{x^2 + y^2}}{c}\right) \bmod 2\pi \tag{5.1}$$

where φ if the phase of the received backscatter signal at the reader position, f_0 is the carrier frequency of the signal and c is the speed of the light.

Collecting many phase measurements closely spaced allowed us to plot the trend of the phase as a function of the reader position. In Figure 5.3 it is possible to see that when $x \sim s$ i.e., the reader is in a lateral position with respect to the tag, the phase φ is linear with respect to x. The result is the characteristic sawtooth wave behaviour due to the 2π periodicity. Instead,

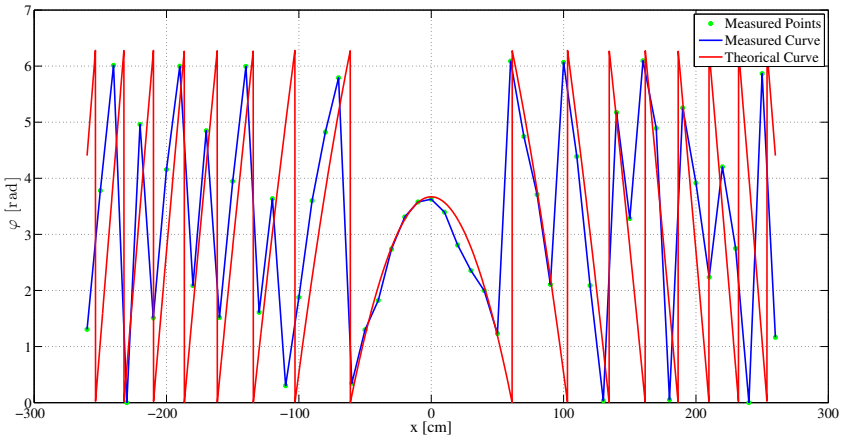

Figure 5.3: Phase trend as function of the position centered respect to tag location.

when the reader approaches the minimum distance with respect to the tag, the relation between s and x is non linear, so the phase has a different trend (central part of the curve). This underlines the importance to measure the tag phase as much as possible with the tag in front of the reader trajectory, where the non linearity can help us to prevent phase ambiguities.

For simplicity we have called the various algorithms used as:

- Algorithm A: it refers to the algorithm present in literature that uses the exponential function. The function to be maximized is in Section 2.4.

- Algorithm B: it refers to the algorithm deriving from the ML criterion. The function to be maximized is in Section 2.3.1.

- Algorithm C: it refers to the algorithm presented in literature that use the exponential function weighted with the received power. The function to be maximized is in Section 2.4.

- Algorithm D: it refers to the algorithm derived from the ML criterion that uses RSS measurements in additions to phase values. The function to be maximized is in Section 2.3.2

Figure 5.4 and Figure 5.5 refers to the localization process using the four

algorithms propose. Specifically, they show the functions whose maximum indicates the tag position.

From Figure 5.6 to Figure 5.15 the localization is performed considering the different algorithms using a portion of the total trajectory. We have chosen only few central phase measurements (5, 7, 9 or 11 values) in order to use values that belong to the non linear zone of the characteristic phase trend; so the phase ambiguities could be limited. In general, decreasing the number of phase measures N and consequently the length L of the trajectory produces smoother correlation functions where the maximum location is more ambiguous. This effect is amplified in the algorithms presented in literature, that use the exponential function. Usually the algorithm B presents a sharper principal peak than the other methods.

Figure 5.16 and Figure 5.18 show the localization of the tag using phase measurements spaced respectively 0.2 meters and 0.3 meters along overall trajectory.

In general, in all configurations, the algorithm D leads to a wrong localization. The resultant correlation function is almost flat and presents a peak not in the tag position. This behavior could be explained with the low reliability and the randomness of the RSS values. In the 1D localization when the distance between the reader trajectory and the tag is equal to 3 meters, the function is still flat but it leads to a correct localization (see Appendix A).

RSS values work better in the algorithm C where the function to be maximized is exponential.

Table 5.1 and Table 5.2 present the results and the RMSE of the localization for different configurations. N indicates the number of phase measures used and L is the equivalent length of the trajectory. Looking at the table, it is possible to see that the algorithm B, using the ML criterion, has for all the configurations a performance equal or better than that of the algorithm A. Only in the configuration with $N = 5$ and $L = 0.8$ m it presents a wrong localization due to a secondary peak that grews decreasing the number of phase values.

Another test done concerned the choice of the best phase values. In order to use only the more reliable measurements, we implemented a threshold model where a phase value was used in the algorithm only if its received

power level satisfied a determined threshold. Table 5.3 and Table 5.4 show the results of this analysis. A received phase value is used in the localization process only if the corresponding RSS is included between the maximum RSS along the trajectory and the latter less the threshold. The threshold was not set in a unique manner, but relative to the maximum signal power along the trajectory. Decreasing the threshold level less phase values are used in the algorithms. Looking at the tables we notice that the localization results with a threshold equal to 10-12 dB generally is equal or better than the localization with all phase values measured. A threshold equal to 2 dB causes a high RMSE because few phase measurements are collected.

The last experiment done in the 1D localization localization scenario considers, a Monte Carlo simulations. Using one of the configurations seen before, in particular $N = 7$ and $L = 0.6$ m, Gaussian noise was added to the reader position in order to discover the performance of the algorithms when the information about the position is not precise. The test was repeated for several noise variances. The results, shown in Table 5.5 and Table 5.6, reveal that the noise on the reader position does not degrade significantly the localization estimation provided that its standard deviation is lower than 0.032 m. Increasing the noise variance the resulting RMSE raises considerably.

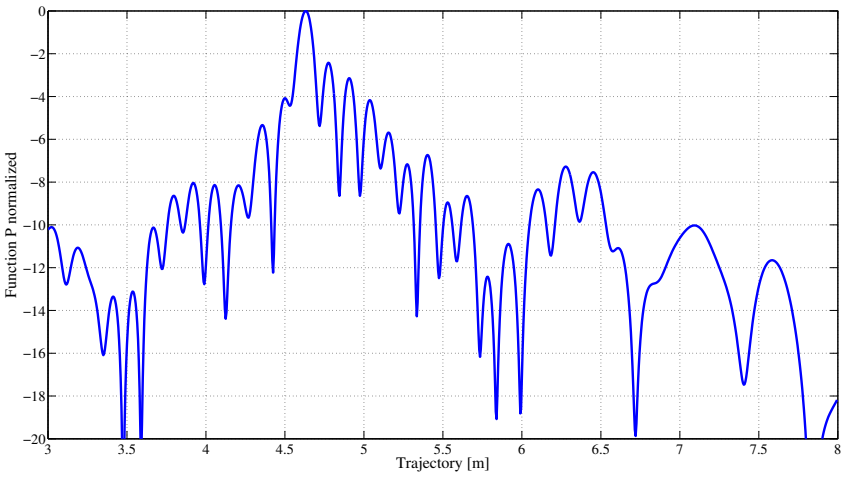

(a) Localization of the tag using algorithm A. Tag estimated in x=4.63 m.

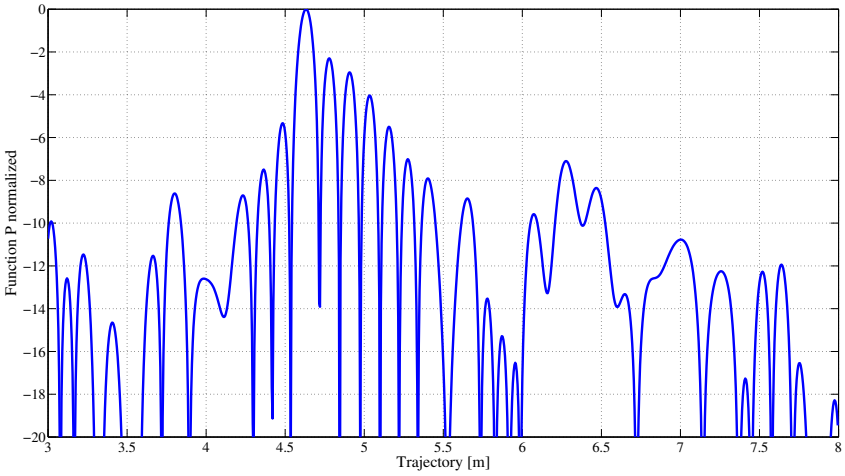

(b) Localization of the tag using algorithm B. Tag estimated in x=4.63 m.

Figure 5.4: Localization using algorithm A and B and 42 phase measurements. True tag position: x=4.65 m. Reader trajectory-tag distance= 2 m.

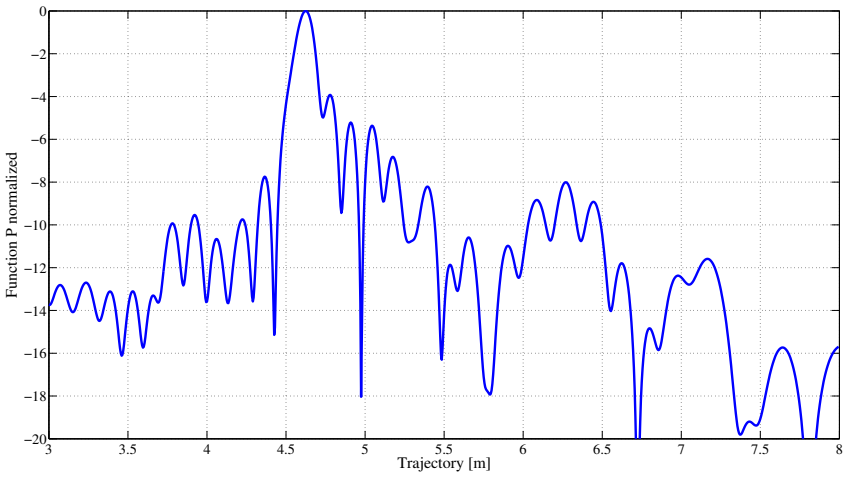

(a) Localization of the tag using algorithm C. Tag estimated in x=4.625 m.

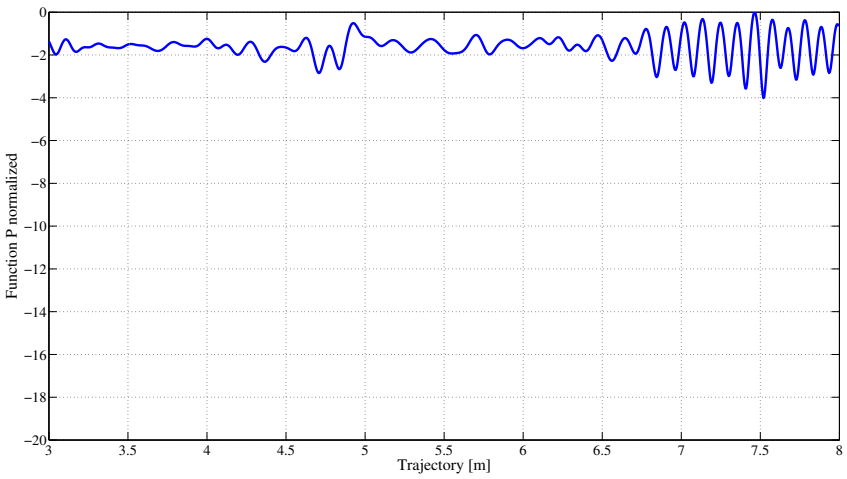

(b) Localization of the tag using algorithm D. Tag estimated in x=7.465 m.

Figure 5.5: Localization using algorithm C and D and 42 phase measurements. True tag position: x=4.65 m. Reader trajectory-tag distance= 2 m.

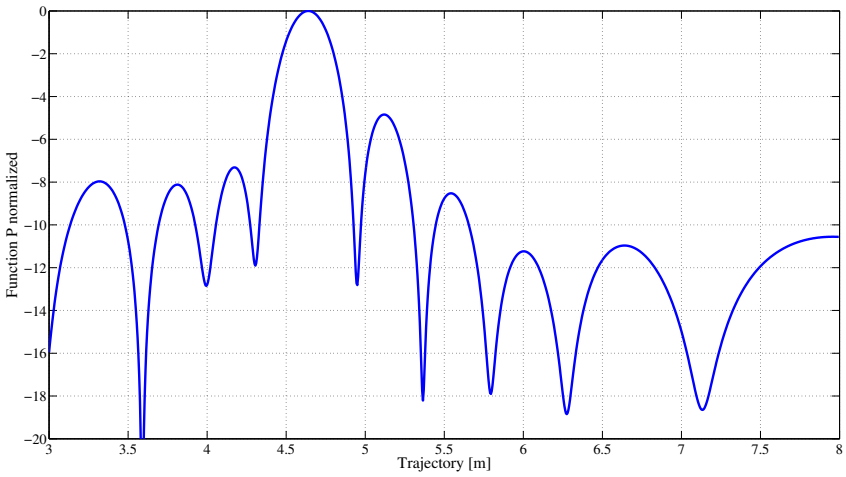

(a) Localization of the tag using algorithm A. Tag estimated in x=4.64 m.

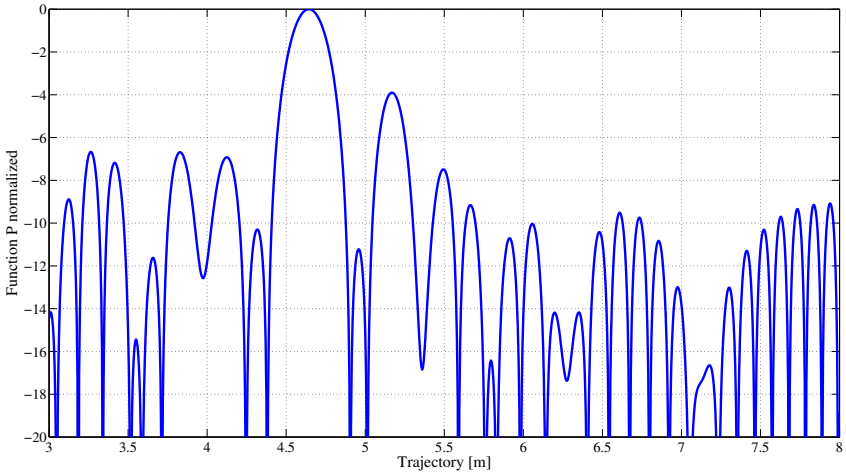

(b) Localization of the tag using algorithm B. Tag estimated in x=4.645 m.

Figure 5.6: Localization with the 11 central measures spaced 0.1 m using algorithm A and B. True tag position: x=4.65 m. Reader trajectory-tag distance= 2 m.

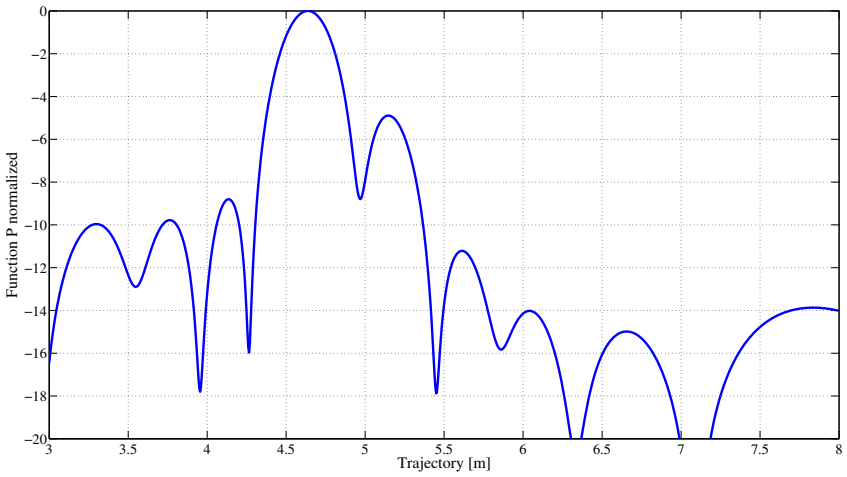

(a) Localization of the tag using algorithm C. Tag estimated in x=4.635 m.

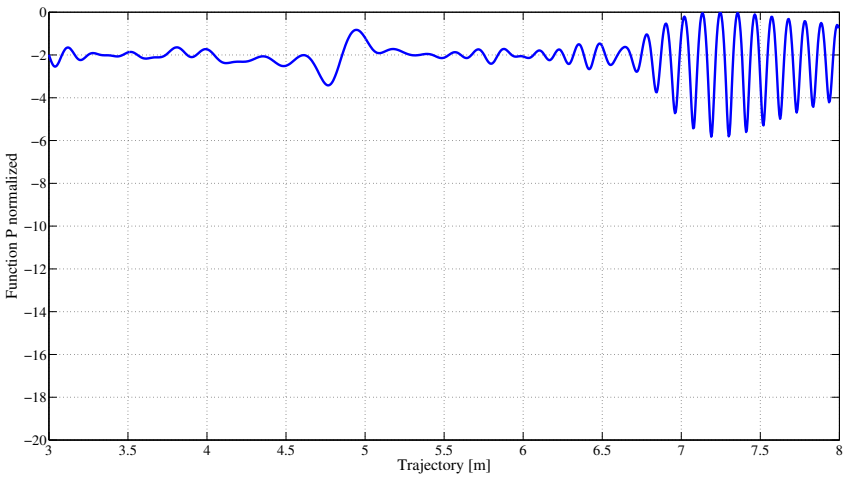

(b) Localization of the tag using algorithm D. Tag estimated in x=7.245 m.

Figure 5.7: Localization with the 11 central measures spaced 0.1 m using algorithm C and D. True tag position: x=4.65 m. Reader trajectory-tag distance= 2 m.

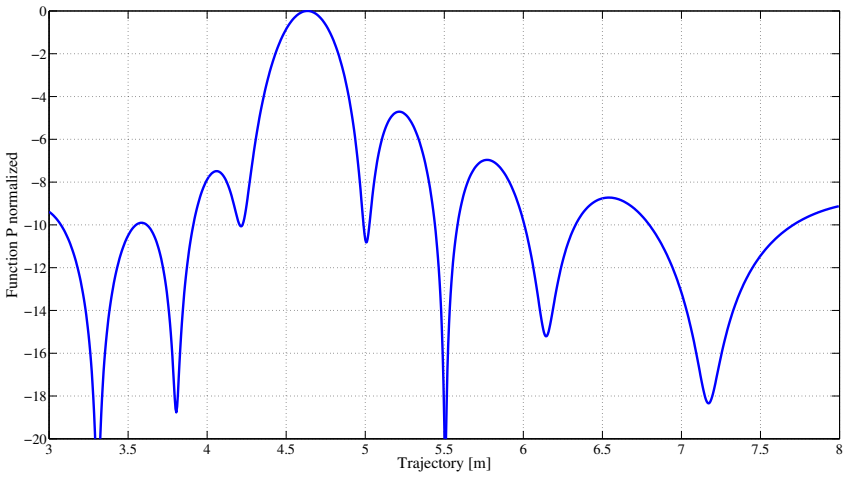

(a) Localization of the tag using algorithm A. Tag estimated in x=4.635 m.

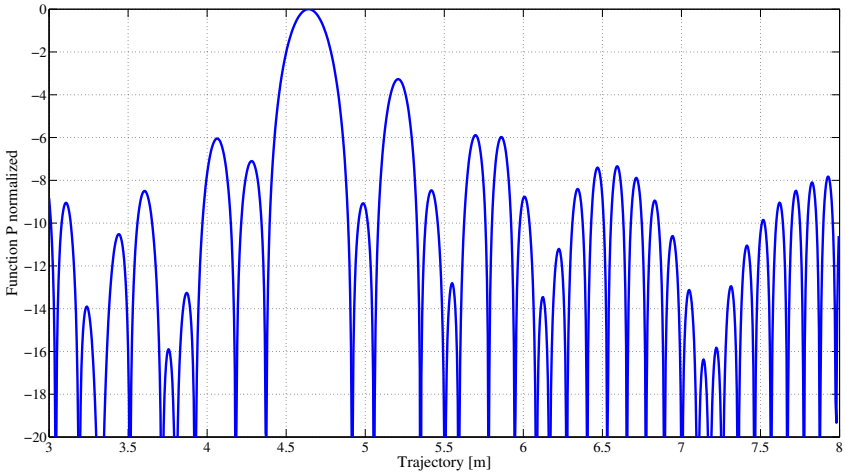

(b) Localization of the tag using algorithm B. Tag estimated in x=4.64 m.

Figure 5.8: Localization with the 9 central measures spaced 0.1 m using algorithm A and B. True tag position: x=4.65 m. Reader trajectory-tag distance= 2 m.

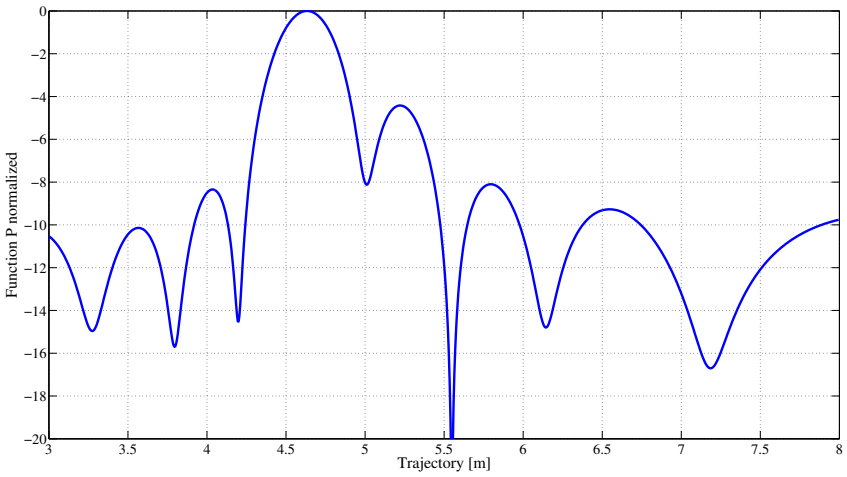

(a) Localization of the tag using algorithm C. Tag estimated in x=4.605 m.

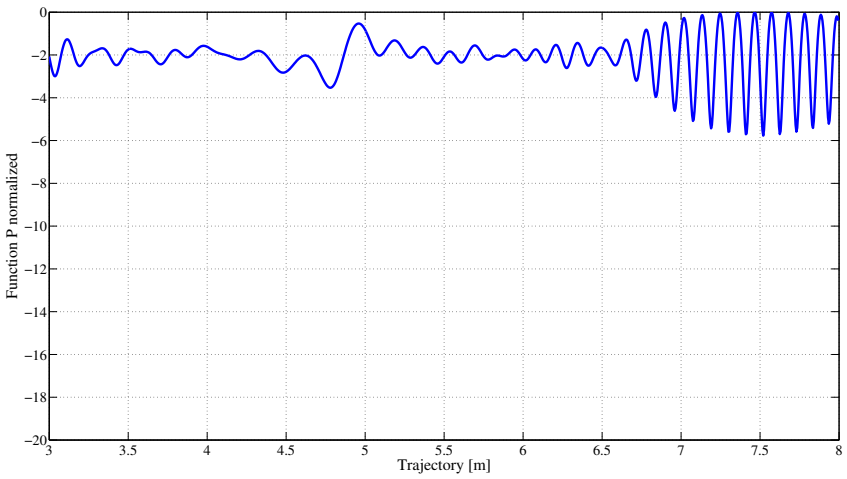

(b) Localization of the tag using algorithm D. Tag estimated in x=7.465 m.

Figure 5.9: Localization with the 9 central measures spaced 0.1 m using algorithm C and D. True tag position: x=4.65 m. Reader trajectory-tag distance= 2 m.

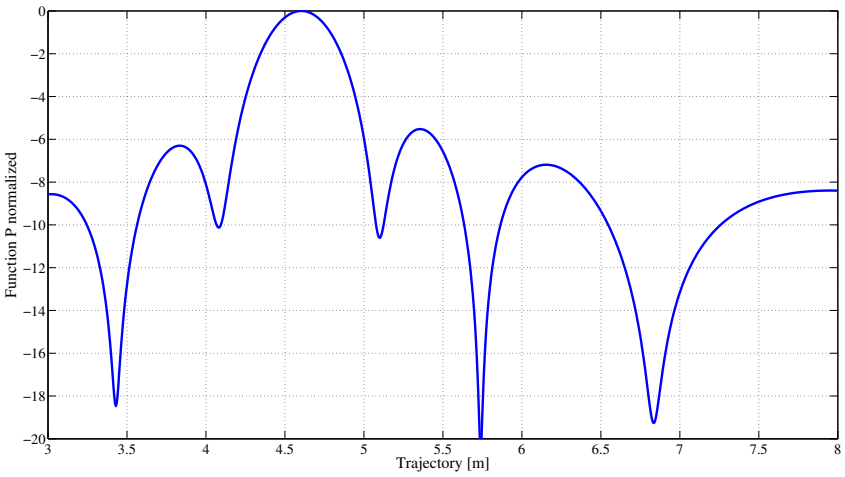

(a) Localization of the tag using algorithm A. Tag estimated in x=4.605 m.

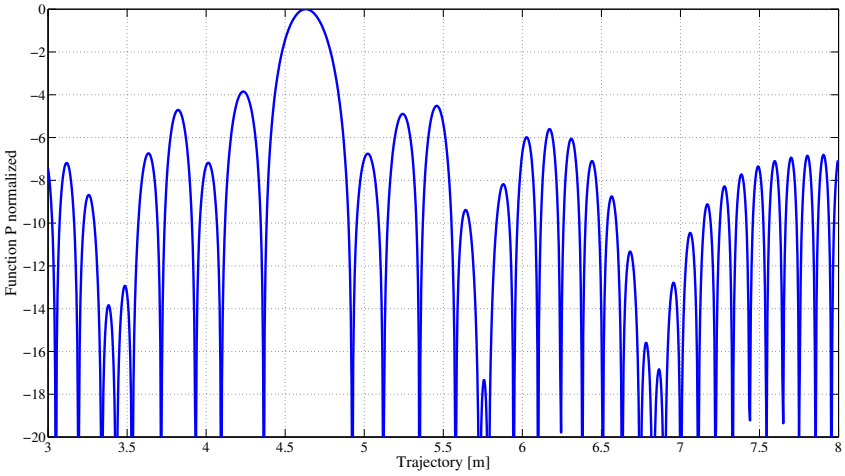

(b) Localization of the tag using algorithm B. Tag estimated in x=4.63 m.

Figure 5.10: Localization with the 7 central measures spaced 0.1 m using algorithm A and B. True tag position: x=4.65 m. Reader trajectory-tag distance= 2 m.

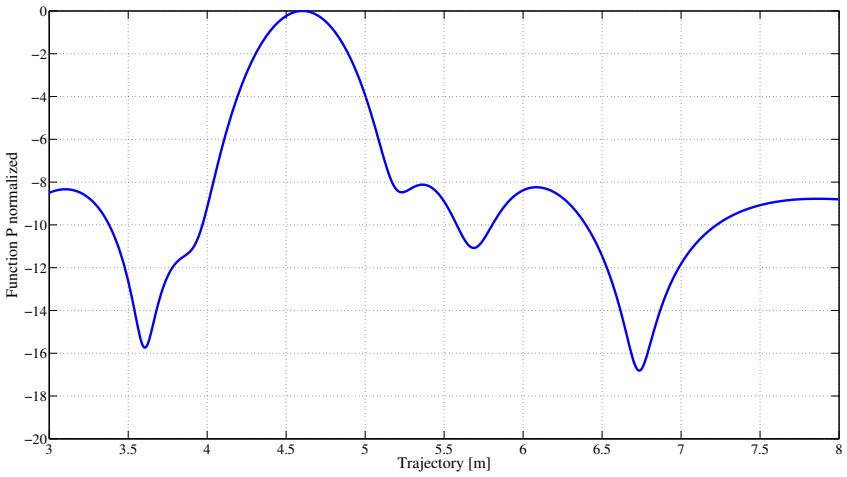

(a) Localization of the tag using algorithm C. Tag estimated in x=4.605 m.

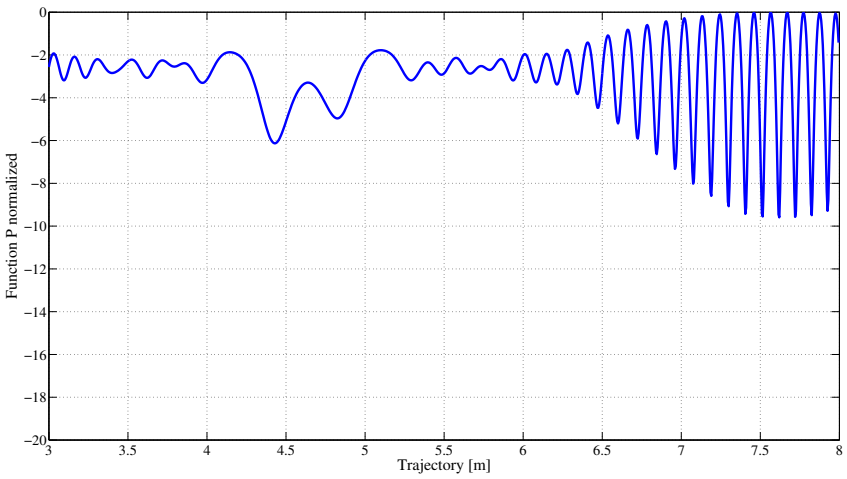

(b) Localization of the tag using algorithm D. Tag estimated in x=7.565 m.

Figure 5.11: Localization with the 7 central measures spaced 0.1 m using algorithm C and D. True tag position: x=4.65 m. Reader trajectory-tag distance= 2 m.

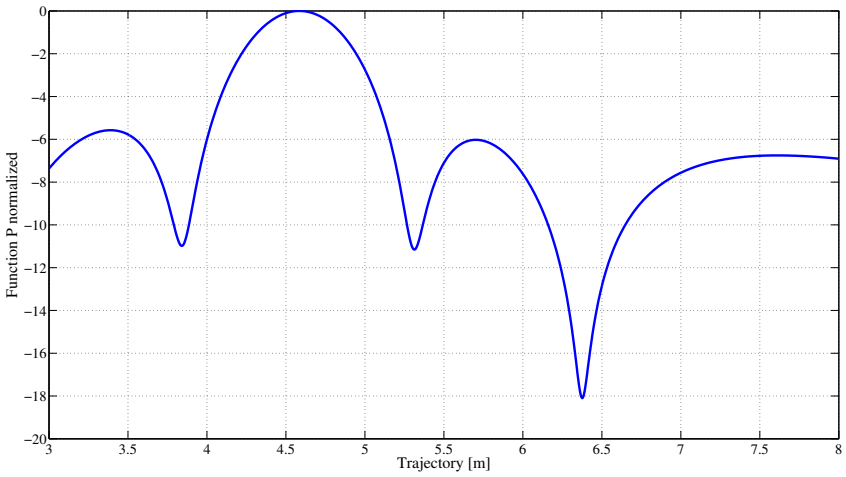

(a) Localization of the tag using algorithm A. Tag estimated in x=4.585 m.

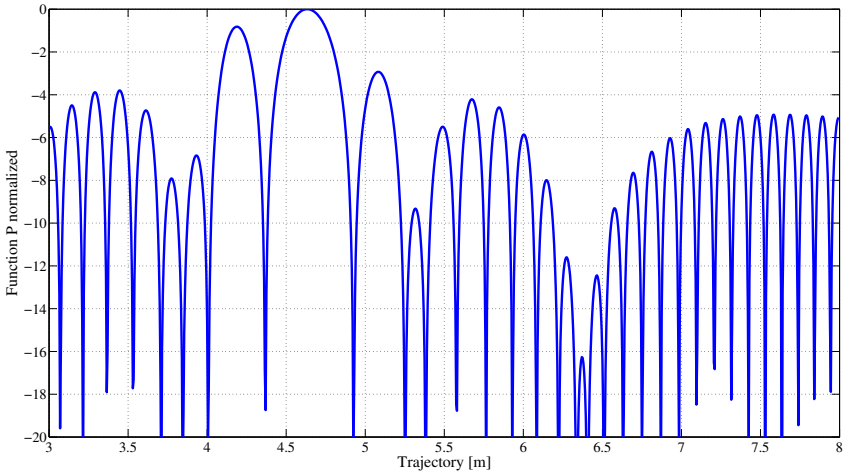

(b) Localization of the tag using algorithm B. Tag estimated in x=4.635 m.

Figure 5.12: Localization with the 5 central measures spaced 0.1 m using algorithm A and B. True tag position: x=4.65 m. Reader trajectory-tag distance= 2 m.

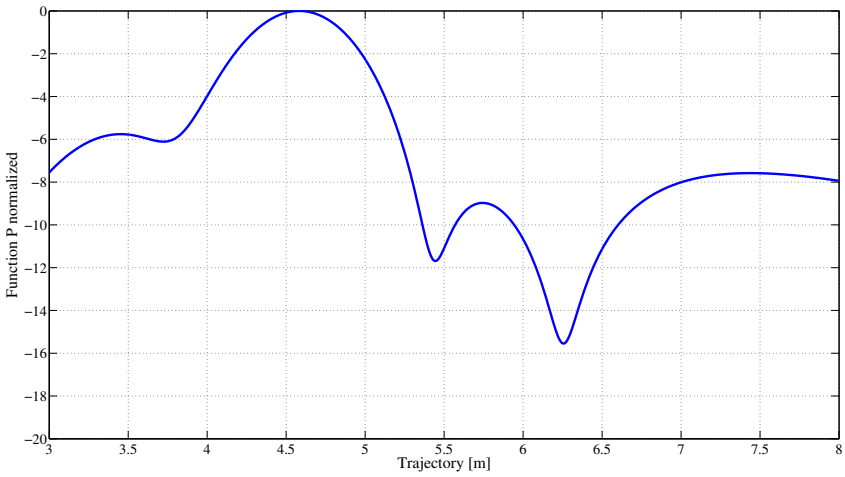

(a) Localization of the tag using algorithm C. Tag estimated in x=4.585 m.

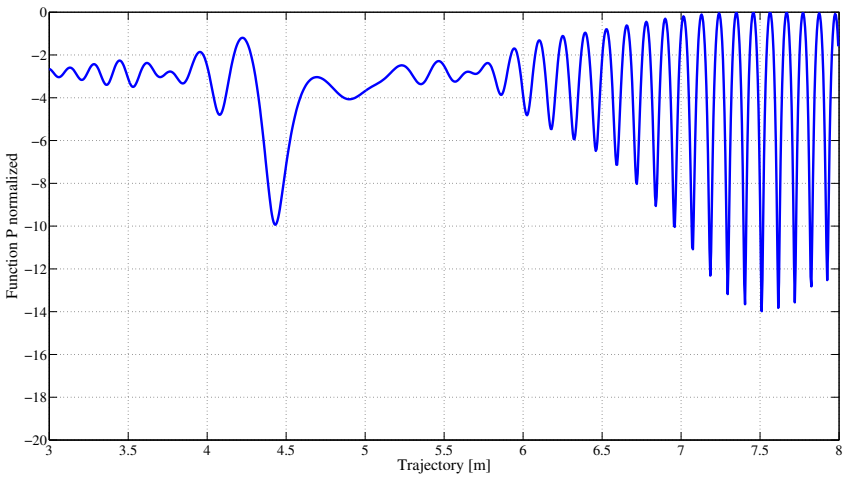

(b) Localization of the tag using algorithm D. Tag estimated in x=7.565 m.

Figure 5.13: Localization with the 5 central spaced 0.1 m measures using algorithm C and D. True tag position: x=4.65 m. Reader trajectory-tag distance= 2 m.

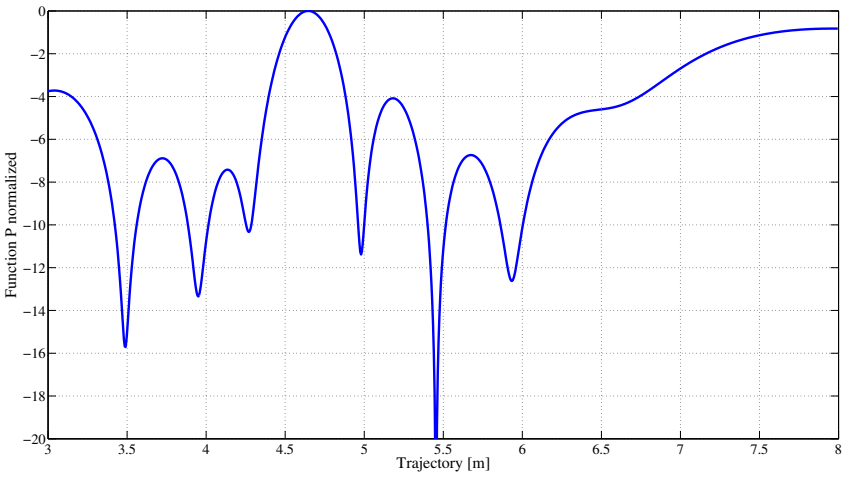

(a) Localization of the tag using algorithm A. Tag estimated in x=4.645 m.

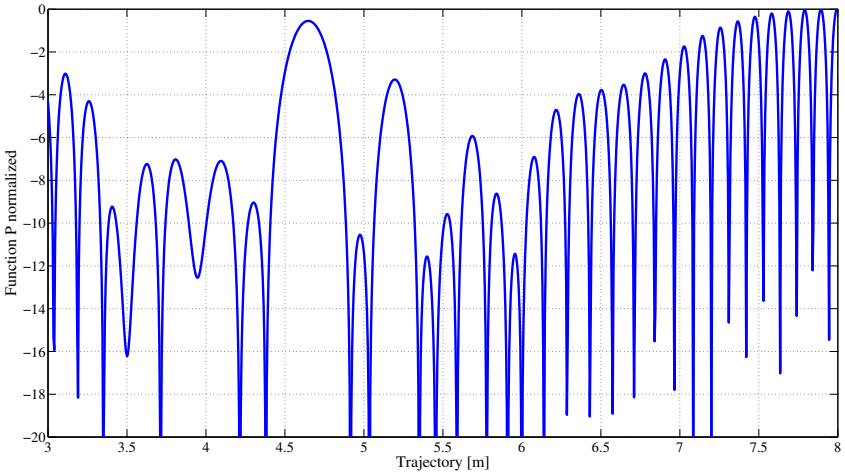

(b) Localization of the tag using algorithm B. Tag estimated in x=7.995 m.

Figure 5.14: Localization with the 5 central spaced 0.2 m measures using algorithm A and B. True tag position: x=4.65 m. Reader trajectory-tag distance= 2 m.

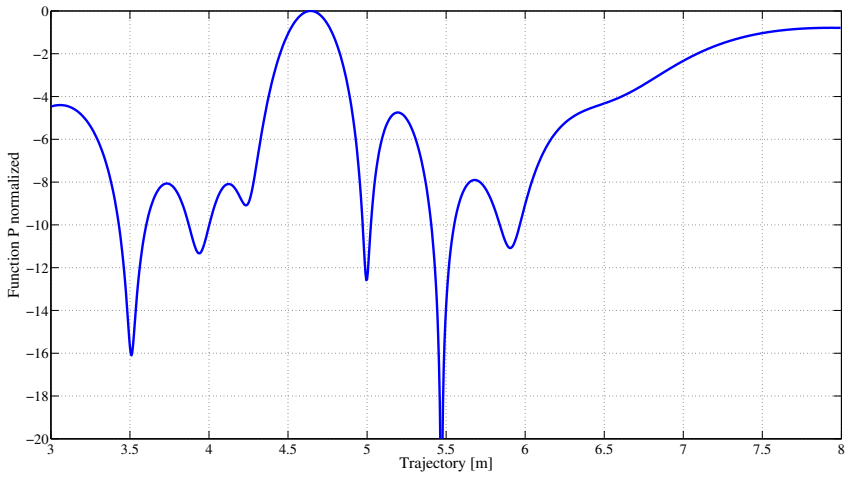

(a) Localization of the tag using algorithm C. Tag estimated in x=4.62 m.

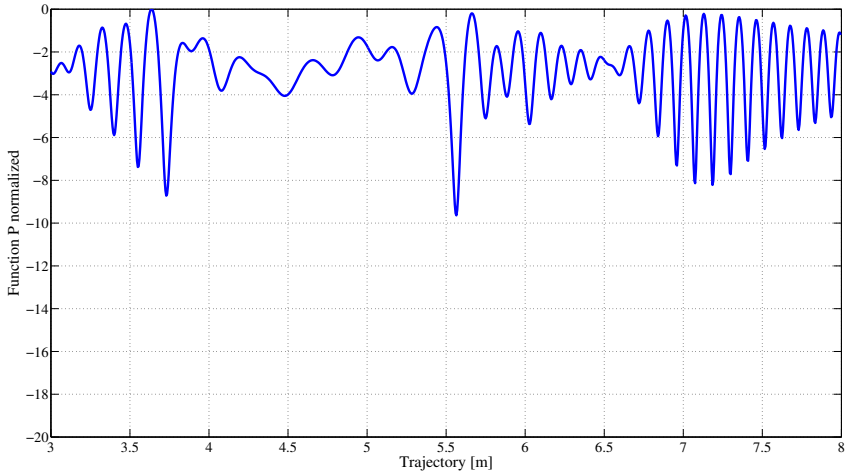

(b) Localization of the tag using algorithm D. Tag estimated in x=3.635 m.

Figure 5.15: Localization with the 5 central measures spaced 0.2 m using algorithm C and D. True tag position: x=4.65 m. Reader trajectory-tag distance= 2 m.

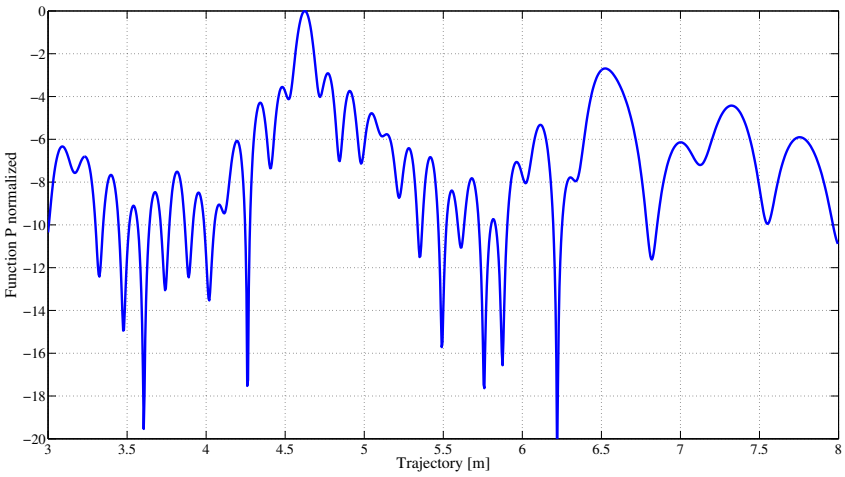

(a) Localization of the tag using algorithm A. Tag estimated in x=4.625 m.

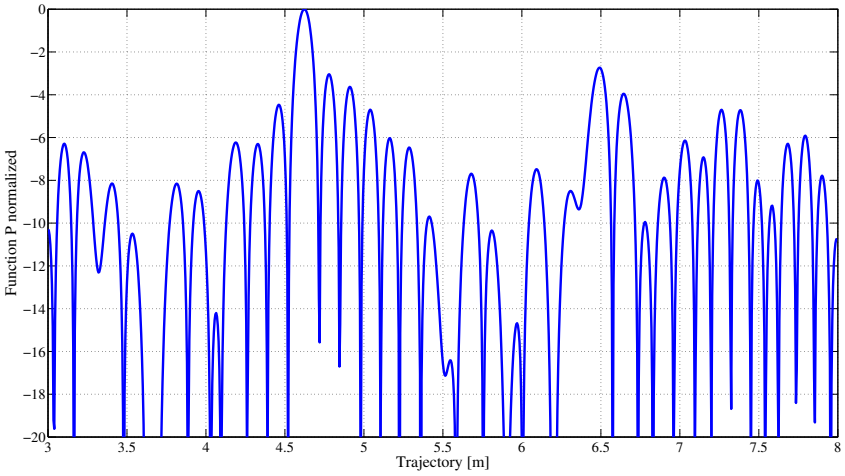

(b) Localization of the tag using algorithm B. Tag estimated in x=4.625 m.

Figure 5.16: Localization with 21 phase measurements spaced 0.2 m measures using algorithm A and B. True tag position: x=4.65 m. Reader trajectory-tag distance= 2 m.

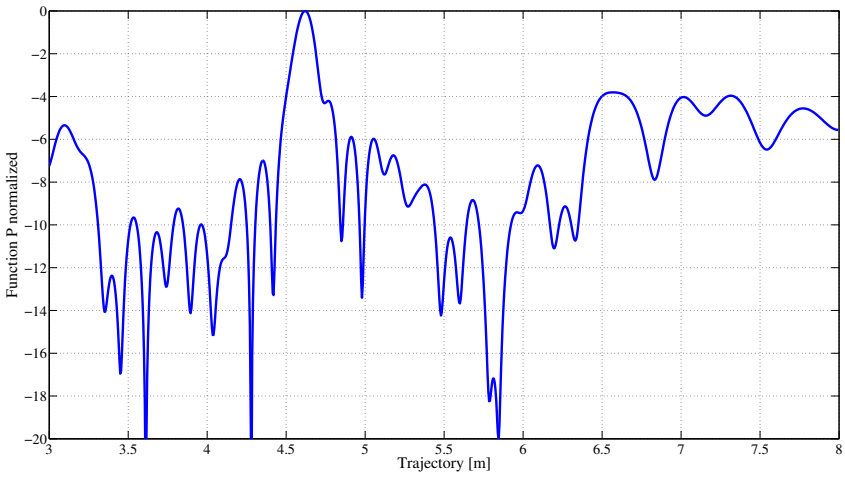

(a) Localization of the tag using algorithm C. Tag estimated in x=4.62 m.

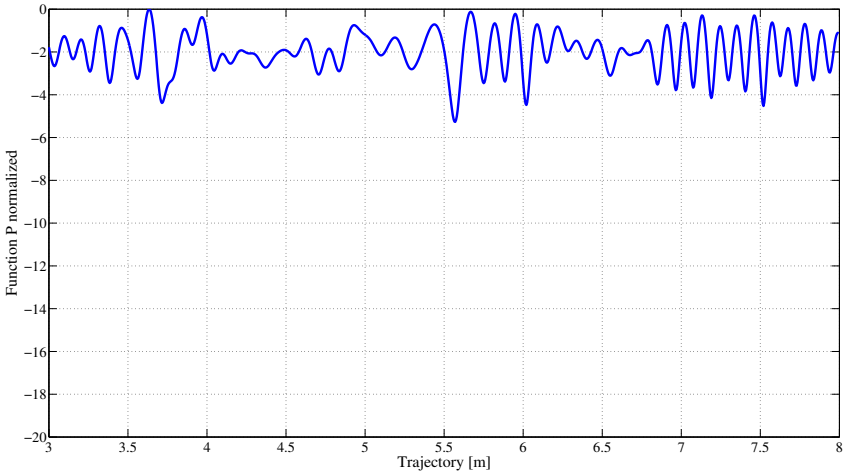

(b) Localization of the tag using algorithm D. Tag estimated in x=3.635 m.

Figure 5.17: Localization with 21 phase measurements spaced 0.2 m using algorithm C and D. True tag position: x=4.65 m. Reader trajectory-tag distance= 2 m.

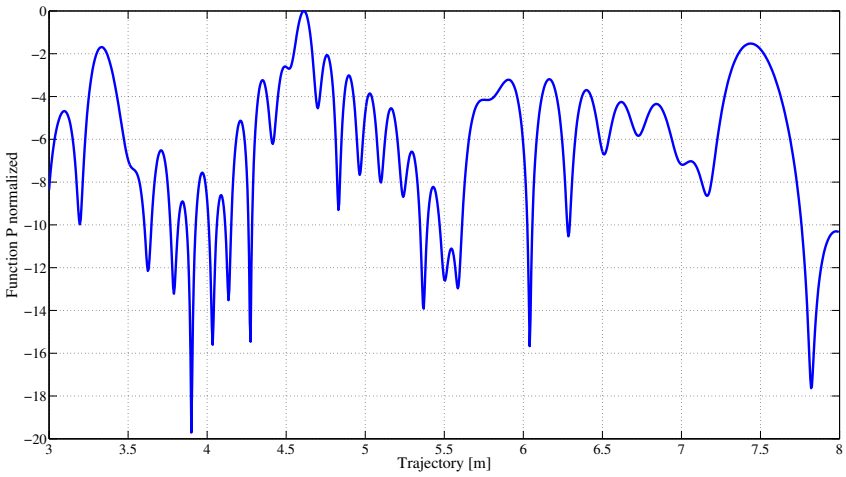

(a) Localization of the tag using algorithm A. Tag estimated in x=4.61 m.

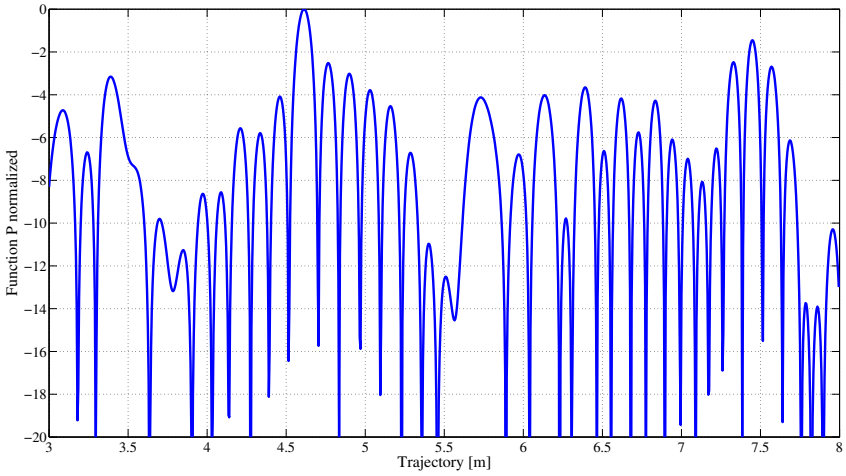

(b) Localization of the tag using algorithm B. Tag estimated in x=4.615 m.

Figure 5.18: Localization with 14 phase measurements spaced 0.3 m measures using algorithm A and B. True tag position: x=4.65 m. Reader trajectory-tag distance= 2 m.

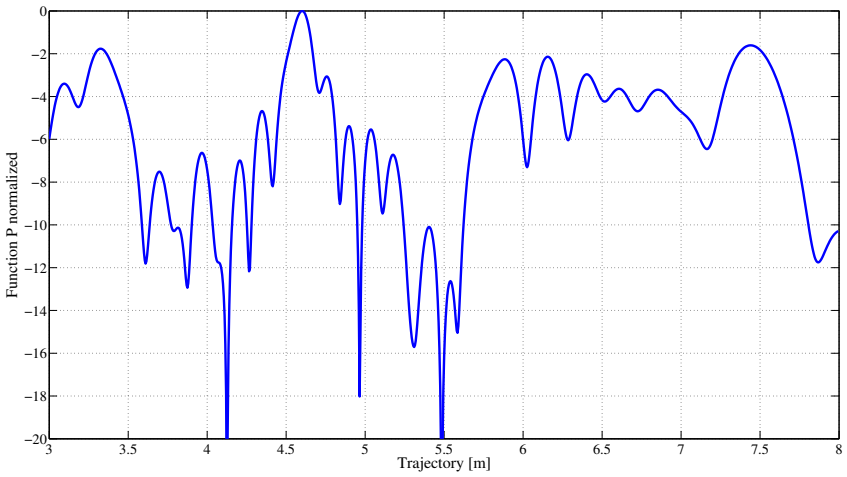

(a) Localization of the tag using algorithm C. Tag estimated in x=4.60 m.

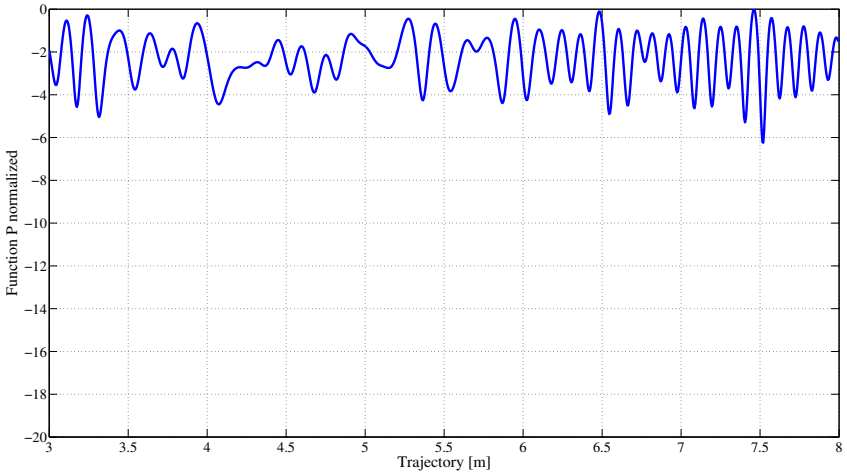

(b) Localization of the tag using algorithm D. Tag estimated in x=7.46 m.

Figure 5.19: Localization with 14 phase measurements spaced 0.3 m using algorithm C and D. True tag position: x=4.65 m. Reader trajectory-tag distance= 2 m.

	Algorithm A		Algorithm B		Algorithm C		Algorithm D	
	$\hat{x}$[m]	RMSE [m]	$\hat{x}$ [m]	RMSE [m]	$\hat{x}$ [m]	RMSE [m]	$\hat{x}$ [m]	RMSE [m]
N=42, L=4m	4.63	0.02	4.63	0.02	4.625	0.025	7.465	2.815
N=11, L=1m	4.64	0.01	4.645	0.005	4.635	0.015	7.245	2.595
N=9, L=0.8m	4.635	0.015	4.64	0.01	4.635	0.015	7.465	2.815
N=7, L=0.6m	4.6050	0.045	4.63	0.02	4.605	0.045	7.565	2.915
N=5, L=0.4m	4.585	0.065	4.635	0.015	4.585	0.065	7.565	2.915
N=5, L=0.8m	4.645	0.005	7.995	3.345	4.645	0.005	3.635	1.015
N=21, L=4m	4.625	0.025	4.625	0.025	4.62	0.03	3.635	1.015
N=14, L=4m	4.61	0.04	4.615	0.035	4.60	0.05	7.46	2.81

Table 5.1: Results for the localization when reader trajectory and tag are distant 2 meters. True tag position: x=4.65 m.

	Algorithm A		Algorithm B		Algorithm C		Algorithm D	
	$\hat{x}$ [m]	RMSE [m]	$\hat{x}$ [m]	RMSE [m]	$\hat{x}$ [m]	RMSE [m]	$\hat{x}$ [m]	RMSE [m]
N=42, L=4m	4.64	0.01	4.64	0.01	4.64	0.01	4.635	0.015
N=11, L=1m	4.645	0.005	4.645	0.005	4.645	0.005	4.64	0.01
N=9, L=0.8m	4.655	0.005	4.65	0	4.655	0.005	4.65	0
N=7, L=0.6m	4.68	0.03	4.675	0.025	4.695	0.045	4.73	0.08
N=5, L=0.4m	4.72	0.07	4.7	0.05	4.735	0.085	4.735	0.085
N=5, L=0.8m	4.645	0.005	4.485	0.165	4.64	0.01	3.12	1.53
N=21, L=4m	4.64	0.01	4.64	0.01	4.64	0.01	4.635	0.015
N=14, L=4m	4.635	0.015	4.63	0.02	4.635	0.015	4.635	0.015

Table 5.2: Results for the localization when reader trajectory and tag are distant 3 meters. True tag position: x=4.65 m.

5.1.2 2D-Localization Results

The 2D-localization algorithm uses the phase measurements collected in the linear trajectory for the previous test but in this case it assumes that the distance between reader trajectory and tag in unknown. The algorithm must localize the tag along the x-coordinate i.e., the position on the same direction of the trajectory and along the y-coordinate; in other words find the distance between reader's trajectory and tag. In this case the correlation functions generated by the algorithms are three dimensional (3D) curves where the maximum indicates the estimated location of the tag.

In this configuration we performed the 2D localization using all phase

Threshold [dBm]	Algorithm A		Algorithm B		Algorithm C		Algorithm D	
	$\hat{x}$ [m]	RMSE [m]	$\hat{x}$ [m]	RMSE [m]	$\hat{x}$ [m]	RMSE [m]	$\hat{x}$ [m]	RMSE [m]
20	4.63	0.02	4.63	0.02	4.625	0.025	7.465	2.815
15	4.625	0.025	4.63	0.02	4.62	0.03	7.465	2.815
12	4.62	0.03	4.63	0.02	4.62	0.03	7.465	2.815
10	4.6150	0.035	4.63	0.02	4.61	0.04	7.465	2.815
8	4.605	0.045	4.625	0.025	4.605	0.045	7.465	2.815
5	4.635	0.015	4.625	0.025	4.635	0.015	7.245	2.595
2	4.68	0.03	4.485	0.165	4.68	0.03	7.98	3.3

Table 5.3: Results for the localization using a threshold in order to choose some phase values. Reader trajectory and tag are distant 2 meters. True tag position: x=4.65 m.

Threshold [dBm]	Algorithm A		Algorithm B		Algorithm C		Algorithm D	
	$\hat{x}$ [m]	RMSE [m]	$\hat{x}$ [m]	RMSE [m]	$\hat{x}$ [m]	RMSE [m]	$\hat{x}$ [m]	RMSE [m]
20	4.64	0.01	4.64	0.01	4.64	0.01	4.635	0.015
15	4.64	0.01	4.64	0.01	4.64	0.01	4.635	0.015
12	4.645	0.005	4.645	0.005	4.64	0.01	4.635	0.015
10	4.64	0.01	4.645	0.005	4.64	0.01	4.635	0.015
8	4.635	0.015	4.63	0.02	4.635	0.015	4.63	0.02
5	4.63	0.02	4.625	0.025	4.63	0.02	4.625	0.025
2	4.655	0.005	4.655	0.005	4.655	0.005	4.655	0.005

Table 5.4: Results for the localization using a threshold in order to choose some phase values. Reader trajectory and tag are distant 3 meters. True tag position: x=4.65 m.

Standard Deviation [m]	Algorithm A	Algorithm B	Algorithm C	Algorithm D
	RMSE [m]	RMSE [m]	RMSE [m]	RMSE [m]
0	0.046	0.018	0.046	2.23
0.003162	0.0461	0.0189	0.0461	2.1754
0.01	0.0468	0.0204	0.0462	2.1521
0.03162	0.0479	0.1716	0.0485	1.7176
0.1	0.1053	0.9825	0.0769	1.3942
0.3162	0.5429	1.2080	0.5935	1.5253

Table 5.5: Results for the localization adding gaussian noise on the reader positions. Reader trajectory and tag are distant 2 meters. True tag position: x=4.65 m.

Standard Deviation [m]	Algorithm A	Algorithm B	Algorithm C	Algorithm D
	RMSE [m]	RMSE [m]	RMSE [m]	RMSE [m]
0	0.03	0.025	0.03	0.02
0.003162	0.0299	0.023	0.0293	0.0207
0.01	0.0308	0.0237	0.0293	0.0217
0.03162	0.0354	0.0281	0.0345	0.2139
0.1	0.0610	0.0851	0.1006	0.7430
0.3162	0.5046	0.7178	0.5501	1.0501

Table 5.6: Results for the localization adding gaussian noise on the reader positions. Reader trajectory and tag are distant 3 meters. True tag position: x=4.65 m.

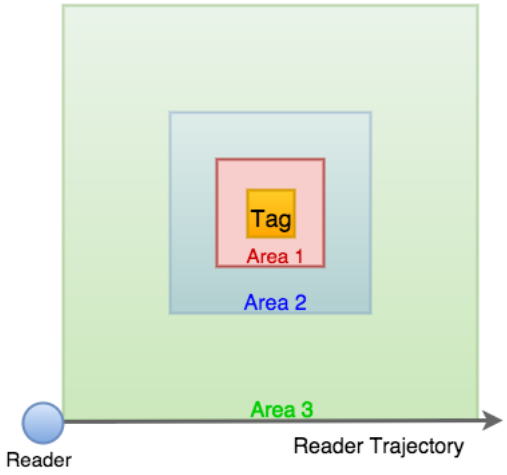

Figure 5.20: Monitored area example.

measurements in the area where the tag could be positioned, called as *monitored area*, in order to mitigate the effects of the secondary lobes. The results for different configurations are shown in Table 5.7 and Table 5.8. In tables $\hat{x}$ and $\hat{y}$ indicate the estimated coordinates of the tag.

Monitored areas are squares centered on the position of the tag with side indicated in the tables (see Figure 5.20). Tables show that the reduction of the monitored area does not improve the localization result probably because the SNR is always high in each configuration.

Looking at Figure 5.24 we can see that the algorithms that use the ML criterion to localize the tag have the correlation function with narrower peak

than other algorithms, implying a more accurate localization, but present secondary peaks with amplitude similar to the main one.

In Figure 5.25 it is possible to see that the localization of the x-coordinate of the tag presents a clear peak in the estimated position and the shape of the curve, looking from the side of the trajectory, is equal to the corresponding configuration in the 1D-localization. The y-coordinate estimation is harder because the phase measures are taken along the x axis, so they do not include reliable information about the distance between tag and reader. Effectively, looking from the y side, the correlation function P presents a not well defined peak.

Monitoring Area Side	Algorithm A			Algorithm B			Algorithm C			Algorithm D		
	$\hat{x}$ [m]	$\hat{y}$ [m]	RMSE [m]	$\hat{x}$ [m]	$\hat{y}$ [m]	RMSE [m]	$\hat{x}$ [m]	$\hat{y}$ [m]	RMSE [m]	$\hat{x}$ [m]	$\hat{y}$ [m]	RMSE [m]
Trajectory length	4.64	1.905	0.0955	4.62	1.8	0.2022	4.62	1.905	0.0996	4.62	1.89	0.114
50cm	4.63	1.89	0.1118	4.63	1.99	0.0224	4.63	1.9	0.1020	4.625	1.89	0.1128
100cm	4.63	1.89	0.1118	4.63	1.99	0.0224	4.63	1.9	0.1020	4.62	1.89	0.114
200cm	4.63	1.90	0.0955	4.63	1.8	0.2010	4.63	1.9	0.1020	4.61	1.8	0.2040

Table 5.7: Results for 2D localization. Reader trajectory and tag are distant 2 meters. True tag position $\mathbf{p} = (4.65, 2)$m.

Monitoring Area Side	Algorithm A			Algorithm B			Algorithm C			Algorithm D		
	$\hat{x}$ [m]	$\hat{y}$ [m]	RMSE [m]	$\hat{x}$ [m]	$\hat{y}$ [m]	RMSE [m]	$\hat{x}$ [m]	$\hat{y}$ [m]	RMSE [m]	$\hat{x}$ [m]	$\hat{y}$ [m]	RMSE [m]
Trajectory length	4.65	3.08	0.08	4.65	3	0	4.65	3.08	0.08	4.65	3.08	0.08
50cm	4.64	3.08	0.0806	4.64	3.175	0.1753	4.64	3.09	0.0906	4.64	3.08	0.0806
100cm	4.64	3.08	0.0806	4.64	2.99	0.0141	4.64	3.09	0.0906	4.64	3.08	0.0806
200cm	4.65	3.08	0.08	4.65	3.18	0.18	4.63	3.1	0.1020	4.63	3.08	0.0825

Table 5.8: Results for 2D localization. Reader trajectory and tag are distant 3 meters. True tag position $\mathbf{p} = (4.65, 3)$m.

5.2 Angular trajectory

Another considered measurement setup was an angular trajectory. The reader is moving along a right angle trajectory around the tag where each 0.1 m performs a phase measurement (see Figure 5.26). The tag is located in $\mathbf{p} = (1.5, 1.5)$ m and in the first setup its position is not parallel with respect to any portion of the trajectory, so it can be read by each reader spot. Instead, in the second setup, the tag is parallel to the x axis of the trajectory. In this situation we have collected many phase measurements along the x axis and few values when the reader is moving along the y axis because

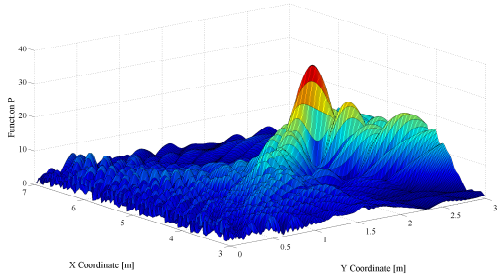

(a) 2D localization using algorithm A.

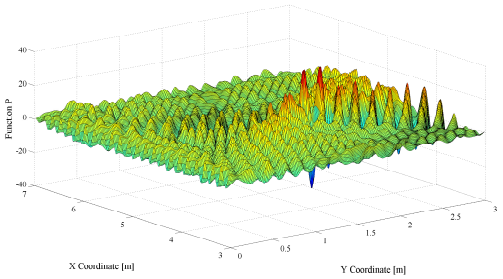

(b) 2D localization using algorithm B.

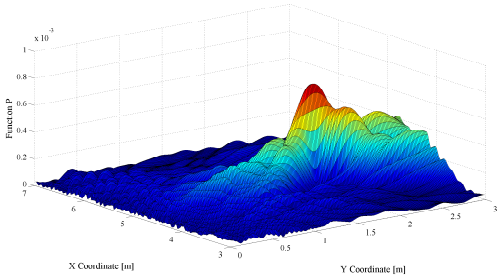

(c) 2D localization using algorithm C.

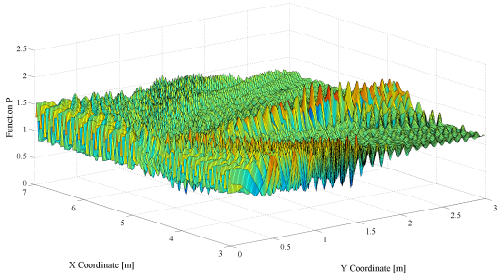

(d) 2D localization using algorithm D.

Figure 5.21: Localization with 42 phase measurements. True tag position $\mathbf{p} = (4.65, 2)$m.

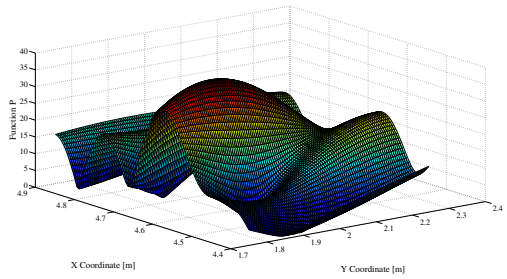

(a) 2D localization using algorithm A.

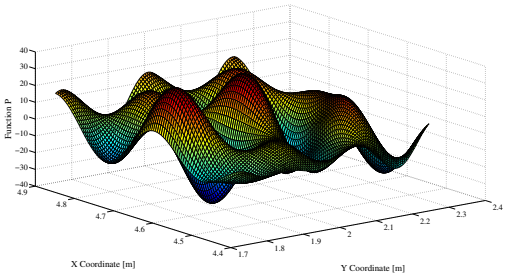

(b) 2D localization using algorithm B.

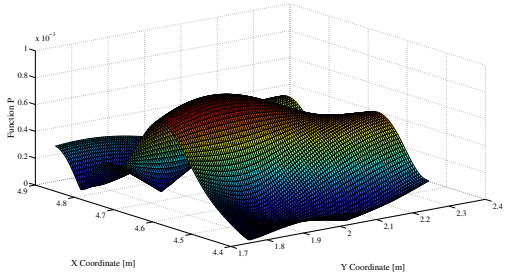

(c) 2D localization using algorithm C.

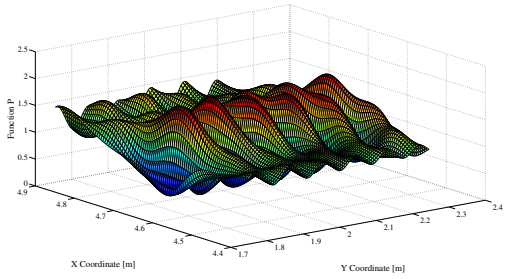

(d) 2D localization using algorithm D.

Figure 5.22: Localization with 42 phase measurements in a monitored area with side equal to 50 cm. True tag position $\mathbf{p} = (4.65, 2)$m.

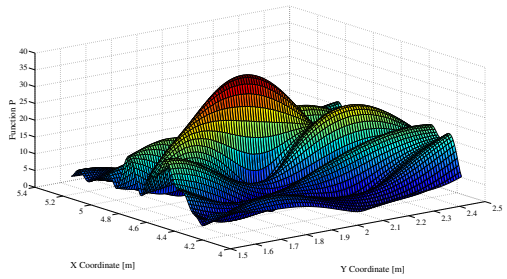

(a) 2D localization using algorithm A.

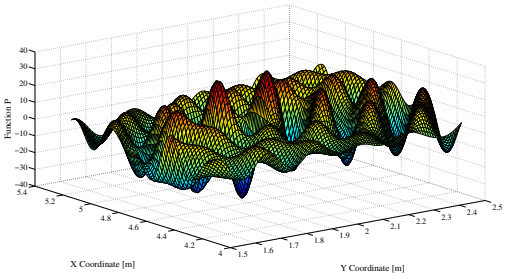

(b) 2D localization using algorithm B.

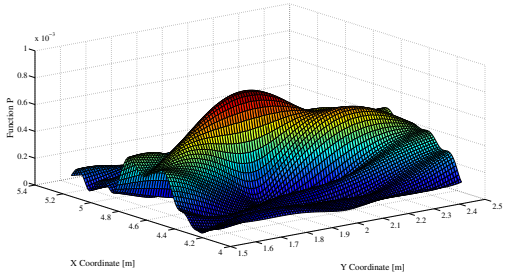

(c) 2D localization using algorithm C.

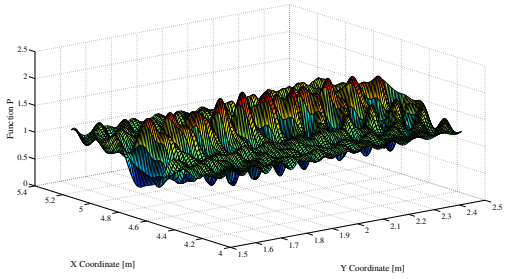

(d) 2D localization using algorithm D.

Figure 5.23: Localization with 42 phase measurements in a monitored area with side equal to 100 cm. True tag position $\mathbf{p} = (4.65, 2)$m.

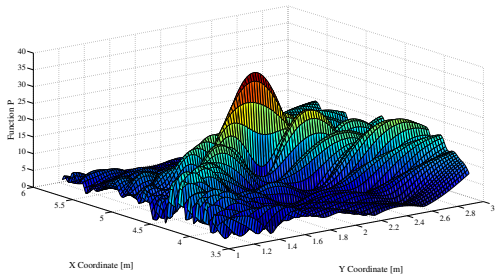

(a) 2D localization using algorithm A.

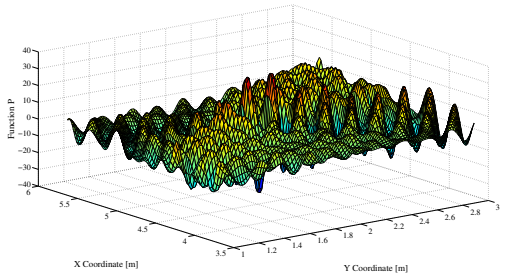

(b) 2D localization using algorithm B.

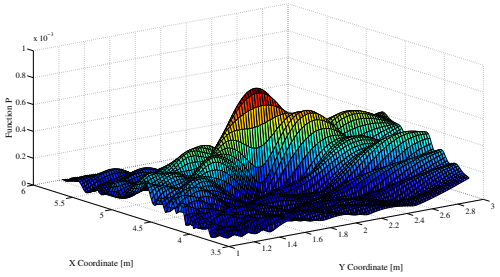

(c) 2D localization using algorithm C.

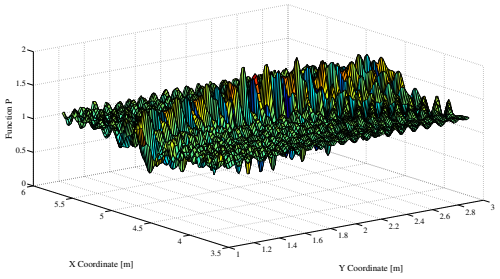

(d) 2D localization using algorithm D.

Figure 5.24: Localization with 42 phase measurements in a monitored area with side equal to 200 cm. True tag position $\mathbf{p} = (4.65, 2)$m.

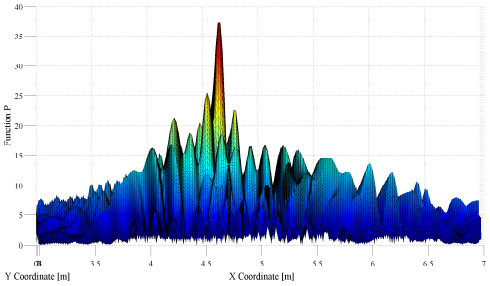

(a) 2D localization using algorithm A looking the function from the x axis.

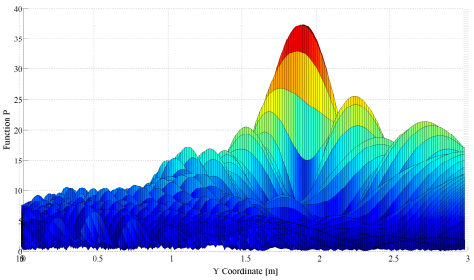

(b) 2D localization using algorithm A looking the function from the y axis.

Figure 5.25: Correlation function of the algorithm A using all phase measurements viewed from x axis and y axis. True tag position $\mathbf{p} = (4.65, 2)$m.

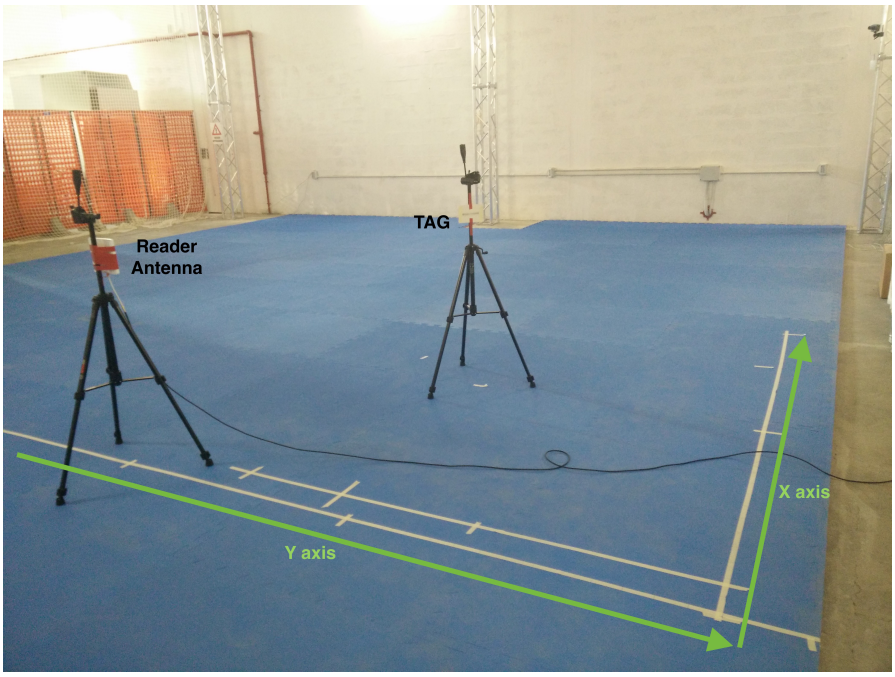

Figure 5.26: Angular trajectory setup.

when the tag is orthogonal to the trajectory hardly it can be read due to its antenna pattern. The reader antenna is always oriented to the target.

Table 5.9 and Table 5.10 show the results of the localization using all phase measurements collected or only a restricted number N of values centered in the portion of the trajectory opposite to the tag location. Reducing the number N of phase values used in the localization process slightly improves the RMSE, but looking for example at Figure 5.27 and Figure 5.28, it increases for all algorithms used, the amplitude of the secondary lobes raising the probability of a wrong localization.

The localization of the x-coordinates when the tag is parallel to the x axis using all the phase values collected is very precise, because we have a lot of measures. Instead the y-coordinate localized has a high error because it was possible to read the tag in few reader positions.

The last test implemented is the localization using phase measures received with a certain power level. The threshold model used is the same as the 1D localization in a linear trajectory i.e., a measured phase is used in the process only if its received power level is between the maximum power

received and the latter minus the threshold. In the case of tag not parallel to any portion of the trajectory, using a threshold approximately equal to 8 dB or 5dB can slightly improve the localization. In the configuration of tag parallel to a side of the trajectory, using this model increases the RMSE. The results are reported in Table 5.11 and Table 5.12

In tables $\hat{x}$ and $\hat{y}$ indicate the estimated coordinates of the tag.

Phase measures used	Algorithm A			Algorithm B			Algorithm C			Algorithm D		
	$\hat{x}$ [m]	$\hat{y}$ [m]	RMSE [m]	$\hat{x}$ [m]	$\hat{y}$ [m]	RMSE [m]	$\hat{x}$ [m]	$\hat{y}$ [m]	RMSE [m]	$\hat{x}$ [m]	$\hat{y}$ [m]	RMSE [m]
All	1.56	1.56	0.0849	1.56	1.56	0.0849	1.56	1.56	0.0849	1.56	1.56	0.0849
N=5	1.515	1.50	0.015	1.485	1.485	0.0335	1.515	1.5	0.015	1.485	1.56	0.0618
N=9	1.56	1.545	0.075	1.575	1.575	0.096	1.575	1.56	0.096	1.575	1.56	0.096

Table 5.9: Results for the localization with an angular trajectory where the tag is not parallel to any portion of the trajectory. N indicates the number of central phase measurements used. True tag position $\mathbf{p} = (1.5, 1.5)$ m.

Phase measures used	Algorithm A			Algorithm B			Algorithm C			Algorithm D		
	$\hat{x}$ [m]	$\hat{y}$ [m]	RMSE [m]	$\hat{x}$ [m]	$\hat{y}$ [m]	RMSE [m]	$\hat{x}$ [m]	$\hat{y}$ [m]	RMSE [m]	$\hat{x}$ [m]	$\hat{y}$ [m]	RMSE [m]
All	1.5	1.635	0.135	1.5	1.635	0.135	1.5	1.635	0.135	1.5	1.74	0.24
N=5	1.62	1.485	0.1209	1.605	1.485	0.1016	1.62	1.485	0.1209	1.515	1.47	0.0335
N=9	1.62	1.485	0.1209	1.605	1.47	0.1092	1.53	1.335	0.1677	1.515	1.47	0.0335

Table 5.10: Results for the localization with an angular trajectory where the tag is parallel to the x axis. N indicates the number of central phase measurements used. True tag position $\mathbf{p} = (1.5, 1.5)$ m.

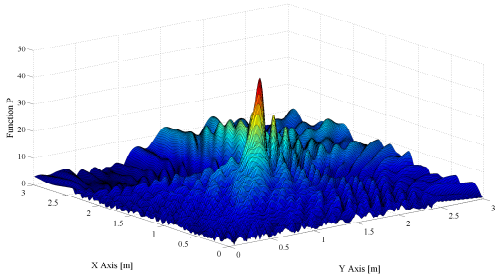

(a) 2D localization using algorithm A.

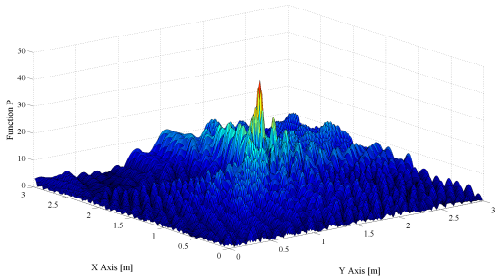

(b) 2D localization using algorithm B.

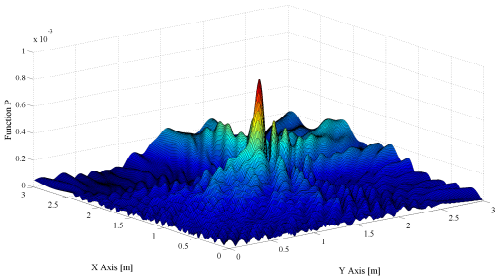

(c) 2D localization using algorithm C.

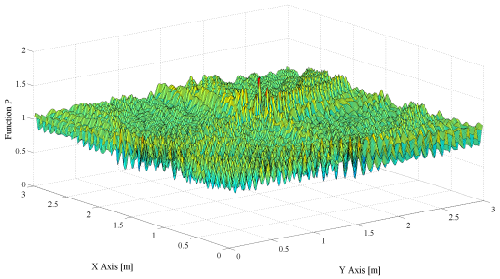

(d) 2D localization using algorithm D.

Figure 5.27: Localization with all phase measurements in angular trajectory with the tag not parallel to any portion of the trajectory. True tag position $\mathbf{p} = (1.5, 1.5)$ m.

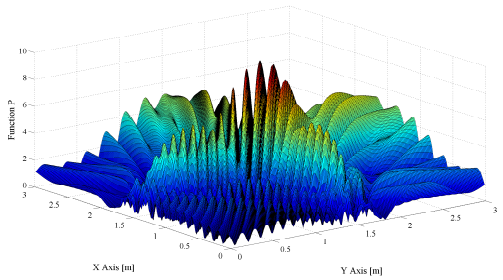

(a) 2D localization using algorithm A.

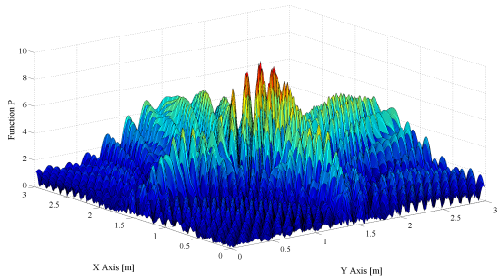

(b) 2D localization using algorithm B.

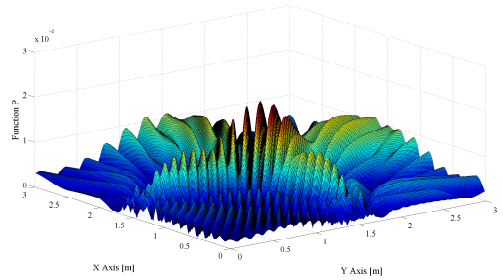

(c) 2D localization using algorithm C.

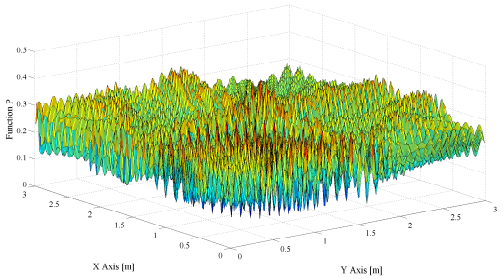

(d) 2D localization using algorithm D.

Figure 5.28: Localization with the 5 central phase measurements in angular trajectory with the tag not parallel to any portion of the trajectory. True tag position $\mathbf{p} = (1.5, 1.5)$ m.

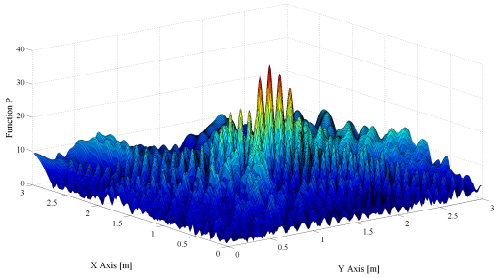

(a) 2D localization using algorithm A.

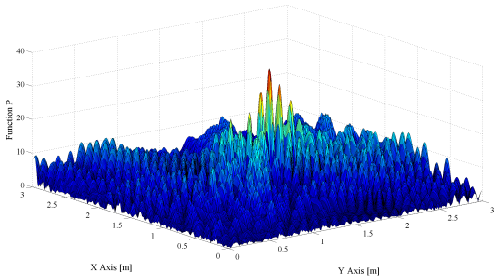

(b) 2D localization using algorithm B.

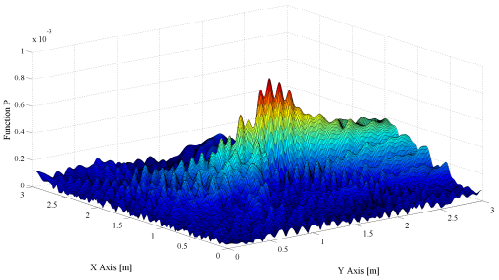

(c) 2D localization using algorithm C.

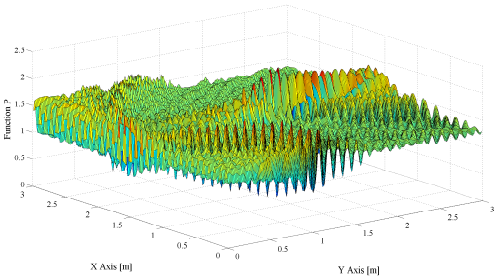

(d) 2D localization using algorithm D.

Figure 5.29: Localization with all phase measurements in angular trajectory with the tag parallel to the x-axis. True tag position $\mathbf{p} = (1.5, 1.5)$ m.

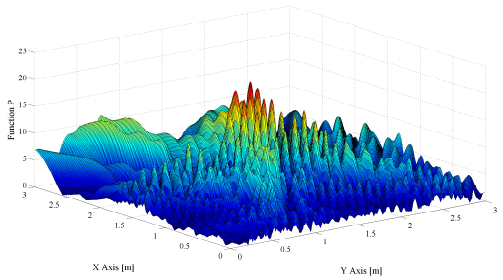

(a) 2D localization using algorithm A.

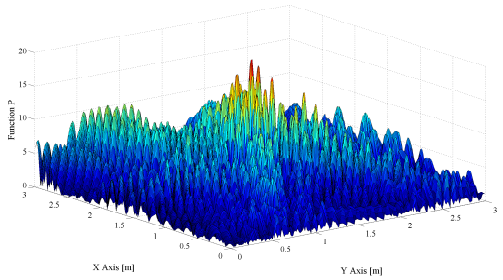

(b) 2D localization using algorithm B.

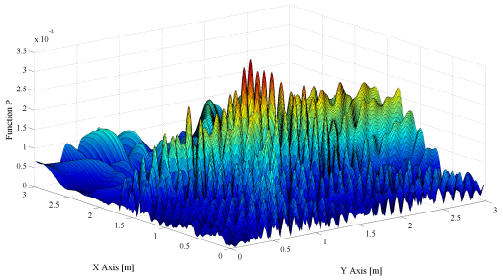

(c) 2D localization using algorithm C.

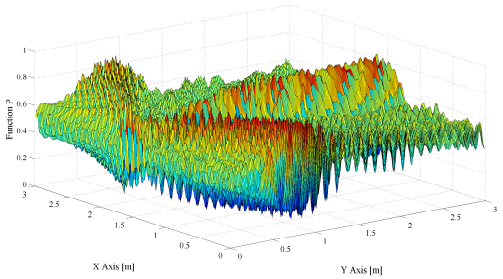

(d) 2D localization using algorithm D.

Figure 5.30: Localization with the 5 central phase measurements in angular trajectory with the tag parallel to the x-axis. True tag position $\mathbf{p} = (1.5, 1.5)$ m.

Threshold [dBm]	Algorithm A			Algorithm B			Algorithm C			Algorithm D		
	$\hat{x}$ [m]	$\hat{y}$ [m]	RMSE [m]	$\hat{x}$ [m]	$\hat{y}$ [m]	RMSE [m]	$\hat{x}$ [m]	$\hat{y}$ [m]	RMSE [m]	$\hat{x}$ [m]	$\hat{y}$ [m]	RMSE [m]
10	1.56	1.56	0.0849	1.56	1.56	0.0849	1.56	1.545	0.075	1.575	1.545	0.0875
8	1.56	1.545	0.075	1.56	1.56	0.0849	1.545	1.53	0.0541	1.575	1.56	0.096
5	1.545	1.53	0.0541	1.575	1.545	0.0875	1.545	1.53	0.0541	1.575	1.545	0.0875
3	1.545	1.515	0.0474	1.575	1.545	0.0875	1.545	1.515	0.0474	1.575	1.545	0.0875

Table 5.11: Results for the localization with an angular trajectory where the tag is not parallel to any portion of the trajectory. A threshold is used to select the phase measures. True tag position $\mathbf{p} = (1.5, 1.5)$ m.

Threshold [dBm]	Algorithm A			Algorithm B			Algorithm C			Algorithm D		
	$\hat{x}$ [m]	$\hat{y}$ [m]	RMSE [m]	$\hat{x}$ [m]	$\hat{y}$ [m]	RMSE [m]	$\hat{x}$ [m]	$\hat{y}$ [m]	RMSE [m]	$\hat{x}$ [m]	$\hat{y}$ [m]	RMSE [m]
10	1.5	1.635	0.135	1.5	1.635	0.135	1.5	1.635	0.135	1.515	1.65	0.1507
8	1.5	1.635	0.135	1.5	1.635	0.135	1.5	1.635	0.135	1.515	1.65	0.1507
5	1.515	1.65	0.1507	1.515	1.65	0.1507	1.515	1.65	0.1507	1.5	1.635	0.135
3	1.515	1.65	0.1507	1.515	1.65	0.1507	1.515	1.65	0.1507	1.515	1.815	0.3154

Table 5.12: Results for the localization with an angular trajectory where the tag is parallel to the x axis of the trajectory. A threshold is used to select the phase measures. True tag position $\mathbf{p} = (1.5, 1.5)$ m.

Chapter 6

Conclusions

In this thesis the performance of RFID tag localization with virtual multi-antenna systems were evaluated. First, the principal RFID phase-based localization techniques present in literature were studied. Then, the ML estimator for the considered problem was derived.

A Matlab simulator was built in order to evaluate the behavior of the system and understand the parameters that influence the performance. We discovered that a reader position not perfectly known can drastically affect the RMSE of the estimated target location.

Successively, we carried out a measurement campaign in a real indoor scenario moving the reader on a linear trajectory and on an angular trajectory. Starting from the measurements taken in the two different configurations we applied the algorithms proposed in order to see their differences. We noticed that there is not a big difference in terms of localization error between the algorithm derived from the ML criterion and the holographic localization method proposed in literature. The first presents a correlation function with a sharper main peak while the second has a smoother function. This means that the ML criterion has a higher accuracy. This method also presents secondary lobes with amplitude higher than the holographic localization method. This increases the possibility of a wrong localization due to ambiguity problems, which leads to outliers generated by high secondary lobes.

Moreover, we discovered that the information about the RSS of the single phase measures used in the localization process does not always improve the performance.

The resultant accuracy of the algorithms is on average equal to few centimeters; in the worst cases seen the RMSE of the localization is always less than 0.2 m.

Future developments of this work could consider the testing of the algorithms using a real time automatic system in an environment with many tags that can collect many phase measurements and accurate odometers to measure the distance between consecutive reader positions. Another research aspect to be addressed could consider efficient methods for estimating the relative distance of unknown tags with respect to reference tags present in the environment.

Appendix A

1D-Localization Results

This appendix shows the results obtained with 1D-localization when reader trajectory and tag distance is equal to 3 meter.

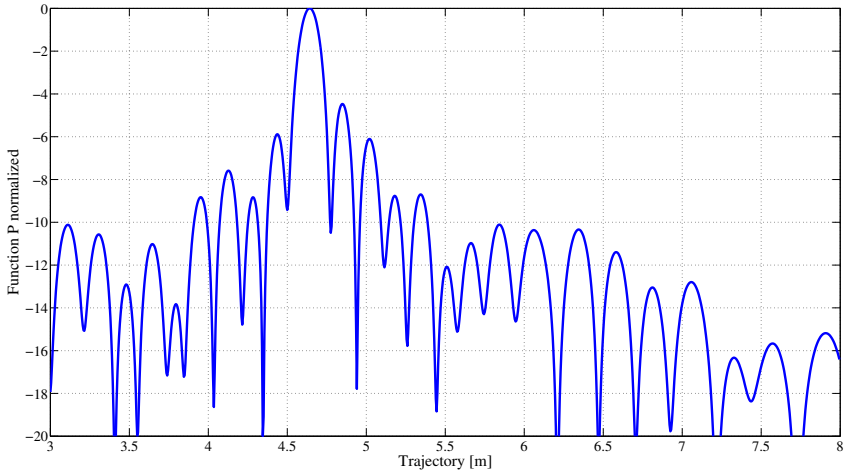

(a) Localization of the tag using algorithm A. Tag estimate in x =4.64 m.

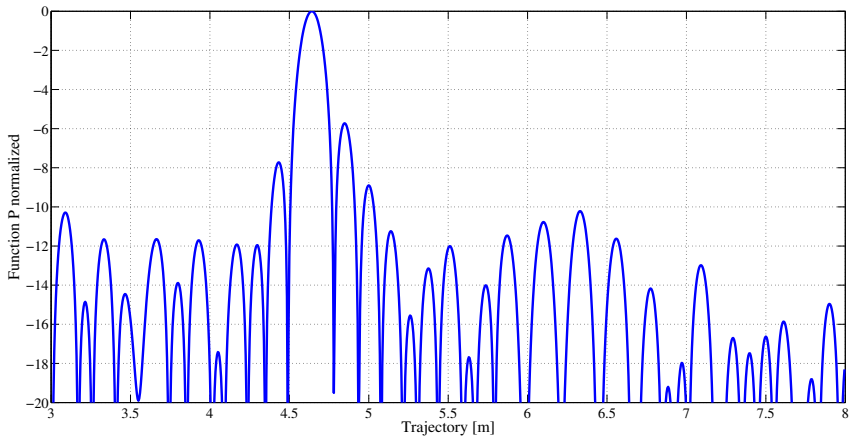

(b) Localization of the tag using algorithm B. Tag estimate in x =4.64 m.

Figure A.1: Localization using algorithm A and B and 42 the phase measurements. True tag position: x =4.65 m. Reader trajectory-tag distance = 3 m.

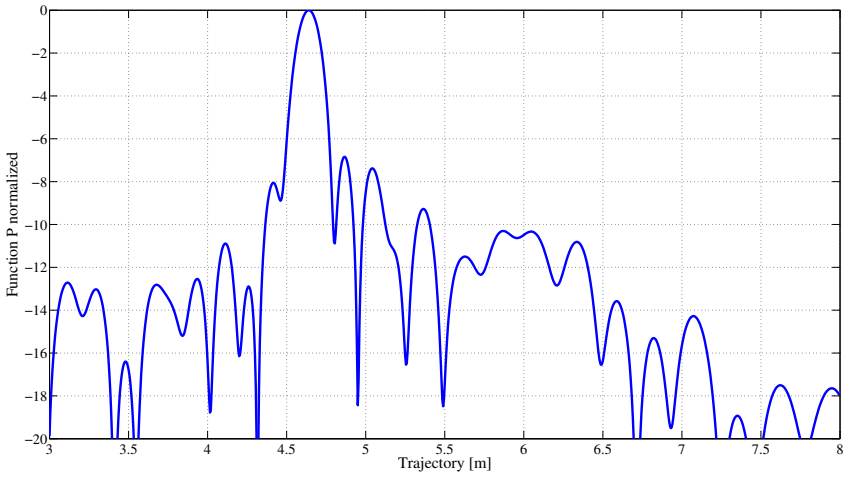

(a) Localization of the tag using algorithm C. Tag estimate in x =4.64 m.

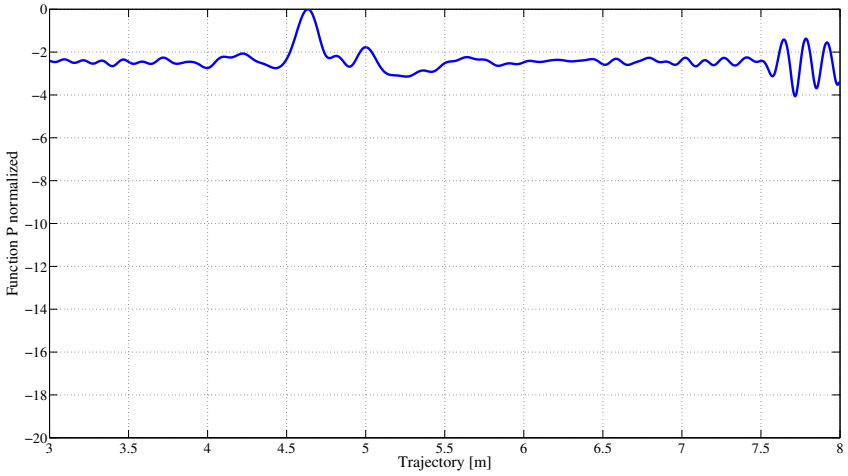

(b) Localization of the tag using algorithm D. Tag estimate in x =4.635 m.

Figure A.2: Localization using algorithm C and D and all the phase measurements. True tag position: x =4.65 m. Reader trajectory-tag distance = 3 m.

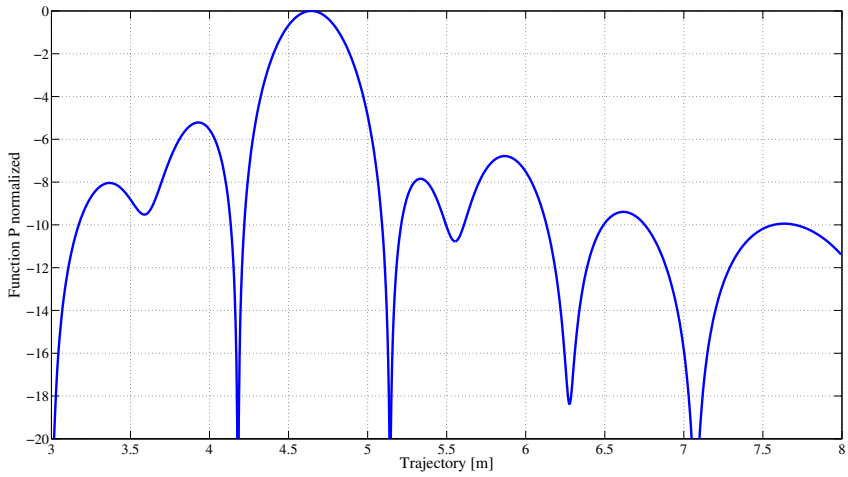

(a) Localization of the tag using algorithm A. Tag estimate in x =4.645 m.

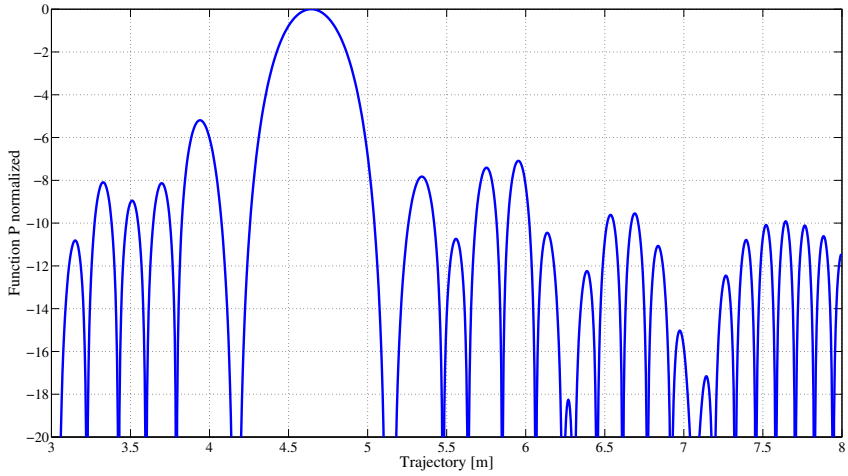

(b) Localization of the tag using algorithm B. Tag estimate in x =4.645 m.

Figure A.3: Localization with the 11 central measures spaced 0.1 m using algorithm A and B. True tag position: x =4.65 m. Reader trajectory-tag distance = 3 m.

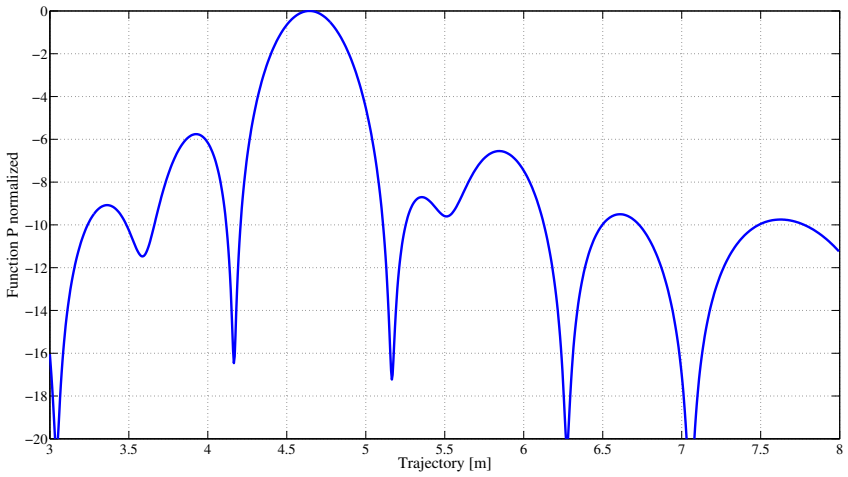

(a) Localization of the tag using algorithm C. Tag estimate in x =4.645 m.

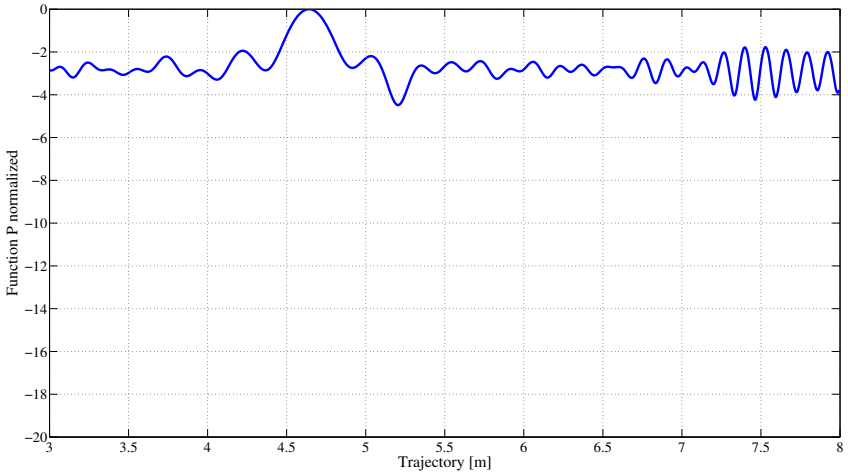

(b) Localization of the tag using algorithm D. Tag estimate in x =4.64 m.

Figure A.4: Localization with the 11 central measures spaced 0.1 m using algorithm C and D. True tag position: x =4.65 m. Reader trajectory-tag distance = 3 m.

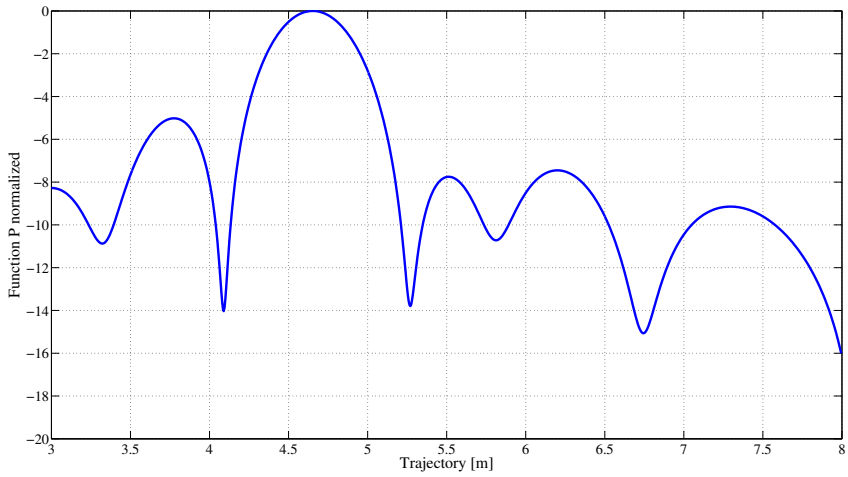

(a) Localization of the tag using algorithm A. Tag estimate in x =4.655 m.

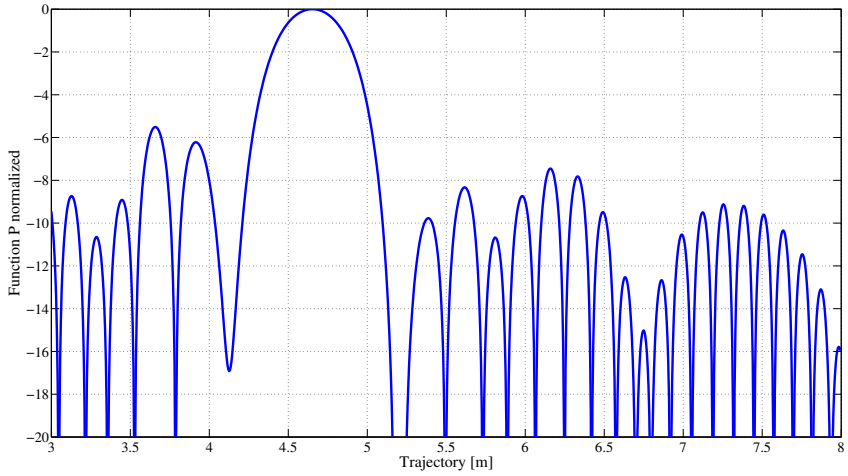

(b) Localization of the tag using algorithm B. Tag estimate in x =4.65 m.

Figure A.5: Localization with the 9 central measures spaced 0.1 m using algorithm A and B. True tag position: x =4.65 m. Reader trajectory-tag distance = 3 m.

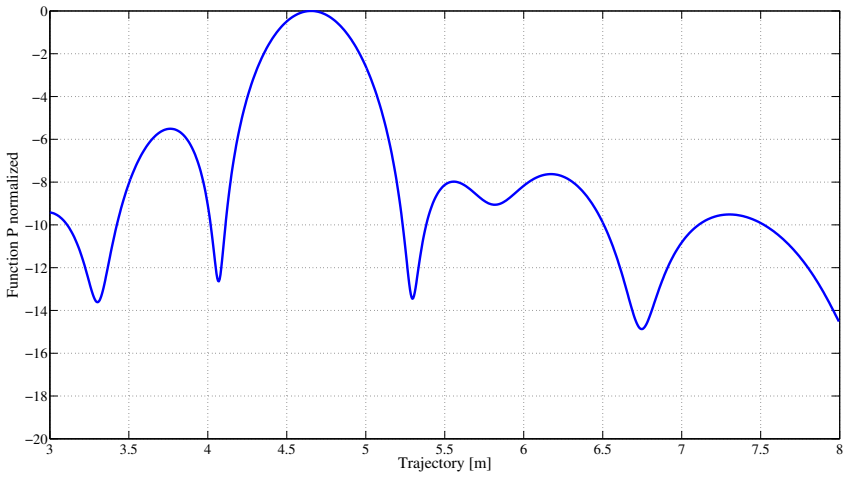

(a) Localization of the tag using algorithm C. Tag estimate in x =4.655 m.

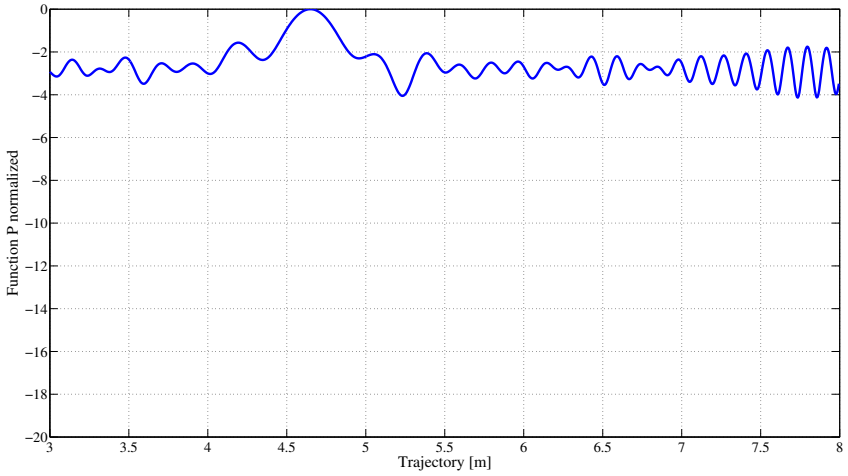

(b) Localization of the tag using algorithm D. Tag estimate in x =4.65 m.

Figure A.6: Localization with the 9 central measures spaced 0.1 m using algorithm C and D. True tag position: x =4.65 m. Reader trajectory-tag distance = 3 m.

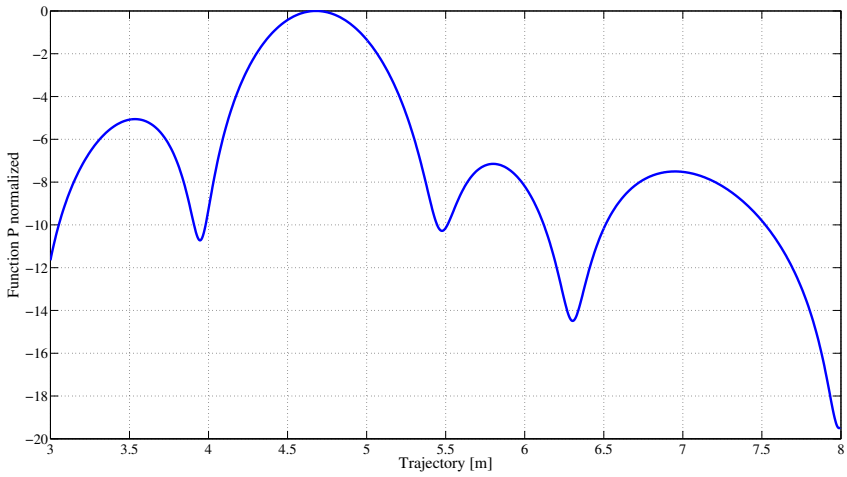

(a) Localization of the tag using algorithm A. Tag estimate in x =4.68 m.

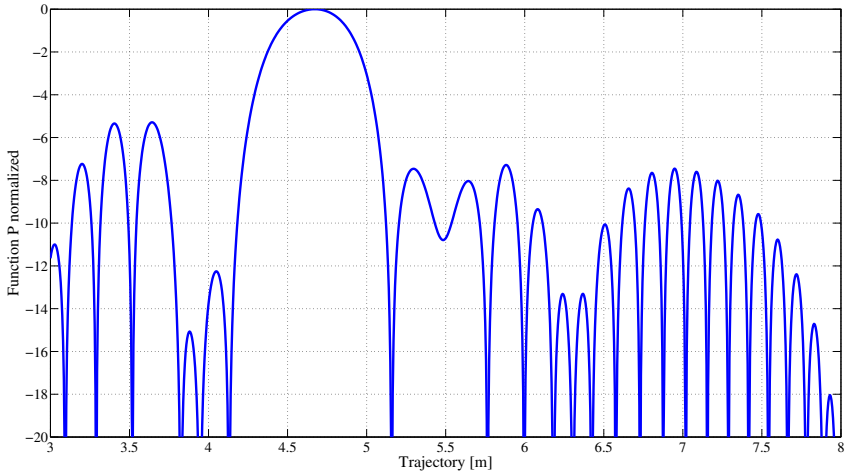

(b) Localization of the tag using algorithm B. Tag estimate in x =4.675 m.

Figure A.7: Localization with the 7 central measures spaced 0.1 m using algorithm A and B. True tag position: x =4.65 m. Reader trajectory-tag distance = 3 m.

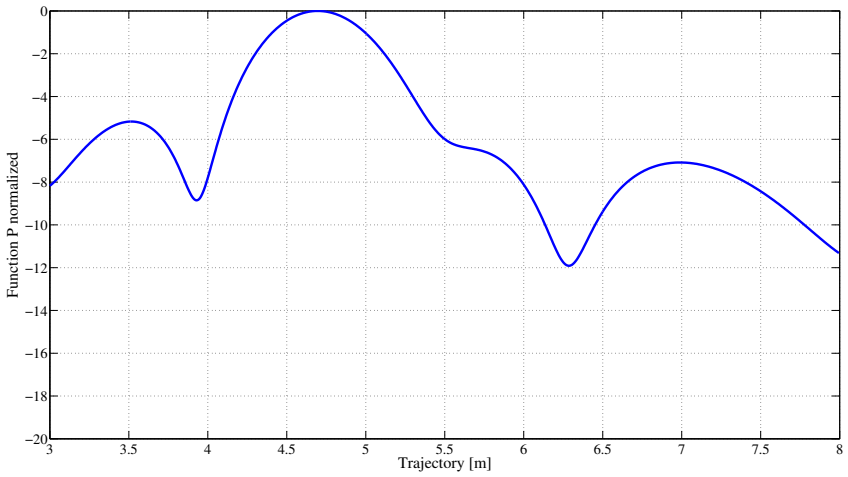

(a) Localization of the tag using algorithm C. Tag estimate in x =4.695 m.

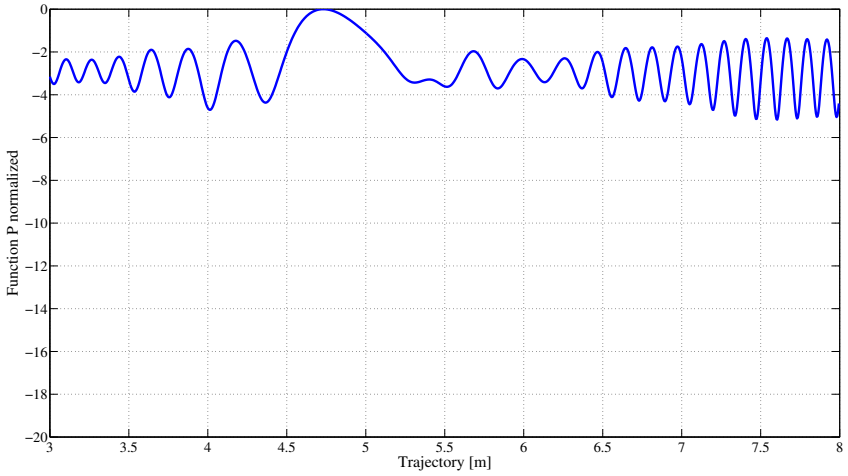

(b) Localization of the tag using algorithm D. Tag estimate in x =4.73 m.

Figure A.8: Localization with the 7 central measures spaced 0.1 m using algorithm C and D. True tag position: x =4.65 m. Reader trajectory-tag distance = 3 m.

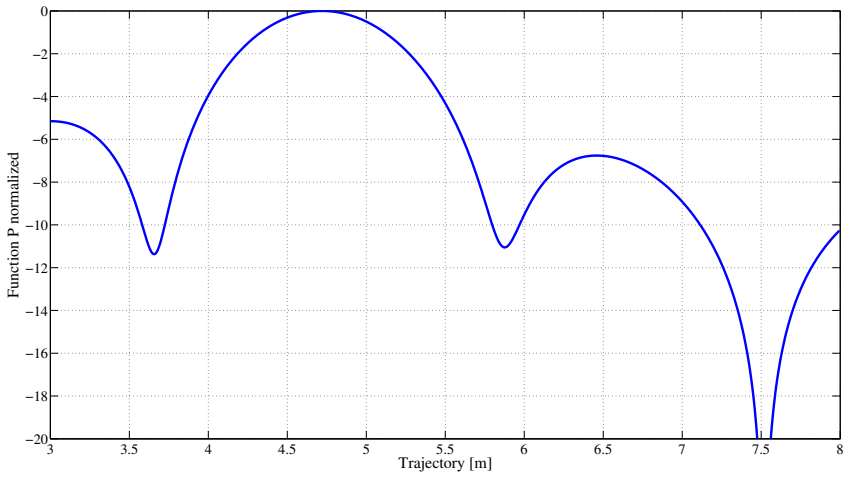

(a) Localization of the tag using algorithm A. Tag estimate in x =4.7 m.

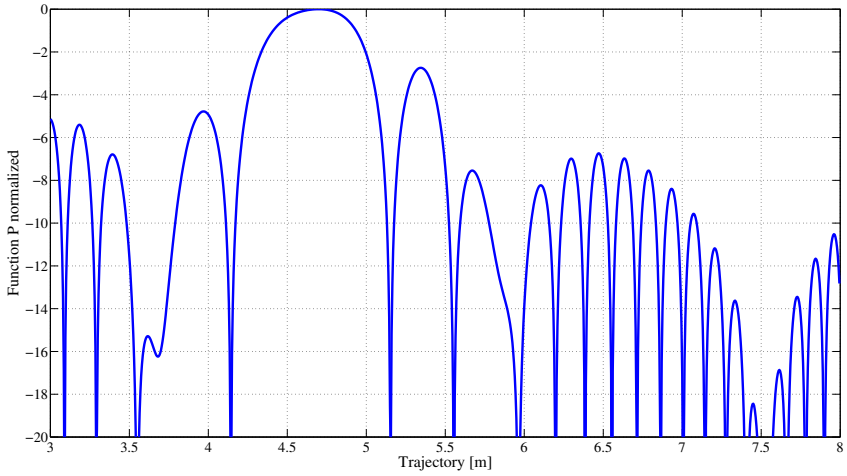

(b) Localization of the tag using algorithm B. Tag estimate in x =4.7 m.

Figure A.9: Localization with the 5 central measures spaced 0.1 m using algorithm A and B. True tag position: x =4.65 m. Reader trajectory-tag distance = 3 m.

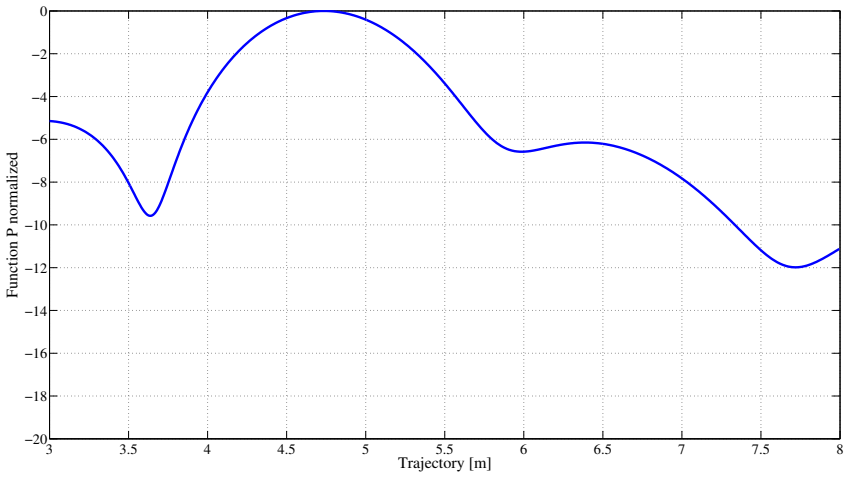

(a) Localization of the tag using algorithm C. Tag estimate in x =4.735 m.

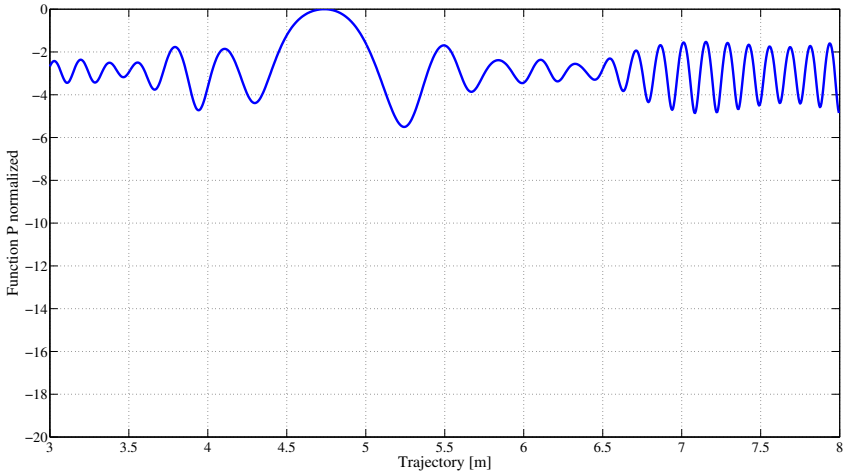

(b) Localization of the tag using algorithm D. Tag estimate in x =4.735 m.

Figure A.10: Localization with the 5 central spaced 0.1 m measures using algorithm C and D. True tag position: x =4.65 m. Reader trajectory-tag distance = 3 m.

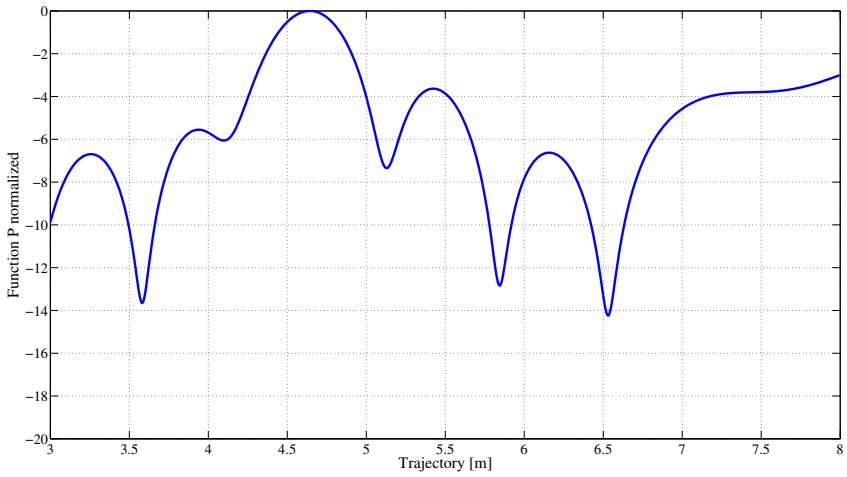

(a) Localization of the tag using algorithm A. Tag estimate in x =4.645 m.

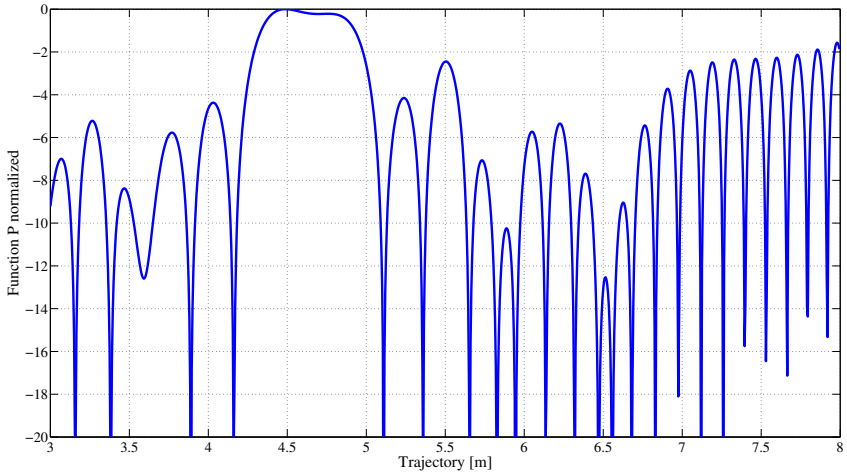

(b) Localization of the tag using algorithm B. Tag estimate in x =4.485 m.

Figure A.11: Localization with the 5 central spaced 0.2 m measures using algorithm A and B. True tag position: x =4.65 m. Reader trajectory-tag distance = 3 m.

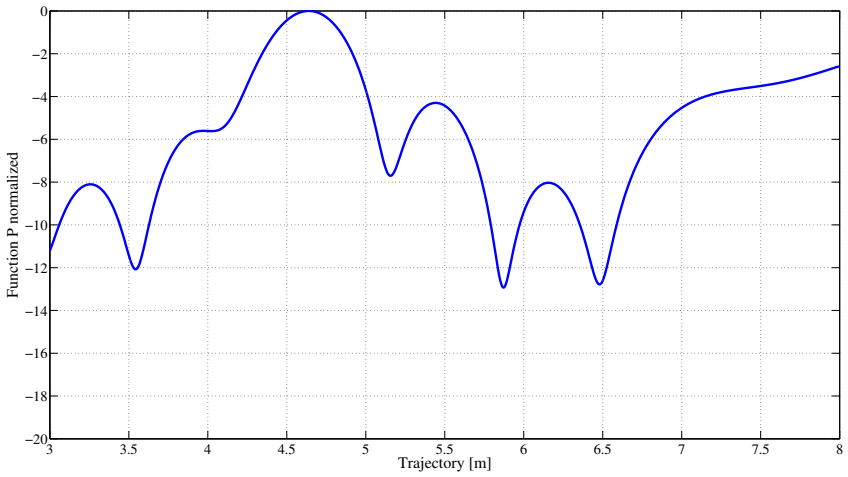

(a) Localization of the tag using algorithm C. Tag estimate in x =4.64 m.

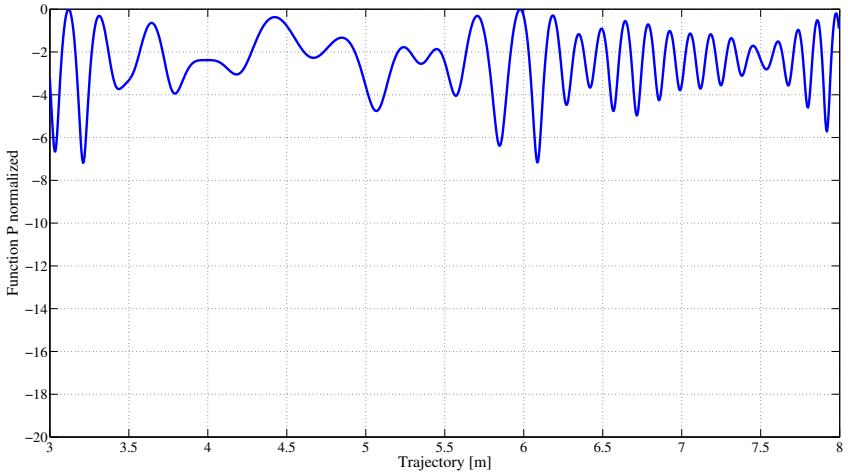

(b) Localization of the tag using algorithm D. Tag estimate in x =3.12 m.

Figure A.12: Localization with the 5 central measures spaced 0.2 m using algorithm C and D. True tag position: x =4.65 m. Reader trajectory-tag distance = 3 m.

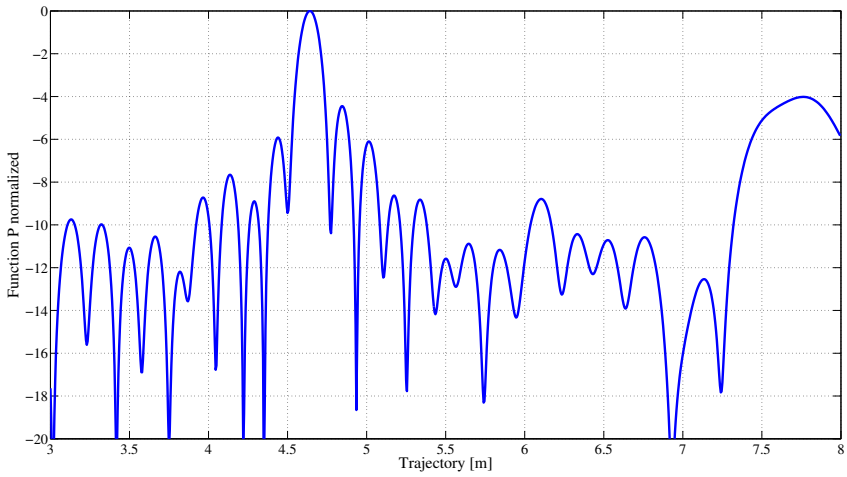

(a) Localization of the tag using algorithm A. Tag estimate in x =4.645 m.

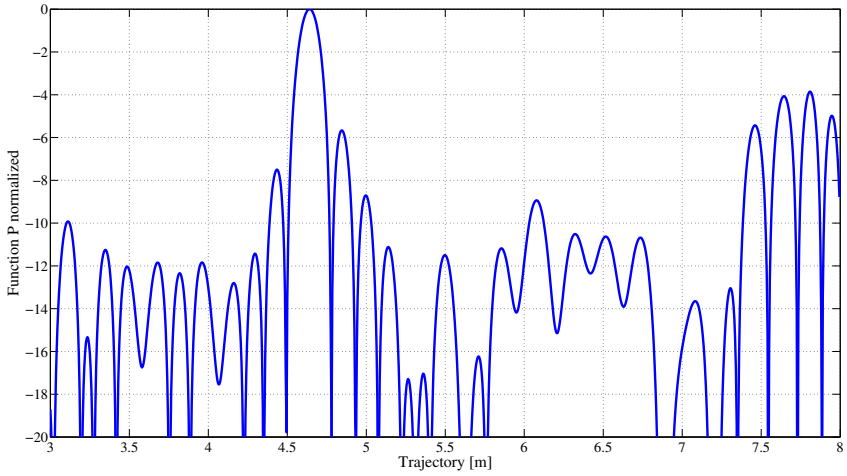

(b) Localization of the tag using algorithm B. Tag estimate in x =4.485 m.

Figure A.13: Localization with 21 phase measurements spaced 0.2 m measures using algorithm A and B. True tag position: x =4.65 m. Reader trajectory-tag distance = 3 m.

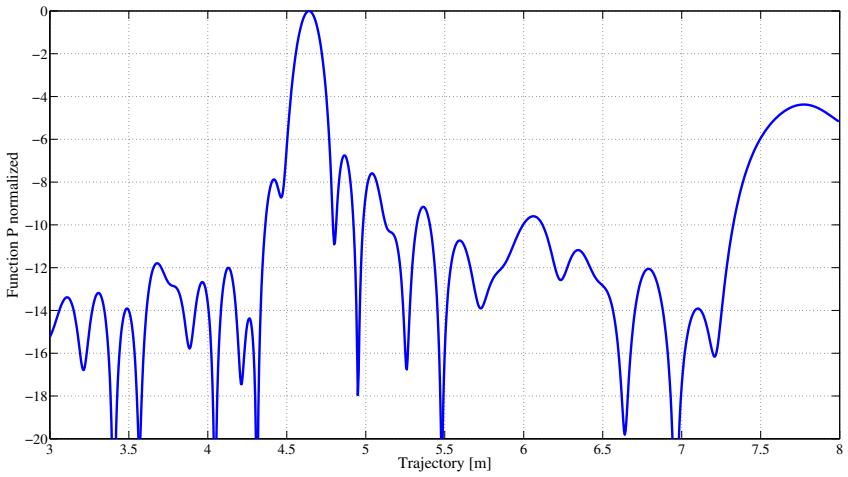

(a) Localization of the tag using algorithm C. Tag estimate in x =4.64 m.

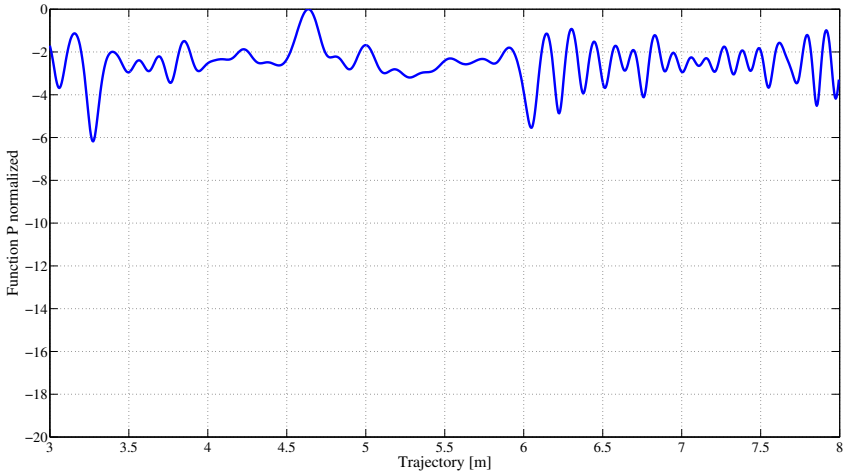

(b) Localization of the tag using algorithm D. Tag estimate in x =4.635 m.

Figure A.14: Localization with 21 phase measurements spaced 0.2 m using algorithm C and D. True tag position: x =4.65 m. Reader trajectory-tag distance = 3 m.

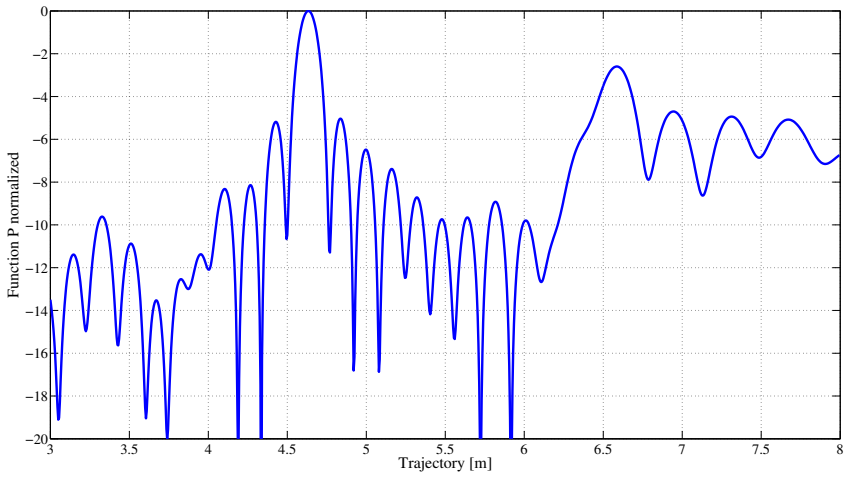

(a) Localization of the tag using algorithm A. Tag estimate in x =4.635 m.

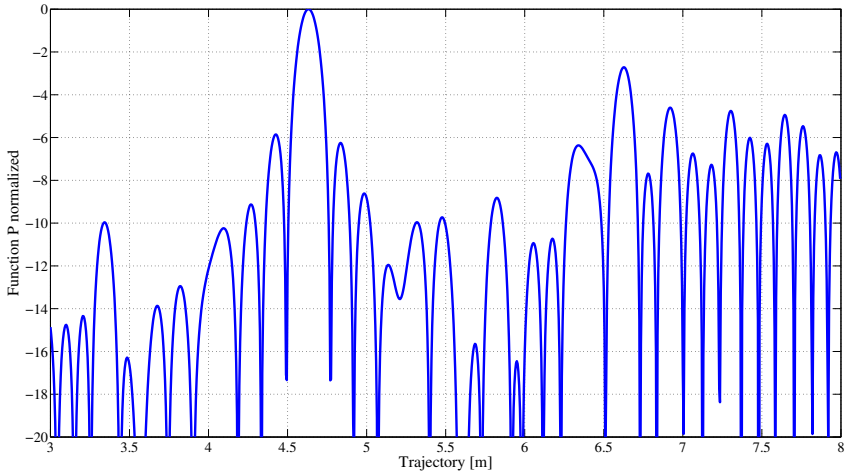

(b) Localization of the tag using algorithm B. Tag estimate in x =4.63 m.

Figure A.15: Localization with 14 phase measurements spaced 0.3 m measures using algorithm A and B. True tag position: x =4.65 m. Reader trajectory-tag distance = 3 m.

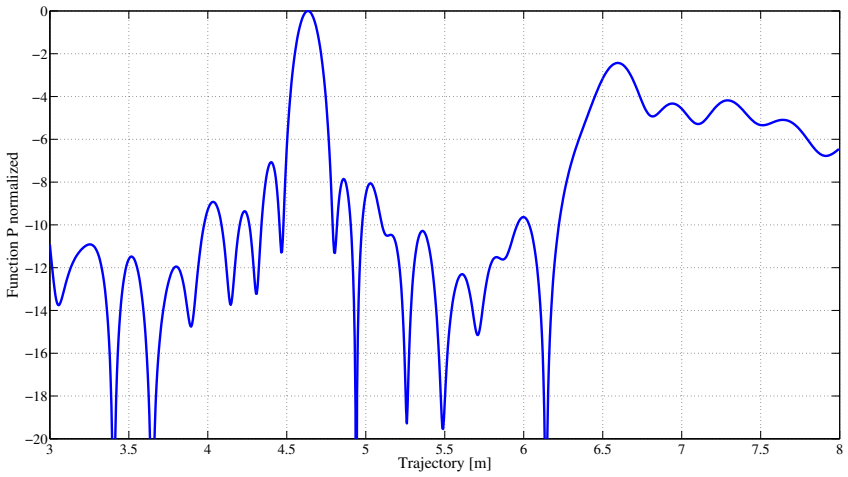

(a) Localization of the tag using algorithm C. Tag estimate in x =4.635 m.

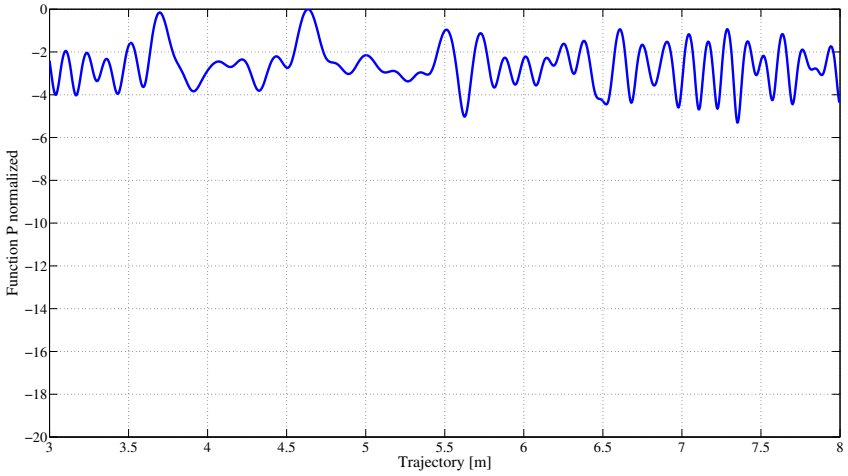

(b) Localization of the tag using algorithm D. Tag estimate in x =4.635 m.

Figure A.16: Localization with 14 phase measurements spaced 0.3 m using algorithm C and D. True tag position: x =4.65 m. Reader trajectory-tag distance = 3 m.

Acknowledgments

Prima di tutti vorrei ringraziare il Prof. Davide Dardari e il Dott. Nicoló Decarli per avermi dato la possibilitá di lavorare a questo interessante progetto, per avermi aiutato e dato preziosi consigli durante tutto questo periodo di tesi.

Vorrei ringraziare tutta la mia famiglia per avermi supportato e sopportato durante questi ultimi anni, per avermi dato la possibilitá di studiare serenamente e per non avermi mai fatto mancare nulla.

Infine un caloroso ringraziamento va agli amici di sempre, a tutti i compagni di corso che mi hanno accompagnato durante questo percorso e a tutte le persone incontrate durante questi ultimi 5 anni.

List of Tables

List of Figures

Bibliography

[1] "http://www.xcycle-h2020.eu/home/index."

[2] D. Dardari, E. Falletti, and M. Luise, *Satellite and terrestrial radio positioning techniques: a signal processing perspective*. Academic Press, 2012.

[3] L. M. Ni, D. Zhang, and M. R. Souryal, "RFID-based localization and tracking technologies," *Wireless Communications, IEEE*, vol. 18, no. 2, pp. 45–51, 2011.

[4] T. S. Rappaport *et al.*, *Wireless communications: principles and practice*. prentice hall PTR New Jersey, 1996, vol. 2.

[5] D. Dardari, P. Closas, and P. M. Djuric, "Indoor tracking: Theory, methods, and technologies," *Vehicular Technology, IEEE Transactions on*, vol. 64, no. 4, pp. 1263–1278, 2015.

[6] M. Bouet and A. L. Dos Santos, "RFID tags: Positioning principles and localization techniques," in *Wireless Days, 2008. WD'08. 1st IFIP*. IEEE, 2008, pp. 1–5.

[7] S. Knedlik, "http://www.zess.uni-siegen.de/home/das-zess/forschung/navigation.html."

[8] H. Liu, H. Darabi, P. Banerjee, and J. Liu, "Survey of wireless indoor positioning techniques and systems," *Systems, Man, and Cybernetics, Part C: Applications and Reviews, IEEE Transactions on*, vol. 37, no. 6, pp. 1067–1080, 2007.

[9] G. R. Paolo Talone, *RFID Fondamenti di una tecnologia silenziosamente pervasiva*. Fondazione Ugo Bordoni, 2008.

[10] J. Hightower, R. Want, and G. Borriello, "Spoton: An indoor 3D location sensing technology based on RF signal strength," *UW CSE 00-02-02, University of Washington, Department of Computer Science and Engineering, Seattle, WA*, vol. 1, 2000.

[11] T. F. Bechteler and H. Yenigün, "2-D localization and identification based on SAW ID-tags at 2.5 ghz," *Microwave Theory and Techniques, IEEE Transactions on*, vol. 51, no. 5, pp. 1584–1590, 2003.

[12] A. Stelzer, K. Pourvoyeur, and A. Fischer, "Concept and application of LPM-a novel 3-D local position measurement system," *Microwave Theory and Techniques, IEEE Transactions on*, vol. 52, no. 12, pp. 2664–2669, 2004.

[13] Y. Zhang, M. G. Amin, and S. Kaushik, "Localization and tracking of passive RFID tags based on direction estimation," *International Journal of Antennas and Propagation*, vol. 2007, 2007.

[14] L. M. Ni, Y. Liu, Y. C. Lau, and A. P. Patil, "Landmarc: indoor location sensing using active RFID," *Wireless networks*, vol. 10, no. 6, pp. 701–710, 2004.

[15] Y. Zhao, Y. Liu, and L. M. Ni, "VIRE: Active RFID-based localization using virtual reference elimination," in *Parallel Processing, 2007. ICPP 2007. International Conference on.* IEEE, 2007, pp. 56–56.

[16] C. Wang, H. Wu, and N.-F. Tzeng, "RFID-based 3-D positioning schemes," in *INFOCOM 2007. 26th IEEE International Conference on Computer Communications. IEEE.* IEEE, 2007, pp. 1235–1243.

[17] A. Bekkali, H. Sanson, and M. Matsumoto, "RFID indoor positioning based on probabilistic RFID map and kalman filtering," in *Wireless and Mobile Computing, Networking and Communications, 2007. WiMOB 2007. Third IEEE International Conference on.* IEEE, 2007, pp. 21–21.

[18] M. Bouet and G. Pujolle, "A range-free 3D localization method for RFID tags based on virtual landmarks," in *Personal, Indoor and Mobile Radio*

Communications, 2008. PIMRC 2008. IEEE 19th International Symposium on. IEEE, 2008, pp. 1–5.

[19] L. E. Miller, *Indoor navigation for first responders: a feasibility study.* Citeseer, 2006.

[20] Y. Liu, Y. Zhao, L. Chen, J. Pei, and J. Han, "Mining frequent trajectory patterns for activity monitoring using radio frequency tag arrays," *Parallel and Distributed Systems, IEEE Transactions on*, vol. 23, no. 11, pp. 2138–2149, 2012.

[21] D. Zhang, Y. Yang, D. Cheng, S. Liu, and L. M. Ni, "Cocktail: an RF-based hybrid approach for indoor localization," in *Communications (ICC), 2010 IEEE International Conference on.* IEEE, 2010, pp. 1–5.

[22] D. Zhang, J. Ma, Q. Chen, and L. M. Ni, "An RF-based system for tracking transceiver-free objects," in *Pervasive Computing and Communications, 2007. PerCom'07. Fifth Annual IEEE International Conference on.* IEEE, 2007, pp. 135–144.

[23] A. J. Smola and B. Schölkopf, "A tutorial on support vector regression," *Statistics and computing*, vol. 14, no. 3, pp. 199–222, 2004.

[24] P. V. Nikitin, R. Martinez, S. Ramamurthy, H. Leland, G. Spiess, and K. Rao, "Phase based spatial identification of UHF RFID tags," in *RFID, 2010 IEEE International Conference on.* IEEE, 2010, pp. 102–109.

[25] M. Vossiek, A. Urban, S. Max, and P. Gulden, "Inverse synthetic aperture secondary radar concept for precise wireless positioning," *Microwave Theory and Techniques, IEEE Transactions on*, vol. 55, no. 11, pp. 2447–2453, 2007.

[26] J. Fuhl, J.-P. Rossi, and E. Bonek, "High-resolution 3D direction-of-arrival determination for urban mobile radio," *Antennas and Propagation, IEEE Transactions on*, vol. 45, no. 4, pp. 672–682, 1997.

[27] R. Miesen, F. Kirsch, and M. Vossiek, "Holographic localization of passive uhf rfid transponders," in *RFID (RFID), 2011 IEEE International Conference on.* IEEE, 2011, pp. 32–37.

[28] A. Costanzo, D. Masotti, T. Ussmueller, and R. Weigel, "Tag, you're it: Ranging and finding via rfid technology," *Microwave Magazine, IEEE*, vol. 14, no. 5, pp. 36–46, 2013.

[29] R. Miesen, R. Ebelt, F. Kirsch, T. Schäfer, G. Li, H. Wang, and M. Vossiek, "Where is the tag?" *Microwave Magazine, IEEE*, vol. 12, no. 7, pp. S49–S63, 2011.

[30] D. Dardari, R. D. Errico, C. Roblin, A. Sibille, and M. Z. Win, "Ultra-wide bandwidth rfid: The next generation?" *Proceedings of the IEEE*, vol. 98, no. 9, pp. 1570–1582, 2010.

[31] F. Guidi, N. Decarli, S. Bartoletti, A. Conti, and D. Dardari, "Detection of multiple tags based on impulsive backscattered signals," *Communications, IEEE Transactions on*, vol. 62, no. 11, pp. 3918–3930, 2014.

[32] N. Decarli, F. Guidi, and D. Dardari, "A novel joint rfid and radar sensor network for passive localization: design and performance bounds," *Selected Topics in Signal Processing, IEEE Journal of*, vol. 8, no. 1, pp. 80–95, 2014.

[33] R. Miesen, F. Kirsch, and M. Vossiek, "UHF RFID localization based on synthetic apertures," *Automation Science and Engineering, IEEE Transactions on*, vol. 10, no. 3, pp. 807–815, 2013.

[34] C. Hekimian-Williams, B. Grant, X. Liu, Z. Zhang, and P. Kumar, "Accurate localization of RFID tags using phase difference," in *RFID, 2010 IEEE International Conference on*. IEEE, 2010, pp. 89–96.

[35] D. Dardari, "Notes of the course of telecommunication systems LM."

[36] Impinj, "Impinj speedway revolution user guide."

[37] ——, "Impinj speedway readers product brief."

[38] *EPC Radio-Frequency Identity Protocols Class-1 Generation-2 UHF RFID Protocol for Communications at 860 MHz 960 MHz Version 1.2.0*, EPC Global Inc Std., 2008.

[39] *Low Level Reader Protocol (LLRP), Version 1.0*, EPC Global Inc Std., 2007.

[40] http://fosstrak.github.io/llrp/, "Fosstrak llrp commander documentations."